

Assessment of individual pharmacokinetic processes in renal drug elimination

Inaugural Dissertation

zur

Erlangung des Doktorgrades  
*philosophiae doctor* (PhD) in Health Sciences  
der Medizinischen Fakultät  
der Universität zu Köln

vorgelegt von

Qian Dong

aus Qinghai, China

Copy-Star Druck und Werbung GmbH, Köln

2025

Assessment of individual pharmacokinetic processes in renal drug elimination

Inaugural Dissertation

zur

Erlangung des Doktorgrades  
*philosophiae doctor* (PhD) in Health Sciences  
der Medizinischen Fakultät  
der Universität zu Köln

vorgelegt von

Qian Dong

aus Qinghai, China

Copy-Star Druck und Werbung GmbH, Köln

2025

Betreuerin / Betreuer: Prof. Dr. Uwe Fuhr

Gutachterin / Gutachter: Prof. Dr. Christine Kurschat  
Prof. Dr. Martin Hellmich

Datum der Mündlichen Prüfung: 02.07.2025

## Table of contents

Abstract.....	III
Zusammenfassung .....	IV
List of abbreviations.....	V
1. Introduction .....	1
1.1 Concepts of renal clearance .....	1
1.1.1 Glomerular filtration .....	1
1.1.2 Tubular secretion .....	2
1.1.3 Tubular reabsorption.....	2
1.1.4 Renal clearance .....	2
1.2 Mechanisms of tubular drug transport .....	3
1.2.1 Cationic drug transporters.....	5
1.2.2 Anionic drug transporters .....	8
1.3 The clinical significance of GFR.....	9
1.4 The clinical significance of transporter-mediated active renal secretion .....	10
1.4.1 Unwanted DDIs involving OCT2 and MATE1/2-K.....	11
1.4.2 Exploiting OCT2 DDIs to protect from cisplatin nephrotoxicity .....	12
1.4.3 Desirable and unwanted DDIs involving OATs.....	13
1.4.4 DDIs involving P-gp.....	14
1.4.5 Sensitive populations .....	15
1.5 Methods and challenges in the quantification of renal PK processes .....	17
1.5.1 Measured GFR to validate estimated GFR.....	17
1.5.2 Estimated GFR using creatinine and/or cystatin C.....	18
1.5.3 Measured GFR using iohexol .....	19
1.5.4 In vitro assessment of renal TDDIs .....	20
1.5.5 Probes and biomarkers for renal TDDI assessment .....	24
1.5.6 In vivo phenotyping for predicting renal TDDIs .....	30
1.5.7 Understanding probe PK in phenotyping cocktails using PopPK modeling.....	34
2. Aims and objectives .....	36
3. Relevant publications and contributions.....	37

3.1 Publication I.....	37
3.2 Publication II.....	40
3.3 Publication III.....	44
4. Summary .....	47
4.1 Key findings .....	47
4.2 Limitations.....	47
4.3 Future directions .....	49
4.3.1 Advancing GFR assessment in diverse patient groups.....	49
4.3.2 Further improvement and validation of the current cocktail approach .....	51
5. Acknowledgment .....	57
Reference.....	58
Publication I .....	78
Publication II .....	81
Publication III .....	112
Erklärung.....	127

## **Abstract**

Renal elimination is a major route of drug clearance, influencing exposure and therapeutic outcomes, especially in patients with impaired kidney function. This cumulative dissertation aims to improve the evaluation of renal drug elimination by optimizing iohexol-based methods for measuring glomerular filtration rate (GFR) and examining the role of kidney transporters.

Three complementary studies were conducted. The first evaluated simplified methods to estimate iohexol clearance from blood samples. Using correction formulas in one- and two-compartment pharmacokinetic (PK) models, reliable GFR estimates were achieved. Both approaches showed acceptable performance, offering practical alternatives to complex models in clinical settings.

The second study assessed the PK and transporter involvement of a reduced iohexol dose (259 mg). Results confirmed iohexol is cleared solely by glomerular filtration, with no significant transporter interaction. Its predictable and dose-proportional PK support its use as a safe and reliable GFR marker, even in patients with kidney impairment.

The third study used population PK modeling to explore adefovir disposition, a substrate of the renal organic anion transporter (OAT) 1, within a transporter probe cocktail. Co-administration slightly increased adefovir exposure, likely due to altered absorption rather than transporter interaction. Renal clearance ( $CL_R$ ) was unaffected, and no saturation of OAT1-mediated elimination was observed. Adefovir  $CL_R$  is thus a suitable marker of OAT1 activity.

Together, these studies offer practical tools and insights for assessing kidney function and transporter-related drug clearance, supporting more individualized and efficient clinical decision-making.

## Zusammenfassung

Die renale Elimination ist ein wesentlicher Weg der Arzneistoffausscheidung und beeinflusst sowohl die Wirkstoffexposition als auch die therapeutischen Ergebnisse – insbesondere bei Patienten mit eingeschränkter Nierenfunktion. Diese kumulative Dissertation zielt darauf ab, die Bewertung der renalen Arzneistoffelimination zu verbessern, indem iohexolbasierte Methoden zur Bestimmung der glomerulären Filtrationsrate (GFR) optimiert und die Rolle renaler Transporter untersucht werden.

Es wurden drei komplementäre Studien durchgeführt. Die erste Studie bewertete vereinfachte Methoden zur Schätzung der Iohexol-Clearance aus Blutproben. Durch Korrekturformeln in pharmakokinetischen (PK) Ein- und Zwei-Kompartimentmodellen konnten zuverlässige GFR-Schätzungen erzielt werden. Beide Ansätze zeigten eine akzeptable Leistungsfähigkeit und stellen eine praxisnahe Alternative zu komplexen Modellierungen in der klinischen Anwendung dar.

Die zweite Studie untersuchte die Pharmakokinetik und mögliche Transporterbeteiligung einer reduzierten Iohexol-Dosis (259 mg). Die Ergebnisse bestätigten, dass Iohexol ausschließlich durch glomeruläre Filtration eliminiert wird, ohne signifikante Beteiligung renaler Transporter. Die vorhersagbare und dosisproportionale Pharmakokinetik unterstützt den Einsatz dieser niedrigeren Dosis als sicheren und zuverlässigen GFR-Marker – auch bei Patienten mit Nierenfunktionsstörung.

Die dritte Studie verwendete populationsbasierte PK-Modellierung zur Untersuchung der Verteilung von Adefovir – einem Substrat des organischen Anionentransporters (OAT) 1 – im Rahmen eines Cocktails mit mehreren Transporter-Sonden. Die gleichzeitige Verabreichung führte zu einem leichten Anstieg der Adefovir-Exposition, vermutlich aufgrund veränderter Absorption und nicht infolge von Transporterinteraktionen. Die renale Clearance ( $CL_R$ ) blieb unbeeinflusst, und es wurde keine klinisch relevante Sättigung der OAT1-vermittelten Elimination beobachtet. Die Adefovir- $CL_R$  eignet sich somit als Marker für die OAT1-Aktivität.

Insgesamt liefern diese Studien praxisnahe Ansätze und Erkenntnisse zur Beurteilung der Nierenfunktion und der Transporter-vermittelten Arzneistoffelimination und unterstützen eine individuellere und effizientere klinische Entscheidungsfindung.

## List of abbreviations

Abbreviation	Full term
ABC	ATP-Binding Cassette
ADR	Adverse Drug Reaction
AKI	Acute Kidney Injury
AUC	Area Under the Curve
AUC <sub>0-8h</sub>	Area Under the Curve from Time Zero to 8 Hours Post-Administration
BCRP	Breast Cancer Resistance Protein
BIS	Berlin Initiative Study
BM	Bröchner-Mortensen
CCC	Concordance Correlation Coefficient
CHO	Chinese Hamster Ovary (cells)
Ch	Chantler
CILDI	Continuous Infusion of Low-Dose Iohexol
CKD	Chronic Kidney Disease
CKD-EPI	Chronic Kidney Disease Epidemiology Collaboration
CKD-EPI <sub>cr2009</sub>	Chronic Kidney Disease Epidemiology Collaboration Creatinine Equation (2009)
CKD-EPI <sub>cr2021</sub>	Chronic Kidney Disease Epidemiology Collaboration Creatinine Equation (2021)
CKD-EPI <sub>cr-cys2012</sub>	Chronic Kidney Disease Epidemiology Collaboration Combined Creatinine and Cystatin C Equation (2012)
CKD-EPI <sub>cys2012</sub>	Chronic Kidney Disease Epidemiology Collaboration Cystatin C Equation (2012)
CI-AKI	Contrast-Induced Acute Kidney Injury



CI	Confidence Interval
C <sub>max</sub>	Maximum Plasma Concentration
C <sub>max,u</sub>	Unbound Maximum Plasma Concentration
CL <sub>R</sub>	Renal Clearance
CL1	Iohexol clearance estimated using a one-compartment model
CL2	Iohexol clearance estimated using a two-compartment model
CL3	Iohexol clearance estimated using a three-compartment model
CMPF	3-Carboxy-4-methyl-5-propyl-2-furanpropionate
CP	Coverage Probability
DDI	Drug-Drug Interaction
DME	Drug-Metabolizing Enzyme
eGFR	Estimated Glomerular Filtration Rate
eGFR <sub>cr</sub>	Creatinine-Based Estimated Glomerular Filtration Rate
eGFR <sub>cys</sub>	Cystatin C-Based Estimated Glomerular Filtration Rate
EBV	Epstein–Barr Virus
EKFC	European Kidney Function Consortium
EMA	European Medicines Agency
FDA	U.S. Food and Drug Administration
GCDCA-S	Glycochenodeoxycholate-3-sulfate
GFR	Glomerular Filtration Rate
GLUT2	Glucose Transporter 2
HA	Hippurate
HEK293	Human Embryonic Kidney 293

HPLC–MS/MS	High-Performance Liquid Chromatography coupled with Tandem Mass Spectrometry
HVA	Homovanillic Acid
IA	Indoleacetate
IC <sub>50</sub>	Half Maximal Inhibitory Concentration
IS	Indoxyl sulfate
ITC	International Transporter Consortium
K <sub>i</sub>	Inhibition Constant
K <sub>m</sub>	Michaelis-Menten Constant
KDIGO	Kidney Disease: Improving Global Outcomes
LLC-PK1	Porcine Kidney Epithelial Cells
MATE	Multidrug and Toxic Compound Extrusion Protein
MDR1	Multidrug Resistance Protein 1
MDRD	Modification of Diet in Renal Disease
MDCK	Madin-Darby Canine Kidney
m <sup>1</sup> A	N <sup>1</sup> -Methyladenosine
mGFR	Measured Glomerular Filtration Rate
MPP <sup>+</sup>	1-Methyl-4-phenylpyridinium
MRP	Multidrug Resistance-Associated Protein
NCA	Non-Compartmental Analysis
NCE	New Chemical Entity
NMN	N <sup>1</sup> -Methylnicotinamide
NMQ	N-Methyl-Quinidine
NSAID	Nonsteroidal Anti-Inflammatory Drug

OA	Organic Anion
OAT	Organic Anion Transporter
OATP	Organic Anion Transporting Polypeptide
OC	Organic Cation
OCT	Organic Cation Transporter
PAH	Para-Aminohippuric Acid
PBPK	Physiologically Based Pharmacokinetic
PDA	4-Pyridoxic Acid
PD	Pharmacodynamic
PET	Positron Emission Tomography
PK	Pharmacokinetic
PMAT	Plasma Membrane Monoamine Transporter
PopPK	Population Pharmacokinetic
P-gp	P-glycoprotein
RLM	Revised Lund-Malmö
RMSE	Root Mean Squared Error
SBI	Single Bolus Injection
sEV	Small Extracellular Vesicle
SLC	Solute Carrier
SmPC	Summary of Product Characteristic
SNP	Single-Nucleotide Polymorphism
TDDI	Transporter-Mediated Drug-Drug Interaction
TDI	Total Deviation Index
TDI <sub>90</sub>	Total Deviation Index at 90% Coverage Probability

TEA	Tetraethylammonium
TMD	Transmembrane Domain
URAT1	Urate Transporter 1
$V_{\max}$	Maximum Reaction Velocity

## **1. Introduction**

The kidneys play a central role in the systemic elimination of xenobiotics and endogenous metabolic byproducts.<sup>1</sup> Approximately one-third of clinically used drugs are primarily cleared via the kidneys, making renal elimination a key determinant of drug disposition and therapeutic outcomes.<sup>2</sup> This process involves glomerular filtration, along with transporter-mediated active tubular secretion and reabsorption in the renal proximal tubule.<sup>1</sup> The involvement of transporters comes with a potential for renal drug-drug interactions (DDIs), which may lead to inappropriate dosing and preventable adverse drug reactions.<sup>3</sup> In individuals with renal impairment, alterations in transporter activity and glomerular filtration rate (GFR) can markedly affect the pharmacokinetics of both renally and non-renally eliminated drugs.<sup>1</sup> Thus, an early and mechanistic understanding of renal pharmacokinetics is essential for optimizing dosing strategies, minimizing adverse effects, and improving translational predictions throughout drug development.<sup>1</sup>

This dissertation comprises three original publications that collectively address the assessment of individual pharmacokinetic (PK) processes contributing to renal drug elimination. The first study focuses on improving the estimation of GFR through practical approaches using iohexol plasma clearance.<sup>4</sup> The second evaluates the PK properties and transporter interaction potential of low-dose iohexol to support its use as a selective GFR marker, also in the presence of co-medications, including those given in cocktail phenotyping studies.<sup>5</sup> The third applies population PK (PopPK) modeling to characterize adefovir as a probe for organic anion transporter (OAT) 1 within a clinical transporter cocktail.<sup>6</sup> Together, these studies provide complementary insights into renal filtration and secretion processes and offer methodological advances relevant to renal transporter phenotyping and DDI assessment.

### **1.1 Concepts of renal clearance**

#### **1.1.1 Glomerular filtration**

Glomerular filtration occurs in the renal corpuscles, where the glomerulus, enclosed by Bowman's capsule, enables passive filtration driven by hydrostatic pressure. This process selectively permits substances to pass based on molecular size and charge.<sup>7,8</sup> Approximately 10% of total renal blood flow undergoes ultrafiltration at the glomerulus, with the filtration rate of drugs influenced by blood flow rate, hematocrit, and the plasma fraction of unbound

drug ( $f_u$ ).<sup>9,10</sup> The total volume filtered by the glomeruli of the kidneys per unit of time is known as the GFR.<sup>11</sup>

### **1.1.2 Tubular secretion**

After glomerular filtration, renal blood flows through peritubular capillaries, where tubular secretion occurs. This process transfers drugs and other substances from plasma into the proximal tubular lumen, primarily via a number of transporters in the proximal tubule. Secretion depends on transporter kinetics, plasma free fraction, and blood flow rate. Since transporters are involved, secretion is saturable and may be inhibited by co-administered drugs, increasing the risk of DDIs.<sup>9,10</sup>

### **1.1.3 Tubular reabsorption**

Tubular drug reabsorption in the nephron occurs via passive or active transport. Passive reabsorption, driven by diffusion, allows unionized drugs to re-enter circulation, while polar drugs are poorly reabsorbed. This process depends on passive permeability, influenced by urine flow and pH.<sup>10</sup> Active reabsorption is relatively uncommon and primarily observed for vitamins and amino acids. It occurs at the luminal (apical) membrane of the proximal tubule via uptake and efflux transporters and shares properties with secretion, being energy-dependent, saturable, stereospecific, and susceptible to competitive drug interactions.<sup>9,10</sup>

### **1.1.4 Renal clearance**

Renal clearance ( $CL_R$ ) represents the volume of plasma from which a drug is completely removed by the kidneys per unit of time.<sup>12</sup> It integrates the contributions of glomerular filtration and tubular secretion, offset by any reabsorption that occurs.  $CL_R$  is a critical parameter for assessing the renal elimination of drugs.<sup>9,13</sup>

In both clinical and preclinical settings,  $CL_R$  is typically estimated by measuring the amount of unchanged drug excreted in urine relative to its plasma concentration over time. This can be assessed following either intravenous or oral administration, provided sufficient urine and plasma data are available.<sup>9</sup>

To interpret  $CL_R$ , it is often compared to the theoretical clearance expected from filtration alone ( $GFR \times f_u$ ).<sup>9</sup> A  $CL_R$  higher than this value indicates net secretion, while a lower value suggests net reabsorption.<sup>9</sup> If the observed value approximates filtration clearance, the drug

is primarily eliminated via glomerular filtration.<sup>9</sup> This comparative approach enables the identification of the dominant elimination pathways and supports a mechanistic interpretation of PK data in drug development and clinical pharmacology.<sup>9</sup> (Figure 1)

## **1.2 Mechanisms of tubular drug transport**

Renal drug handling is largely mediated by a variety of transport proteins located in the proximal tubules of the kidney.<sup>14</sup> These proteins, many of which are polyspecific, recognize a broad spectrum of endogenous and exogenous compounds and are responsible for the active secretion and reabsorption of numerous drugs.<sup>14,15</sup> A key feature influencing their function is the strong negative transmembrane potential that exists between the intracellular and extracellular environments.<sup>14</sup> This electrochemical gradient can either hinder or facilitate the movement of charged substrates, depending on their ionic nature.<sup>14</sup> As a result, the mechanisms underlying tubular secretion differ significantly between organic anions and cations (OAs and OCs).<sup>14</sup>

Two major and distinct tubular secretion systems are recognized: the OA transport system and the OC transport system.<sup>14</sup> Transporters involved in these processes mainly belong to two large protein families: the solute carrier (SLC) family and the ATP-binding cassette (ABC) family.<sup>16,17</sup>

SLC transporters utilize either passive or secondary active transport mechanisms. Facilitative SLC transporters enable the passive diffusion of substrates along their electrochemical gradients, while secondary active SLC transporters mediate the uptake of substrates against their gradients by coupling transport to the movement of co-transported ions, such as Na<sup>+</sup> or H<sup>+</sup>.<sup>2</sup> Members of the SLC family relevant to renal drug handling include OATs, organic cation transporters (OCTs), organic anion transporting polypeptides (OATPs), urate transporter (URAT) 1, multidrug and toxic compound extrusion proteins (MATEs), nucleoside transporters, among others.<sup>16</sup>

In contrast, ABC transporters function as primary active transporters. They use the energy derived from ATP hydrolysis to actively export substrates against their electrochemical gradients.<sup>2,16</sup> In the kidney, key ABC transporters involved in drug secretion include multidrug resistance-associated proteins (MRPs) 2 and 4, P-glycoprotein (P-gp), and the breast cancer resistance protein (BCRP).<sup>16</sup>

This dissertation emphasizes the role of renal membrane transporters, particularly a defined subset of SLC and ABC transporters that are implicated in DDIs and/or drug-induced nephrotoxicity, as highlighted in recent regulatory guidelines.<sup>18-20</sup> These transporters are strategically localized on both the basolateral (blood-facing) and apical (urine-facing) membranes of proximal tubular epithelial cells.<sup>2</sup> Typically, renal elimination of a given drug is mediated by different transporters in the basolateral and the apical membrane, with the potential for more than one mechanism to cause respective DDIs. Basolateral uptake transporters such as OATs and OCTs mediate the cellular influx of drugs from the circulation, while apical efflux transporters such as MATEs and MRPs facilitate the elimination of drugs into the tubular lumen for urinary excretion.<sup>2</sup> The subsequent sections will explore the expression patterns, subcellular localization, and transport mechanisms of these transporters in greater detail. (Figure 1)

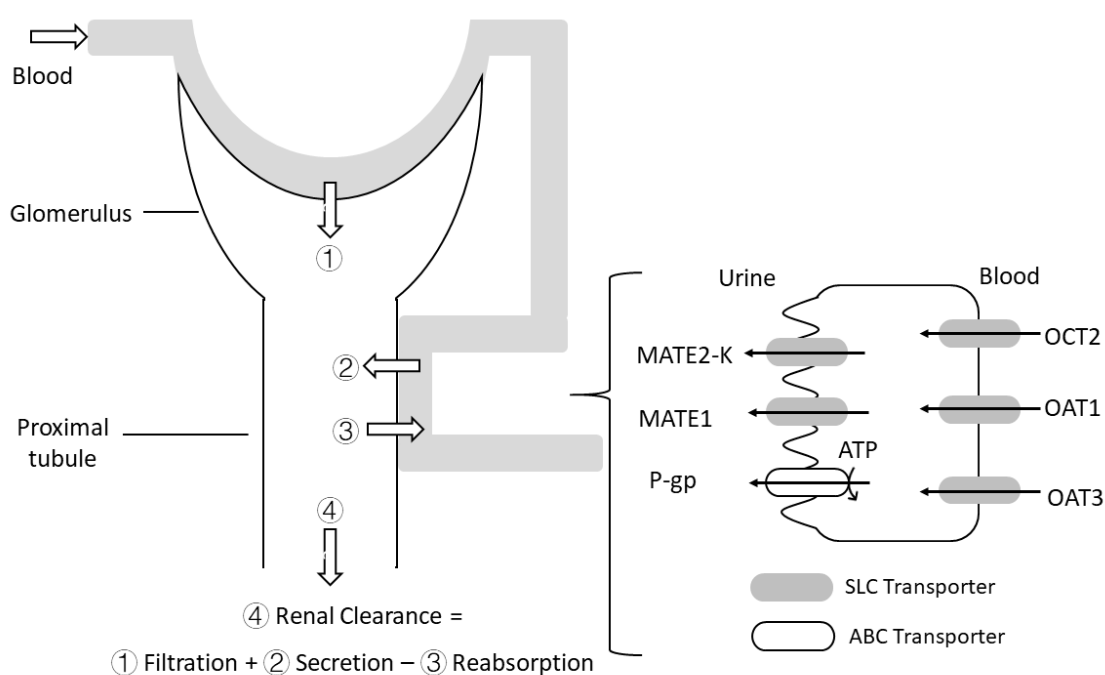


Figure 1. Overview of renal drug elimination pathways and key transporters in the proximal tubule. Renal clearance is governed by the interplay of three processes: ① glomerular filtration, ② active tubular secretion, and ③ tubular reabsorption. The net renal clearance ④ is determined by filtration minus reabsorption plus secretion. In the proximal tubule, drug uptake from the blood across the basolateral membrane is mediated by SLC transporters, including OAT1, OAT3, and OCT2. Efflux into the tubular lumen is facilitated by apical SLC



transporters (MATE1, MATE2-K) and ABC transporters such as P-gp, which utilize ATP hydrolysis for active transport. Gray rounded rectangles represent SLC transporters, and white rounded rectangles indicate ABC transporters.

### 1.2.1 Cationic drug transporters

#### OCTs (SLC family *SLC22A*)

OCTs are part of the *SLC22A* family.<sup>21</sup> In humans, three distinct OCTs have been identified: OCT1 (*SLC22A1*), OCT2 (*SLC22A2*), and OCT3 (*SLC22A3*). These membrane transporters consist of 553–556 amino acids and are predicted to contain 12 transmembrane domains (TMDs).<sup>21</sup> The amino acid sequence of OCT2 shares 70% identity with OCT1,<sup>22</sup> whereas OCT3 exhibits approximately 50% sequence similarity with both OCT1 and OCT2.<sup>23</sup>

Among the OCTs, OCT2 is primarily expressed in the kidneys and is generally regarded as a “kidney-specific” uptake OCT,<sup>24</sup> localized to the basolateral membrane of renal proximal tubules.<sup>21</sup> OCT1, in contrast, is predominantly found in the sinusoidal membrane of hepatocytes in the liver, with very low expression levels detected in other tissues, including the luminal membrane of proximal and distal renal tubules.<sup>21</sup> Meanwhile, OCT3 has a broader tissue distribution, being present in skeletal muscle, heart, placenta, and salivary glands.<sup>21</sup> However, because OCT3 is expressed at lower levels than its paralogs in key drug absorption (e.g., intestine) and elimination organs (e.g., liver and kidney), its contribution to DDIs is generally considered to be very limited.

Within the kidneys, among the OCTs, mainly OCT2 plays a crucial role in the renal secretion of OCs by facilitating their transport from systemic circulation into renal tubule cells.<sup>25</sup> This process is electrogenic, sodium (Na<sup>+</sup>)-independent, and driven by the negative membrane potential within kidney tubular cells. By mediating this initial step, OCT2 significantly contributes to drug clearance and the renal excretion of both endogenous and exogenous OCs.<sup>16</sup> While OCT1 is primarily involved in the hepatic uptake of OCs, it may also participate in their renal secretion, with some degree of reabsorption possible, as observed with OCs like metformin.<sup>3,26,27</sup>

OCT2 transports a broad spectrum of substrates, primarily OCs with one or two positive charges, as well as weak bases that are protonated at physiological pH.<sup>28</sup> Well-established model substrates for OCT2 used in in vitro studies include creatinine, tetraethylammonium

(TEA), and metformin.<sup>19</sup> Despite the wide array of substrates suitable for in vitro studies, metformin remains the only clinically approved probe used for OCT2 phenotyping in human trials.<sup>19</sup> In addition, several compounds, such as cimetidine, clonidine, pyrimethamine, and verapamil, are recommended as inhibitors in these in vitro assays.<sup>19</sup> Notably, dolutegravir is generally a more potent in vivo inhibitor of OCT2 than of MATE transporters.<sup>19</sup>

### **MATEs (SLC Family *SLC47A*)**

MATEs belong to the SLC47 family.<sup>16</sup> Among them, MATE1 (gene symbol *SLC47A1*) and hMATE2-K (gene symbol *SLC47A2*) are the most extensively studied transporters. MATE1 and MATE2-K consist of 570 and 566 amino acids, respectively, and are predicted to contain 13 TMDs.<sup>16,29,30</sup> This structural prediction has been experimentally validated for human MATE1,<sup>29</sup> but confirmation of MATE2-K topology is still pending.<sup>30</sup>

Among the MATE transporters, MATE1 is most abundantly expressed in the kidney but is also significantly present in other tissues, such as the liver, skeletal muscle, and adrenal gland,<sup>16</sup> while MATE2-K is primarily expressed in the kidney.<sup>16</sup> In the human kidney, MATE1 is localized together with MATE2-K in the brush-border membrane of the proximal tubule epithelial cells.<sup>30</sup>

MATE1 and MATE2-K are OC/proton exchangers that mediate the apical efflux of OCs in the kidney.<sup>16</sup> Their transport activity is driven by a proton gradient oriented from the tubular lumen into the cytosol, which is established by the typically higher acidity of the lumen compared to the intracellular environment.<sup>16,31,32</sup> As protons move into proximal tubule epithelial cells, MATE1 and MATE2-K facilitate the concurrent extrusion of OCs into the urine.<sup>16</sup> These transporters share extensive substrate and inhibitor overlap with OCT2 and act in concert with it to support renal OC secretion.<sup>16,33</sup> For instance, in the case of metformin, uptake from the blood into tubular epithelial cells occurs mainly via basolateral OCT2, followed by apical excretion into the urine predominantly through MATE1 and MATE2-K.<sup>27</sup>

To assess MATE1 and MATE2-K activity in vitro, commonly used probe substrates such as creatinine, metformin, 1-methyl-4-phenylpyridinium (MPP<sup>+</sup>), and TEA are frequently employed.<sup>19</sup> However, these compounds are also substrates of OCT transporters, which can complicate the interpretation of MATE-specific transport.<sup>16</sup> Although metformin is widely used as a probe substrate, its dual transport by OCTs and MATEs limits its suitability for

selectively probing MATE function in clinical settings.<sup>3,19</sup> Inhibition studies often utilize cimetidine, pyrimethamine, and quinidine, which are widely used in vitro inhibitors of MATE1 and MATE2-K.<sup>19</sup> Among these, pyrimethamine is considered a relatively selective MATE inhibitor in vivo,<sup>19</sup> whereas cimetidine exhibits potent in vivo inhibition of MATEs.<sup>16,34</sup>

### **P-gp (ABC Family *ABCB1*)**

P-gp, encoded by the *ABCB1* gene and also known as multidrug resistance protein 1 (MDR1), is one of the most extensively studied members of the ABC transporter family.<sup>16</sup> This 1280-amino-acid membrane protein is both phosphorylated and glycosylated and is composed of two homologous halves, each containing six hydrophobic transmembrane segments and an intracellular ATP-binding domain.<sup>35</sup> Acting as a broad-spectrum efflux transporter, P-gp is vital in regulating drug distribution and is predominantly found in tissues such as the intestine, kidney, liver, brain, and placenta.<sup>17</sup>

In the kidney, P-gp is positioned on the apical membrane of proximal tubule cells, facilitating the active excretion of both endogenous compounds and xenobiotics into the urine, counteracting their concentration gradients.<sup>16</sup> Its substrates are typically large, lipophilic or amphipathic compounds with molecular weights exceeding 400 Da and a net positive charge at physiological pH.<sup>16</sup>

P-gp transports a wide range of therapeutics across multiple drug classes, including: chemotherapeutic agents (e.g., docetaxel, etoposide, vincristine), immunosuppressants (e.g., cyclosporine A, tacrolimus), antibiotics (e.g., macrolides), statins (e.g., atorvastatin, lovastatin), cardiac medications (e.g., digoxin, digitoxin), beta-adrenergic blockers (e.g., carvedilol).<sup>17</sup>

Several well-established P-gp substrates, including digoxin, N-methyl-quinidine (NMQ), quinidine, and vinblastine, are commonly used in vitro to study the kinetic properties of P-gp.<sup>19</sup> To evaluate P-gp activity, inhibitors such as verapamil, valspodar (PSC833), zosuquidar (LY335979), and GF120918, which also inhibits BCRP, are frequently applied in experimental setups.<sup>19</sup>

For in vivo evaluation of transporter activity, regulatory agencies recommend specific probe substrates such as digoxin, dabigatran etexilate (primarily affected by intestinal P-gp), and fexofenadine (also a substrate for OATP1B1, OATP1B3, and OATP2B1).<sup>19</sup> Commonly

recommended P-gp inhibitors include itraconazole, which also inhibits BCRP and CYP3A; verapamil, which also affects CYP3A; and quinidine.<sup>19</sup> These agents are widely used in clinical DDI studies to assess P-gp function and its influence on drug disposition.

### 1.2.2 Anionic drug transporters

#### OATs (SLC Family *SLC22A*)

OATs enable the transport of various anionic substrates and are classified within the SLC family SLC22, which also includes OCTs.<sup>16</sup> ten distinct OAT family members have been found in humans, including OAT1–8, OAT10, and URAT1. The majority of OATs are predominantly expressed in the renal proximal tubule, with the exception of OAT7, which is solely located in the liver.<sup>16,36</sup> Among these, OAT1 (*SLC22A6*) and OAT3 (*SLC22A8*) are of particular PK relevance due to their significant role in renal drug elimination.<sup>37</sup> Structurally, OAT1 and OAT3 are composed of 563 and 542 amino acids, respectively, and both share a common topology featuring 12 TMDs.<sup>38</sup> In the kidney, these transporters are localized to the basolateral membrane of proximal tubule epithelial cells. OAT1 is predominantly expressed in the S2 segment, while OAT3 is distributed throughout the S1 to S3 segments.<sup>17</sup> Under normal physiological conditions, OAT1 and OAT3 function as OA/ $\alpha$ -ketoglutarate exchangers, mediating the initial uptake step in the renal secretion of OAs.<sup>36</sup> Their activity is driven by an outward  $\alpha$ -ketoglutarate gradient, maintained by the  $\text{Na}^+$ - $\alpha$ -ketoglutarate cotransporter, which facilitates the uptake of OAs from the blood into renal tubular cells.<sup>16,36</sup>

While OAT1 and OAT3 have overlapping substrate preferences, they exhibit distinct affinities for specific compounds.<sup>36</sup> Both transport relatively small and hydrophilic OAs, but OAT3 tends to favor larger, more hydrophobic molecules, particularly those containing multiple ring structures.<sup>37</sup> A notable example is estrone-3-sulfate, a commonly used substrate in in vitro assays for OAT3 function.<sup>37</sup> In contrast, para-aminohippuric acid (PAH) shows markedly higher affinity for OAT1, with an apparent affinity in the low micromolar range, making it a well-established probe for studying OAT1-mediated transport.<sup>38</sup>

Numerous clinically relevant drugs are recognized substrates of OAT1 and OAT3, including antibiotics, antivirals, antihypertensives, diuretics, cytotoxic agents,  $\text{H}_2$ -receptor antagonists, nonsteroidal anti-inflammatory drugs (NSAIDs), statins, and uricosurics.<sup>16</sup> In clinical research, adefovir is used to assess renal OAT1 function, while sitagliptin is employed to evaluate renal

OAT3 activity.<sup>3,39</sup> Although selective inhibitors for individual OATs remain unavailable, several broad-spectrum inhibitors have been identified. Among these, probenecid is the most widely used. It binds to both OAT1 and OAT3 with similar affinity and effectively inhibits their transport function without itself being translocated.<sup>36</sup>

### **1.3 The clinical significance of GFR**

GFR is widely recognized as the most reliable indicator of renal function and has broad implications in clinical practice.<sup>40</sup> Changes in GFR are fundamental for diagnosing, staging, and monitoring chronic kidney disease (CKD), as well as predicting CKD-related complications and mortality.<sup>12</sup> Additionally, in acute care settings, GFR trends help evaluate the onset and progression of acute kidney injury (AKI).<sup>12</sup> This is particularly important in patients with fluctuating renal function, such as the critically ill, for whom timely assessment can guide clinical decision-making.<sup>41-44</sup> Furthermore, in kidney transplant recipients, GFR serves as a key marker of allograft function.<sup>12</sup> It guides immunosuppressive therapy adjustments, aids in early detection of rejection or nephrotoxicity, and helps evaluate the long-term risk of chronic allograft dysfunction.<sup>12,45</sup> Similarly, in dialysis patients, residual kidney function, as reflected by GFR, contributes significantly to overall dialysis adequacy and is associated with improved clinical outcomes.<sup>46,47</sup> Moreover, renal function is a key determinant of the clearance of renally excreted drugs, such as angiotensin-converting enzyme inhibitors, beta-lactam antibiotics, and antineoplastic agents, to name just a few.<sup>2</sup> As such, GFR plays a central role in determining safe and effective dosing regimens.<sup>12</sup> Inaccurate estimation of GFR can result in toxicity or therapeutic failure, particularly with drugs that are renally cleared or contraindicated at low GFR levels, such as metformin, alendronate, dabigatran etexilate, and certain chemotherapeutics and antibiotics.<sup>12,48</sup>

Beyond its essential role in clinical decision-making, GFR assessment is also relevant in evaluating the impact of interventions (e.g., drug treatments, dietary modifications) and conditions (e.g., genetic polymorphisms, diseases) on renal transporter activity in clinical studies.<sup>49</sup> Assessment of renal transporter activity is achieved through phenotyping procedures, which involve administering a selective transporter substrate and analyzing PK metrics that reflect transporter function<sup>39</sup> (see section “1.5.6 In vivo phenotyping for predicting renal TDDIs” for details). The choice of appropriate probe drugs and relevant PK metrics is essential for identifying factors that influence transporter activity.<sup>49</sup> However, many

currently used phenotyping approaches remain insufficiently validated, indicating the need for further methodological refinement.<sup>49</sup> In addition, certain PK metrics may be influenced by confounding factors unrelated to transporter activity, but these effects can often be quantified and adjusted for, thereby improving the accuracy and interpretability of transporter function assessments.<sup>49</sup>

CL<sub>R</sub> and, when applicable, net renal secretion are frequently used as metrics to assess renal transporter activity in clinical studies.<sup>39</sup> These parameters offer important advantages over broader metrics such as systemic clearance or area under the concentration-time curve (AUC), as they are not influenced by factors such as drug absorption, distribution, alternative elimination routes, or external variables affecting these processes.<sup>39</sup> However, as described above, renal elimination comprises multiple components. Since glomerular filtration is a passive process, estimating CL<sub>R</sub> or net renal secretion using an inaccurate GFR can introduce bias and lead to a misrepresentation of actual renal transporter activity.<sup>3,39</sup> This issue is particularly critical for compounds whose CL<sub>R</sub> values are close to the GFR, for instance digoxin, where small errors in GFR estimation may significantly distort conclusions about active transport. In contrast, this limitation is less pronounced for drugs primarily cleared by active tubular secretion, such as metformin.<sup>39</sup> Therefore, accurate measurement of GFR is essential for distinguishing the contribution of active secretion to CL<sub>R</sub> and for ensuring robust phenotyping of renal transporter function in clinical studies.<sup>3,39</sup>

#### **1.4 The clinical significance of transporter-mediated active renal secretion**

Renal tubular secretion is a common process involved in transporter-mediated DDIs (TDDIs). However, most tubular-based DDIs are of limited magnitude and rarely reach clinical significance.<sup>14</sup> Even when a drug primarily depends on renal elimination, defined as at least 25% of the absorbed dose being excreted unchanged in urine, complete inhibition of renal transporters typically leads to less than a twofold increase in systemic drug exposure (AUC).<sup>2,50</sup> An exception is probenecid, a potent *in vivo* inhibitor of OATs, which can increase concentrations of other drugs by up to fourfold.<sup>1</sup> However, such a significant increase occurs only in drugs whose clearance is heavily reliant on transporter-mediated secretion.<sup>1</sup>

Unlike CYP- or OATP-mediated hepatic DDIs, clinically significant renal DDIs are relatively rare, even in patients with impaired kidney function.<sup>1</sup> This is mainly because tubular secretion often

represents only one of several elimination pathways.<sup>1,14</sup> When secretion is inhibited, drugs may still be eliminated through glomerular filtration or other compensatory routes.<sup>1,14</sup> Additionally, many renally secreted drugs are transported by multiple proteins, so inhibition of a single transporter may have a limited effect on overall clearance.<sup>1,14</sup> Furthermore, perpetrator drugs often need to achieve unbound plasma concentrations far exceeding those typically encountered in clinical practice, making significant effects on renal elimination less probable.<sup>1,14</sup>

Despite their low frequency, renal DDIs still need to be evaluated, especially when new chemical entities (NCEs) are co-administered with renally cleared drugs that have narrow therapeutic windows, such as digoxin or methotrexate.<sup>1,50</sup> In vulnerable populations, including patients with kidney failure or critical illness, even small changes in renal clearance can increase the risk of adverse effects.<sup>1,50</sup> Additionally, renal DDIs can lead to drug accumulation in proximal tubule cells, increasing the potential for nephrotoxicity and kidney injury.<sup>1,50</sup>

To address these concerns, interested scientists, along with regulatory agencies such as the U.S. Food and Drug Administration (FDA) and the European Medicines Agency (EMA), have established guidelines for assessing the DDI potential of NMEs with key renal transporters. These include OCT2, OAT1, OAT3, MATE1, MATE2-K, and P-gp.<sup>18-20</sup> The next section examines several clinically relevant renal DDIs caused by transporter inhibition.

#### **1.4.1 Unwanted DDIs involving OCT2 and MATE1/2-K**

A major route for the renal elimination of small, hydrophilic, positively charged drugs is mediated by OCT2 and MATE1/2-K.<sup>16</sup> Inhibition of either transporter has been associated with clinically relevant DDIs involving cationic drugs.<sup>16</sup>

One well-characterized example is the interaction between cimetidine, a histamine H<sub>2</sub>-receptor antagonist, and metformin, a drug predominantly cleared unchanged by the kidneys via active tubular secretion through OCT2 and MATE1/2-K.<sup>16,27,51-55</sup> Co-administration of cimetidine reduces the CL<sub>R</sub> of metformin, resulting in increased systemic exposure.<sup>16,52,53</sup> When administered at 400 mg twice daily, cimetidine increases metformin's AUC by approximately 1.5-fold and decreases CL<sub>R</sub> by about 42.4%.<sup>16,54</sup>

In vitro data suggest that cimetidine is a stronger inhibitor of MATE1 and MATE2-K (inhibition constant  $[K_i] = 1.1\text{--}6.9\ \mu\text{mol/L}$ ) than of OCT2 ( $K_i = 95\text{--}146\ \mu\text{mol/L}$ ), implicating MATE inhibition as the primary mechanism underlying the observed DDI.<sup>16,34</sup> Notably, cimetidine is also a substrate of both OCT2 and MATE transporters, and its uptake via OCT2 at the basolateral membrane is believed to promote intracellular accumulation, thereby enhancing its inhibitory effect on apical MATE1/2-K.<sup>55,56</sup> This mechanistic pathway is further supported by pharmacogenetic evidence showing that OCT2 polymorphisms can modulate the magnitude of the interaction, as demonstrated in studies involving Chinese populations.<sup>54</sup> Therefore, this DDI is thought to be primarily driven by cimetidine's potent inhibition of apical MATE1/2-K, enhanced through OCT2-mediated intracellular accumulation.<sup>16</sup>

Another example is dolutegravir, an antiretroviral drug and potent in vitro inhibitor of OCT2 (half maximal inhibitory concentration  $[IC_{50}]$  approximately  $1.9\ \mu\text{M}$ ) and MATE1/2-K ( $IC_{50}$  ranging from  $6.3$  to  $25\ \mu\text{M}$ ).<sup>16,57</sup> When co-administered with metformin, dolutegravir increases metformin AUC by approximately 2.5-fold, which is a greater effect than that observed with cimetidine.<sup>16,57</sup> Despite its high in vitro potency, dolutegravir's unbound  $C_{\text{max}}$  suggests it is unlikely to inhibit MATE1/2-K in vivo, while it may act as a moderate in vivo inhibitor of OCT2.<sup>16,58,59</sup> The magnitude of the interaction exceeds expectations based solely on OCT2 inhibition, indicating that additional mechanisms may be involved,<sup>16</sup> although no changes in metformin absorption or distribution have been reported.<sup>16,27,57,60</sup> These observations underscore the importance of dose adjustment and therapeutic monitoring when OCT2/MATE substrates are used concurrently with inhibitors such as dolutegravir.<sup>16</sup>

#### **1.4.2 Exploiting OCT2 DDIs to protect from cisplatin nephrotoxicity**

Beyond DDIs, OCT2-mediated uptake and accumulation of drugs in renal proximal tubule cells can contribute to drug-induced nephrotoxicity, as seen in the case of cisplatin-induced kidney damage.<sup>16</sup>

Cisplatin, a widely used anticancer agent, is limited by nephrotoxicity, primarily affecting renal proximal tubules.<sup>61,62</sup> This toxicity is closely linked to its uptake via OCT2, with minimal efflux through MATE1 and MATE2-K, leading to cisplatin accumulation in renal cells.<sup>63-65</sup> Animal studies have shown that Oct1/2-deficient mice are protected from cisplatin-induced renal injury,<sup>66,67</sup> and a single-nucleotide polymorphism (SNP) at the 808G>T locus in the OCT2 gene



*SLC22A2* (rs316019) is associated with reduced nephrotoxicity, reinforcing the critical role of OCT2 in renal cisplatin handling.<sup>66</sup>

These findings support the use of OCT2 inhibitors to reduce nephrotoxicity.<sup>16</sup> For instance, high-dose cimetidine reduced kidney damage in humans without affecting cisplatin pharmacokinetics or efficacy.<sup>68</sup> However, many OCT inhibitors also block MATE transporters, whose activity facilitates cisplatin efflux.<sup>16</sup> As a result, dual inhibition may lead to increased intracellular cisplatin accumulation and worsen nephrotoxicity.<sup>16</sup> This concern is supported by studies showing that MATE inhibition, whether through genetic deletion in *Mate1* knockout mice or pharmacological inhibition using pyrimethamine or ondansetron, leads to elevated cisplatin retention and increased renal toxicity.<sup>69,70</sup>

Given the opposing roles of OCT2 and MATE transporters in cisplatin handling, caution is needed when considering their inhibitors as nephroprotective strategies.<sup>1,16</sup> Future research should prioritize the development of highly selective OCT2 inhibitors that minimize nephrotoxicity while preserving cisplatin's anticancer efficacy.<sup>1,16</sup>

#### **1.4.3 Desirable and unwanted DDIs involving OATs**

Clinically, DDIs involving the OAT-mediated renal proximal tubular transport system can be a double-edged sword, offering therapeutic benefits while also posing risks of adverse effects.

On the one hand, inhibiting renal anion secretion can enhance drug activity or reduce nephrotoxicity. A well-established example is probenecid, a prototypical inhibitor of renal anion secretion, which exhibits similar inhibitory potency for OAT1 and OAT3, with  $K_i$  ranging from 4 to 12  $\mu\text{mol/L}$ .<sup>16</sup> At standard oral doses (0.5–2 g), its unbound plasma concentrations range from 3 to 50  $\mu\text{M}$ ,<sup>71</sup> making both OAT1 and OAT3 likely sites of interaction with probenecid *in vivo*.<sup>16</sup> In addition to the well-known (historical) use of probenecid with penicillin to extend its therapeutic effect,<sup>16</sup> it is also co-administered with cephalosporins to enhance their efficacy or minimize renal accumulation and nephrotoxicity. Notably, probenecid has been shown to prolong the elimination half-life of cefazolin from 1.65 to 2.67 hours,<sup>72</sup> and to double the maximum plasma concentration of cefamandole.<sup>73</sup> Besides its use with antibiotics, probenecid is used with antiviral drugs to mitigate nephrotoxicity.<sup>50</sup> Renal cytotoxicity of adefovir and cidofovir is mediated by OAT1, which facilitates excessive drug accumulation in proximal tubular cells.<sup>74,75</sup> Given the evidence that OAT1 inhibitors reduce

cidofovir-induced nephrotoxicity, the respective summary of product characteristics (SmPCs) mandate coadministration of the OAT inhibitor probenecid in patients receiving cidofovir.<sup>76,77</sup>

On the other hand, while OAT inhibition can enhance therapeutic effects, it also impairs renal drug excretion, increasing the risk of toxic accumulation, particularly for drugs with narrow therapeutic indices.<sup>50</sup> Methotrexate, a cytotoxic antineoplastic agent, is primarily excreted unchanged (80%-90%) via glomerular filtration and tubular secretion within 24 hours of intravenous administration.<sup>78</sup> It is transported by multiple renal transporters, including OAT1 and OAT3.<sup>78</sup> However, co-administration with NSAIDs,<sup>79,80</sup> probenecid,<sup>81</sup> or sulfamethoxazole<sup>82-85</sup> has been shown to reduce methotrexate's renal clearance and elevate systemic exposure, thereby increasing the likelihood of toxicity.<sup>50</sup> As a result, the accumulation of methotrexate in the bloodstream can have severe consequences. In rheumatoid arthritis patients receiving low-dose oral methotrexate with probenecid, toxic buildup has been linked to life-threatening pancytopenia.<sup>86</sup> Furthermore, co-administration with trimethoprim-sulfamethoxazole has been associated with an increased risk of myelotoxicity in children undergoing treatment for acute lymphoblastic leukemia.<sup>87</sup> Supporting these concerns, a systematic review incorporating one observational study and 17 case reports has identified this interaction as a significant risk factor for cytopenia in rheumatoid arthritis patients,<sup>88</sup> further underscoring the importance of monitoring methotrexate clearance in polypharmacy settings.

Thus, given the potential for both beneficial and adverse interactions, drugs sharing a common renal tubular transport pathway (OA system) require careful evaluation in clinical practice.<sup>50</sup> Understanding the balance between enhanced therapeutic effects and increased toxicity risk is critical for optimizing treatment outcomes.<sup>50</sup>

#### **1.4.4 DDIs involving P-gp**

In addition to the inhibition of renal uptake transporters, renal DDIs may also result from the inhibition of efflux transporters expressed on the apical membrane of proximal tubule cells.<sup>1</sup> Although in vivo evidence remains limited, apical transporters such as P-gp, MRP2/4, and BCRP may contribute to renal drug clearance and DDIs.<sup>1</sup> Among these, P-gp-mediated DDIs are the most extensively studied, with the interaction between P-gp and digoxin serving as a well-established example.<sup>1,89,90</sup> Digoxin, a cardiac glycoside widely used in the management

of congestive heart failure and atrial fibrillation, is a recognized substrate of P-gp.<sup>19,91</sup> Given its narrow therapeutic window, even small changes in serum concentration can lead to toxicity,<sup>92</sup> making close monitoring essential, especially when it is co-administered with drugs that may share P-gp-related disposition pathways, which may be the key site for drug interactions with digoxin.<sup>1</sup>

Quinidine, which functions as both a substrate and a potent inhibitor of P-gp,<sup>93</sup> has been shown to significantly reduce digoxin clearance by up to 64%,<sup>94</sup> thereby increasing the risk of digoxin toxicity. This inhibitory effect has been demonstrated in both preclinical and clinical studies, including evidence of elevated digoxin exposure in wild-type mice but not in P-gp knockout models.<sup>95</sup> Other P-gp inhibitors such as verapamil,<sup>96</sup> clarithromycin,<sup>97</sup> cyclosporin A,<sup>98</sup> and itraconazole<sup>99</sup> have also been reported to reduce the renal clearance of digoxin.<sup>1,16</sup>

Despite these observations, the clinical relevance of P-gp-mediated DDIs is not always consistent.<sup>1</sup> For example, although ritonavir is a known P-gp inhibitor in vitro, its effects in vivo have been variable.<sup>1</sup> One study reported that ritonavir increased digoxin's AUC by 86% and reduced its renal clearance by 35%.<sup>100</sup> Nevertheless, another study has shown no significant impact of ritonavir on digoxin CL<sub>R</sub>.<sup>101</sup> These inconsistencies underscore the complexity of predicting renal P-gp-mediated DDIs and suggest that additional studies are needed to clarify its role in tubular drug secretion.<sup>1</sup> However, monitoring PK changes of P-gp substrates during co-administration with P-gp inhibitors is recommended.<sup>1,16</sup>

#### **1.4.5 Sensitive populations**

Although renal TDDIs are typically of low magnitude, their clinical significance may be increased in specific populations.<sup>50</sup> Individuals with impaired renal function, such as elderly patients or those with diabetes, may be more susceptible to pronounced DDIs.<sup>50</sup> This is exemplified by the shifting balance between glomerular filtration and active tubular secretion in creatinine elimination.<sup>50,102</sup> In individuals with normal renal function, filtration is the primary clearance mechanism, with only 10% to 40% of creatinine eliminated via tubular secretion.<sup>50,102</sup> In contrast, patients with glomerular disease may rely equally on secretion for creatinine clearance.<sup>50,102</sup> A similar compensatory increase in secretion could occur for other drugs and metabolites, warranting further investigation.<sup>50</sup>

CKD, including diabetic nephropathy and glomerulonephritis, not only reduces glomerular filtration but also alters renal transporter activity.<sup>50,103</sup> A decline in GFR is often accompanied by changes in the expression and function of renal transporters.<sup>50,103</sup> In kidney-related diseases, the function of OAT1 and OAT3 is consistently impaired, as evidenced by reduced mRNA expression, protein levels, and transporter activity.<sup>50,103</sup> These transporters are essential for the uptake of endogenous and exogenous substances into renal tubular epithelial cells.<sup>50</sup> Their reduced activity may present both protective and detrimental consequences.<sup>103</sup> On one hand, it limits the entry of potentially nephrotoxic compounds such as uremic toxins, including indoxyl sulfate (IS), 3-carboxy-4-methyl-5-propyl-2-furanpropionate (CMPF), indoleacetate (IA), and hippurate (HA), into renal tissue, potentially reducing further kidney damage.<sup>104</sup> On the other hand, decreased transporter activity impairs drug excretion, leading to elevated plasma drug concentrations and an increased risk of toxicity.<sup>103</sup> Additionally, accumulated uremic toxins can competitively inhibit OATs, further disrupting the CL<sub>R</sub> of both drugs and endogenous organic acids.<sup>104,105</sup> In patients with severe renal impairment, pathophysiological changes lead to a decline in OAT1 and OAT3 expression, which further contributes to drug accumulation.<sup>103</sup> A clinically relevant example involves morinidazole metabolites, which are OAT1/3 substrates.<sup>103</sup> Following a 500 mg intravenous dose, the AUC values for these metabolites were 15.1- to 20.4-fold higher in patients with severe renal impairment compared to healthy individuals.<sup>103,106,107</sup>

Although kidney diseases directly affect renal transporter function and drug elimination, non-renal conditions may also significantly alter these transporters, which makes individualized dose adjustments necessary.<sup>103</sup> Emerging evidence suggests that metabolic disorders, such as hyperuricemia and diabetes, can influence the expression of key renal transporters (e.g., OAT1/3, OCT2, BCRP, and MRP2/4).<sup>103</sup> These changes may affect the CL<sub>R</sub> of various drugs such as cephalexin,<sup>108</sup> metformin,<sup>109</sup> and sitagliptin.<sup>110</sup> Therefore, careful dose adjustments based on altered transporter activity are essential to maintain drug safety and efficacy in patients with kidney-related or systemic diseases that impact renal drug transport.<sup>103</sup>

Age-related changes in renal function, including reduced blood flow, declining GFR, impaired tubular secretion, and increased tubular frailty, also significantly affect drug therapy.<sup>111,112</sup> Elderly individuals aged 65 years and older account for nearly 30 percent of commonly prescribed medications and face a higher risk of adverse drug reactions (ADRs) compared to

the general population.<sup>111</sup> Despite this, the underlying mechanisms contributing to these risks remain poorly understood, partly due to limited clinical research.<sup>50,111</sup> It is unclear to what extent factors such as reduced renal clearance, drug accumulation, increased DDIs, and polypharmacy contribute to the observed outcomes.<sup>50,111</sup> A recent study provides a detailed analysis of the ontogeny of renal drug transporters by assessing mRNA expression, protein abundance, and localization in postmortem kidney tissues from preterm newborns to adults.<sup>113</sup> The study reveals that most renal transporters, including P-gp, URAT1, OAT1/3, and OCT2, exhibit a significant increase in both mRNA expression and protein levels during early childhood. In contrast, others, such as MATE1, glucose transporter 2 (GLUT2), and MRP2/4, remain relatively stable from birth.<sup>113</sup> These findings suggest the crucial role of renal transporter maturation in drug clearance. Medications that depend on OAT1, OAT3, and OCT2 for elimination may be cleared more slowly in neonates and infants due to immature transporter expression, underscoring the need for age-specific drug dosing adjustments in these vulnerable populations.<sup>113</sup>

Beyond age and diseases, other factors, including sex, pregnancy, and ethnic differences, also influence renal drug transporter activity.<sup>103,114</sup> However, these factors are not explored in detail in this thesis. Gaining deeper insights into their impact will enhance our ability to advance personalized medicine and reduce the likelihood of ADRs.

## **1.5 Methods and challenges in the quantification of renal PK processes**

### **1.5.1 Measured GFR to validate estimated GFR**

Estimated GFR (eGFR) based on endogenous filtration markers is the most commonly employed method for assessing GFR in clinical practice and is generally adequate for guiding clinical decisions.<sup>115</sup> However, these estimates may be unreliable in non-steady-state conditions, in individuals whose non-GFR determinants significantly differ from those in the populations used to develop estimation equations,<sup>40</sup> and in clinical transporter phenotyping studies where precise GFR measurement is critical for assessing renal transporter function.<sup>3</sup> In such cases, directly measured GFR (mGFR) using exogenous markers (e.g., iohexol) provide an essential means of confirmation.<sup>40,116</sup> Since conventional mGFR methods are often impractical for routine use,<sup>117</sup> this thesis aims to improve iohexol-based GFR measurement by evaluating practical correction formulas<sup>4</sup> and lower dosing strategies to enhance feasibility and accessibility.<sup>5</sup>

### 1.5.2 Estimated GFR using creatinine and/or cystatin C

The eGFR is routinely reported by clinical laboratories and is calculated based on the blood concentration of an endogenous filtration marker, such as creatinine or cystatin C, supplemented by clinical and demographic factors.<sup>12,40</sup> These additional variables help account for non-GFR determinants such as differences in marker generation, tubular handling (secretion or reabsorption), and extrarenal elimination.<sup>12</sup> By incorporating these factors, eGFR adjusts for individual variability unrelated to GFR, providing more accurate estimates than marker concentrations alone.<sup>12</sup> Furthermore, expressing GFR on a standardized scale enhances its clinical applicability.<sup>12</sup> As a result, eGFR is widely considered a reliable and adequate measure for guiding most clinical decisions.<sup>40</sup>

Creatinine-based eGFR (eGFR<sub>cr</sub>) is widely used due to its affordability, simplicity, and broad availability.<sup>12,118</sup> Creatinine is produced endogenously via muscle metabolism and can be influenced by dietary intake.<sup>12</sup> While it is freely filtered by the glomerulus, creatinine also undergoes tubular secretion, facilitated by transporters such as OCT2, MATE1/2-K, and OAT2, and has extrarenal clearance pathways.<sup>119,120</sup> These non-GFR determinants introduce variability that may affect eGFR<sub>cr</sub> accuracy, particularly in individuals with abnormal body composition, nonsteady-state conditions, or those exposed to TDDIs.<sup>12,121</sup> The 2009 Chronic Kidney Disease Epidemiology Collaboration (CKD-EPI) creatinine equation (CKD-EPI<sub>cr2009</sub>)<sup>122</sup> is recommended by Kidney Disease: Improving Global Outcomes (KDIGO) clinical practice guideline for estimating eGFR<sub>cr</sub> in adults due to its superior performance over earlier equations like Modification of Diet in Renal Disease (MDRD),<sup>123</sup> particularly at higher GFR levels (GFR ≥ 60 mL/min/1.73 m<sup>2</sup>).<sup>12,118,122,124</sup>

Cystatin C-based eGFR (eGFR<sub>cys</sub>) offers an alternative that is less influenced by muscle mass and tubular secretion, potentially improving accuracy in populations where creatinine-based estimates are unreliable.<sup>12,121</sup> Cystatin C is freely filtered and catabolized in the tubules, but not excreted in urine,<sup>12,121</sup> and may be affected by factors such as inflammation, smoking, and thyroid function.<sup>12,121,125</sup> Although its higher cost limits routine use,<sup>121</sup> cystatin C can enhance GFR estimation when combined with creatinine. The 2012 CKD-EPI combined equation (CKD-EPI<sub>cr-cys2012</sub>)<sup>126</sup> demonstrates improved accuracy over either biomarker alone<sup>12,121,126,127</sup> and is recommended when greater precision is required, such as in transplant evaluations or critical

drug dosing.<sup>115,128</sup> However, because it still incorporates creatinine, it does not serve as an entirely independent confirmatory test.<sup>12,121</sup>

Despite ongoing development of newer eGFR equations, such as those that remove race-based adjustments (e.g., 2021 CKD-EPI creatinine equation [CKD-EPI<sub>cr2021</sub>])<sup>129</sup> or are tailored for specific populations (e.g., the European Kidney Function Consortium [EKFC] equation,<sup>130</sup> the Revised Lund-Malmö [RLM] equation,<sup>131</sup> and the Berlin Initiative Study [BIS] equation<sup>132</sup>), no estimation method has demonstrated sufficient accuracy across all clinical contexts.<sup>12,127,130</sup> Therefore, in cases where an accurate assessment of kidney function is essential, mGFR using exogenous markers such as iohexol remains necessary.<sup>127</sup>

### **1.5.3 Measured GFR using iohexol**

Plasma clearance of iohexol following a single dose, typically around 3,235 mg, has become a key tool to measure GFR, primarily due to its favorable PK properties.<sup>133</sup> Unlike endogenous filtration markers, iohexol-based assessments are not affected by variations in body composition or illness, making it a good candidate for routine clinical use.<sup>5,115</sup> Moreover, iohexol is particularly in clinical scenarios that demand precise GFR assessment, such as in patients with unstable kidney function,<sup>41,134</sup> those suffering from severe conditions like HIV, heart failure, or liver failure,<sup>12,40,135</sup> and in clinical trials where GFR is essential in evaluating drug pharmacokinetics.<sup>3,116,136</sup>

Although iodinated contrast agents such as iohexol are generally well tolerated, ADRs occur in up to 3% of cases and may occasionally be clinically significant.<sup>5,137</sup> Acute reactions include allergic-like symptoms such as hives, itching, difficulty swallowing, shortness of breath, and, in severe instances, anaphylaxis.<sup>137,138</sup> Physiologic reactions, including pain, nausea, vomiting, arrhythmias, and visual disturbances, are also reported.<sup>137,138</sup> The risk of these reactions, particularly physiological ones, tends to increase with higher doses.<sup>137,138</sup> The most serious ADR associated with contrast media is contrast-induced acute kidney injury (CI-AKI).<sup>5,139</sup> While its incidence is relatively low at 1% to 2% in individuals with normal kidney function, it may rise to as high as 25% in patients with CKD or other risk factors such as comorbidities, advanced age, or nephrotoxic drug exposure.<sup>5,139</sup> Notably, the risk of CI-AKI increases with the volume of contrast media administered, doubling with every additional 20 mL in patients with CKD.<sup>5,140</sup> “Given the dose dependency of ADRs, it is desirable to validate and use iohexol at

the lowest possible dose for GFR assessment, particularly in patients with impaired renal function or those requiring repeated GFR monitoring.”<sup>5</sup>

“While iohexol elimination in humans is considered to be mediated exclusively by glomerular filtration, there is limited evidence suggesting that iohexol may interact with membrane transporters.<sup>3,141-143</sup> Minor inconsistencies have been observed when comparing iohexol clearance to that of inulin, which is regarded as an ideal GFR marker,<sup>3</sup> though inulin is no longer preferred due to practical limitations.<sup>144</sup> Additionally, beyond glomerular filtration iohexol might be reabsorbed through a saturable mechanism in rats.<sup>141</sup> Moreover, iohexol downregulated the expression of OCT2 in both rat kidneys and HK-2 cells.<sup>142</sup> It also exerted a mild inhibitory effect on P-glycoprotein in human cancer cell lines.<sup>143</sup> The involvement of membrane transporters in iohexol pharmacokinetics may lead to nonlinearity in its pharmacokinetics, particularly at low concentrations. Similar to creatinine, this can make iohexol susceptible to TDDIs when coadministered with drugs that affect transporter activity.<sup>119</sup> Both nonlinearity and TDDIs with iohexol as a victim could cause discrepancies between iohexol clearance and GFR.”<sup>5</sup>

Additionally, iohexol has the potential to influence the pharmacokinetics of co-administered drugs, potentially altering their therapeutic effects.<sup>5</sup> Furthermore, its interactions with transporters may also affect the pharmacokinetics of probe drugs used in transporter phenotyping cocktail studies (see Section 1.5.6 “In vivo phenotyping for predicting renal TDDIs” for details).<sup>5,39</sup> Before incorporating iohexol into future phenotyping approaches, it is essential to ensure that it does not lead to clinically significant DDIs.<sup>5</sup> Lowering its standard dose may help reduce the risk of such interactions, minimize adverse effects,<sup>138,140</sup> and decrease overall drug consumption.<sup>5</sup> However, PK data on low-dose iohexol remain limited,<sup>5,41,42</sup> highlighting the need for further research to assess its safety and efficacy.<sup>5</sup>

#### **1.5.4 In vitro assessment of renal TDDIs**

In the early phases of drug research, in vitro models serve as essential preclinical tools for determining whether a drug candidate functions as a transporter substrate or inhibitor.<sup>145</sup> These models offer mechanistic insights into TDDIs and help predict their in vivo relevance.<sup>18,19,145</sup> Additionally, they provide critical kinetic data, including the Michaelis-



Menten constant ( $K_m$ ), maximum reaction velocity ( $V_{max}$ ) for substrates, as well as  $K_i$  and  $IC_{50}$  for inhibitors, enabling a comprehensive evaluation of potential DDIs.<sup>18,19,145</sup>

A range of in vitro transporter assays are available to assess the risk of TDDIs in investigational drugs.<sup>146</sup> This thesis focuses on in vitro methodologies for studying renal TDDIs, particularly transfected cell-based and membrane vesicle-based assays, both of which are endorsed by regulatory authorities.<sup>19</sup>

#### **1.5.4.1 In vitro system**

##### **1.5.4.1.1 Transfected cell-based assays**

In vitro transfected cell-based uptake assays are widely used to study whether an investigational drug is a substrate or inhibitor of SLC transporters such as OCTs, OATs, OATPs, and MATEs. These assays can also be utilized to study efflux transporters, such as P-gp and BCRP.<sup>18,19</sup>

Several mammalian host cell lines are commonly used for constructing transfected cells, including human embryonic kidney (HEK293) cells, Chinese hamster ovary (CHO) cells, porcine kidney epithelial cells (LLC-PK1), and Madin-Darby canine kidney (MDCK) cells.<sup>146</sup> Among these, HEK293 and CHO cells are preferred for expressing uptake transporters due to their low endogenous transporter activity and ease of maintenance. In contrast, MDCK and LLC-PK1 cells are often used for efflux transporter studies, as they form tight, polarized monolayers suitable for such investigations.<sup>147</sup>

To construct recombinant cell lines for in vitro studies in this thesis, two transfection methods were employed to introduce transporter cDNA into host cells. The first method utilized the pEBTetD vector, an Epstein–Barr virus (EBV)-derived episomal vector,<sup>148</sup> which enables stable and efficient propagation in human cell lines without genomic integration. This vector also features a doxycycline-inducible expression system,<sup>148</sup> allowing precise control of transporter expression levels. The inducible system facilitates direct comparisons between cells with and without transporter expression, improving the reliability of functional analyses.<sup>148</sup> The second method involved the Flp-In system, which enables site-specific genomic integration of the transporter cDNA via Flp recombinase-mediated recombination.<sup>147</sup> This approach enhances stable transfection efficiency by ensuring cDNA insertion at a fixed genomic locus, thereby

reducing variability in expression levels compared to the episomal pEBTetD system. The detailed construction processes for these plasmids have been described previously.<sup>147,149</sup>

#### **1.5.4.1.2 Inside-out membrane vesicles**

Inside-out membrane vesicles are widely used in vitro systems for evaluating whether an investigational drug is a substrate or inhibitor of efflux transporters, such as ABC transporters P-gp or BCRP.<sup>18,19,146</sup> These vesicles, derived from cells transfected with specific transporter genes, offer several advantages, including simplicity, reduced variability, high assay throughput, and a direct means of estimating in vitro kinetic parameters.<sup>146,147</sup>

These vesicles are artificially created by disrupting the plasma membrane of transfected cells in a way that flips the orientation of the transport proteins, exposing their ATP-binding sites to the external environment.<sup>147</sup> This configuration allows for the direct assessment of ATP-dependent drug transport activity, making it easier to determine whether a compound acts as a substrate or inhibitor of the transporter.<sup>147</sup> When ATP is added, the transporter actively moves drugs into the vesicle interior, allowing for precise quantification of transport efficiency.<sup>147</sup> However, this system has inherent limitations, particularly in identifying drugs that have high passive permeability or significant nonspecific binding. Such properties can interfere with the recognition of true transporter substrates, leading to potential misinterpretation of results.<sup>18,19,146</sup>

#### **1.5.4.2 Substrate assessments**

To determine whether a drug is a substrate of renal uptake transporters, regulatory agencies recommend conducting in vitro studies.<sup>18-20</sup> These studies assess transporters such as OAT1/3, OCT2, and MATE1/2-K when active renal secretion contributes to  $\geq 25\%$  of the drug's systemic clearance.<sup>18,19</sup> Similarly, P-gp evaluation is necessary when active renal secretion plays a major role in drug elimination.<sup>18,19</sup> Beyond renal transporters, assessing P-gp and BCRP-mediated transport is valuable for understanding a drug's brain penetration, oral bioavailability, and biliary excretion.<sup>18,19</sup> For drugs primarily eliminated through hepatic metabolism or biliary excretion ( $\geq 25\%$  of total clearance), or those targeting the liver pharmacologically, evaluating their interaction with OATP1B1 and OATP1B3 transporters is recommended.<sup>18,19</sup> These assessments help determine whether hepatic uptake influences drug disposition, potentially affecting efficacy and safety.

In in vitro transporter studies, a drug is considered a potential substrate if it exhibits at least a twofold higher uptake in transporter-expressing cells compared to control cells, and if this uptake is inhibited by 50% or more in the presence of a known transporter inhibitor. For vesicle-based assays, alternative evaluation approaches may be applied, guided by internal data and prior experience.<sup>18,19</sup>

When a drug meets the criteria for transporter substrate identification, further kinetic characterization is necessary. This involves a two-step process: First, time-dependent uptake is evaluated to establish the period during which uptake remains linear before reaching saturation. Second, kinetic parameters such as  $K_m$  and  $V_{max}$  are determined by measuring uptake rates across a range of drug concentrations in both transporter-expressing and control cells. This approach ensures a comprehensive understanding of the drug's interaction with transporters, which is critical for predicting its pharmacokinetic behaviour.<sup>146,147</sup>

#### **1.5.4.3 Inhibition Assays**

To evaluate the potential of the test drug to inhibit specific transporters and contribute to TDDIs in vivo, inhibition assays were conducted. These experiments assessed intracellular accumulation of a standard substrate in cell-based systems or intravesicular accumulation via ATP-dependent uptake in inside-out membrane vesicles. Measurements were taken with and without the test drug.

The initial assessment of transporter inhibition typically involves testing the drug at its highest clinically relevant concentrations. According to the latest established guidelines, recommended concentrations include 10 times the unbound maximum plasma concentration ( $C_{max,u}$ ) for OAT1/3 and OCT2, 50 times  $C_{max,u}$  for MATEs, 10 times the liver inlet  $C_{max,u}$  for OATP1B1/3, and 0.1 times the highest therapeutic dose per 250 mL for orally administered P-gp or BCRP inhibitors.<sup>18,19</sup> For parenterally administered drugs or inhibitory metabolites formed post-absorption, the recommended concentration is 50 times  $C_{max,u}$ . Since transporters are widely expressed across various tissues, such as P-gp, which is localized in the intestine, liver, and kidney, the highest relevant concentration was selected to ensure a robust in vitro evaluation of potential impact of the drug on TDDIs. Drug concentrations should remain within solubility limits while avoiding cytotoxic effects.<sup>18,19</sup> If inhibitory activity is detected at the threshold concentration, further testing at multiple concentrations is recommended to determine  $IC_{50}$  or  $K_i$  values.<sup>147</sup>

#### **1.5.4.4 Strengths and challenges of in vitro DDI studies**

In vitro DDI studies are widely used due to their controlled experimental conditions, cost-effectiveness, and ability to provide rapid preliminary assessments of potential interactions before clinical trials.<sup>147</sup> However, in vitro models cannot fully replicate the coordinated action of multiple transporters in epithelial cells, limiting their predictive accuracy.<sup>147</sup> Although systems using multiple-transfected cells offer improved representation, they still do not reflect the complexity of drug transport across intact organs, such as renal tubular epithelium.<sup>145</sup> In addition, they also fail to account for drug metabolites, leading to potential underestimation of interactions.<sup>14,145</sup> Variability in experimental conditions and challenges in scaling data to human pharmacokinetics further restrict their reliability.<sup>147</sup> Although in vitro transporter interaction screening is not required for all NCEs in preclinical development, recognizing the potential for TDDIs remains essential for both marketed drugs and compounds undergoing clinical evaluation.<sup>1</sup>

#### **1.5.5 Probes and biomarkers for renal TDDI assessment**

##### **1.5.5.1 Renal OCT2 and MATE1/2-K activity**

###### **1.5.5.1.1 Probe drug**

Metformin is a widely used probe drug for studying the inhibition of renal uptake and efflux transporters, specifically OCT2 and MATE1/2-K.<sup>18</sup> As an oral antidiabetic agent, metformin exhibits an absolute oral bioavailability of approximately 50–60%.<sup>27,150</sup> Although commonly employed in TDDIs studies, its absorption and distribution processes are complex and not yet fully elucidated.<sup>151</sup>

In the intestine, metformin is taken up from the lumen into enterocytes via the plasma membrane monoamine transporter (PMAT) and subsequently transported into the bloodstream by basolateral OCT1.<sup>27,39</sup> Hepatic uptake is primarily mediated by OCT1 and OCT3 on the sinusoidal membrane, with MATE1 facilitating biliary excretion.<sup>27,39</sup> Renal clearance, accounting for approximately 76% of total elimination, involves active tubular secretion via OCT2 and MATE1/2-K.<sup>32,109,151-153</sup> Although functionally relevant genetic polymorphisms in OCT2 and MATE1/2-K have not been strongly linked to altered metformin pharmacokinetics,<sup>154</sup> clinical studies using transporter inhibitors such as dolutegravir (OCT inhibitor) and pyrimethamine (MATE inhibitor) demonstrate significantly increased

metformin exposure.<sup>51,155</sup> These findings underscore the functional relevance of OCT2 and MATE1/2-K in metformin elimination and support the use of metformin plasma and urine levels as robust markers for renal transporter activity.<sup>3</sup>

Although metformin is not a highly selective probe for OCT2 or MATE1/2-K, it remains a valuable clinical tool for assessing TDDIs, particularly given the lack of more specific alternatives.<sup>3,39</sup> Its use is supported by regulatory agencies, which acknowledge metformin as an appropriate probe substrate to evaluate the clinical relevance of in vitro inhibition of OCT2 and/or MATEs.<sup>19</sup> The International Transporter Consortium (ITC) has also provided recommendations on study designs to ensure suitable metformin dosing during co-administration scenarios.<sup>156</sup> Nevertheless, the impact of inhibiting a single transporter on metformin disposition is often limited, largely due to the overlapping substrate specificities among renal transporters.<sup>151</sup> Consequently, observed renal DDIs with metformin are generally modest in magnitude.<sup>151</sup>

#### **1.5.5.1.2 Endogenous biomarkers**

Creatinine, a breakdown product of muscle creatine, is widely used as a biomarker of renal function,<sup>157</sup> but it may also serve as an endogenous probe for evaluating renal transporter activity in early clinical studies.<sup>158</sup> Approximately 10–40% of its total renal excretion is attributable to net tubular secretion, after accounting for reabsorption, whereas no metabolism of creatinine has been described previously.<sup>159</sup> Elevated serum creatinine and decreased renal clearance of creatinine may indicate temporary inhibition of active renal transporters, such as OCT2, OAT2, and MATE1/2-K, without any change in GFR.<sup>160,161</sup> However, interpreting changes in creatinine is complicated, as its levels are affected by multiple factors such as age, sex, body weight, muscle mass, and diet.<sup>160-162</sup> Moreover, elevated serum creatinine can also indicate impaired renal function, making it essential to differentiate between transporter inhibition and true nephrotoxicity.<sup>160-162</sup> Although serum creatinine often increases with OCT2/MATE inhibition, it lacks sensitivity and specificity for detecting TDDIs.<sup>160-162</sup>

N<sup>1</sup>-methylnicotinamide (NMN) and N<sup>1</sup>-methyladenosine (m<sup>1</sup>A) have emerged as promising endogenous biomarkers for assessing the activity of renal transporters OCT2 and MATE1/2-K.<sup>162</sup> NMN, a metabolite formed during tryptophan and vitamin B3 metabolism, is generated by aldehyde oxidase and cleared renally through both passive glomerular filtration and active

tubular secretion via OCT2 and MATEs.<sup>159,163,164</sup> Its  $CL_R$  is concentration-dependent, likely due to saturable reabsorption in addition to secretion.<sup>159,165</sup> NMN has been confirmed as a substrate of OCT2 and MATE1/2-K, but not of organic anion transporters (OAT1, OAT2, or OAT3) in vitro.<sup>151,161</sup>  $m^1A$ , an endogenous purine nucleoside derived from transfer RNA, is also secreted by the kidneys and has been identified as a substrate of OCT2 and MATE2-K, though not of MATE1 in vitro.<sup>151,161</sup> While multiple clinical studies have supported the utility of NMN as a biomarker, showing strong and consistent correlations with metformin renal clearance across various transporter inhibition scenarios ( $R^2 = 0.53\text{--}0.87$ ),<sup>161</sup> including co-administration with trimethoprim,<sup>164</sup> pyrimethamine,<sup>166</sup> cimetidine,<sup>167</sup> and investigational inhibitors such as aboricitinib<sup>168</sup> and bevurogant,<sup>169</sup> clinical evidence for  $m^1A$  remains limited.<sup>161</sup> In one comparative clinical study using pyrimethamine,  $m^1A$  demonstrated a stronger correlation with metformin  $CL_R$  ( $R^2 = 0.65$ ) than NMN ( $R^2 = 0.53$ ) and creatinine ( $R^2 = 0.11$ ), suggesting high sensitivity to transporter inhibition.<sup>166</sup> However, the observed increase in the AUC of NMN upon metformin administration in this study was likely due to metabolic modulation unrelated to transporter inhibition, which may explain its slightly lower correlation with metformin  $CL_R$  compared to  $m^1A$ .<sup>161,166,170</sup>

Taken together, these findings suggest that NMN is currently the more clinically validated and reliable biomarker for OCT2 and MATE1/2-K activity, while  $m^1A$  exhibits strong potential and may outperform NMN in specific contexts. Further clinical studies are warranted to confirm the broader applicability of  $m^1A$ .

### **1.5.5.2 Renal OAT1/3 activity**

#### **1.5.5.2.1 Probe drug for OAT1**

Adefovir dipivoxil, the oral prodrug of adefovir, is used clinically to treat chronic hepatitis B.<sup>171</sup> Once administered, it is converted to active adefovir by hepatic esterases, achieving an oral bioavailability of approximately 59%.<sup>171</sup> Adefovir is a highly selective substrate for OAT1 over OAT3 in vitro<sup>172,173</sup> and has been recommended by regulatory guidelines as an in vivo probe to assess the inhibitory potential of NMEs on OAT1.<sup>19</sup>

Following administration, about 45% of the dose is excreted renally, with total  $CL_R$  exceeding GFR by two to three times, indicating substantial active tubular secretion.<sup>171,174</sup> Around 60% of this secretion is mediated by OAT1 at the basolateral membrane of proximal tubule

cells.<sup>171,174</sup> Efflux from renal cells likely involves apical transporters MATE1, MATE2-K, and to a lesser extent, MRP4.<sup>3,175</sup> Although adefovir is a substrate of MRP4, studies in *Mrp4*<sup>-/-</sup> mice suggest that MRP4 has a limited impact on systemic exposure.<sup>175</sup> Despite the absence of clinically significant OAT1 polymorphisms,<sup>154</sup> co-administration of adefovir dipivoxil with probenecid, a potent OAT1 inhibitor, reduces renal clearance of adefovir by 45% and increases AUC from time zero to 8 hours post-administration ( $AUC_{0-8h}$ ) by approximately 80%,<sup>172</sup> highlighting the key role of OAT1 in its elimination. Moreover, clinical DDI studies show that single doses of adefovir dipivoxil do not cause significant interactions with substrates of other transporters, such as metformin, digoxin, sitagliptin, or pitavastatin.<sup>39</sup> These findings support the use of adefovir as a sensitive and selective *in vivo* probe for assessing OAT1 activity.

#### **1.5.5.2.2 Probe drug for OAT3**

Sitagliptin is a selective and reversible inhibitor of dipeptidyl peptidase-4 that has emerged as a potential phenotyping probe for human OAT3 activity.<sup>3,39</sup> *In vitro* data demonstrate marked selectivity for OAT3 over OAT1, making sitagliptin a promising candidate for transporter phenotyping.<sup>110,173</sup> Following oral administration, sitagliptin exhibits high bioavailability (approximately 87%), with around 35% of the absorbed dose undergoing metabolism, primarily via CYP2C8 and CYP3A4.<sup>176</sup> Approximately 79% of the dose is excreted unchanged in urine through renal pathways largely mediated by OAT3.<sup>3</sup>

While sitagliptin exhibits some *in vitro* inhibition of OCT1, OCT2, and MATE2-K, these effects are considered unlikely to be clinically relevant due to low  $C_{max,u}$  to  $K_i$  ratios (0.009, 0.03, and 0.001, respectively).<sup>149</sup> This is further supported by the lack of significant DDIs observed in single-dose studies involving known substrates of OCT1, OCT2, MATE2-K, and other relevant transporters, such as metformin, digoxin, adefovir, and pitavastatin.<sup>39</sup> Sitagliptin is also a substrate of OATP4C1 and P-gp,<sup>3</sup> but its renal elimination is not significantly altered by coadministration with cyclosporine, a potent P-gp inhibitor.<sup>3,177</sup> These findings collectively indicate that the disposition of sitagliptin is primarily governed by OAT3, with minimal influence from other transporters. Although genetic polymorphisms in OAT3 have shown limited impact on sitagliptin clearance,<sup>154</sup> coadministration with gemfibrozil, a known OAT3 inhibitor, results in a significant increase in the  $C_{max}$  and AUC of sitagliptin, along with about

a 35% reduction in clearance.<sup>178</sup> Altogether, these PK features support the suitability of sitagliptin as an *in vivo* probe for OAT3 activity.

Currently, benzylpenicillin (penicillin G) is recommended by the FDA as a probe substrate for OAT3.<sup>19</sup> However, its suitability is limited by uncertainties regarding the contribution of its degradation products following oral administration.<sup>3</sup> Additionally, the observed increase in the CL<sub>R</sub> of sitagliptin in the presence of p-aminohippurate suggests the involvement of other transporters in the elimination of benzylpenicillin, raising concerns about its selectivity for OAT3.<sup>172</sup> Furosemide, a dual substrate of OAT1 and OAT3, has been proposed as a potential alternative for assessing both transporters simultaneously.<sup>19</sup> However, due to its lack of transporter specificity, it falls outside the scope of this thesis and is not discussed further.

#### **1.5.5.2.3 Endogenous biomarkers for OAT1 and OAT3**

Among the investigated endogenous biomarkers, 4-pyridoxic acid (PDA) has emerged as the most promising for assessing OAT1 and OAT3 activity, owing to its high sensitivity and reproducibility.<sup>158</sup> *In vitro* studies using transporter-overexpressing cell systems confirmed that PDA is a substrate for human OAT1, OAT3, and OAT4, but not for OCT2, MATE1/2-K, OATP1B1/1B3, or the sodium taurocholate cotransporting polypeptide.<sup>179</sup> Clinical DDI studies further support the utility of PDA.<sup>180,181</sup> Following administration of the OAT inhibitor probenecid, PDA plasma exposure increased approximately 3.2- to 3.7-fold, accompanied by a reduction in CL<sub>R</sub>.<sup>180,181</sup> Notably, the increase in PDA exposure closely paralleled the increase in the AUC of furosemide, a recognized OAT1/3 probe, reinforcing the value of PDA as a translational biomarker for evaluating OAT1/3-mediated DDIs.<sup>161,182</sup>

Other endogenous candidates include homovanillic acid (HVA), taurine, glycochenodeoxycholate-3-sulfate (GCDCA-S), 6 $\beta$ -hydroxycortisol, and kynurenic acid.<sup>161</sup> Taurine shows selectivity for OAT1, while GCDCA-S and 6 $\beta$ -hydroxycortisol are predominantly transported by OAT3.<sup>161,183,184</sup> GCDCA-S, despite demonstrating high sensitivity in urine-based assessments, has limited specificity due to additional transport via hepatic OATP1B transporters.<sup>161,185</sup> HVA and kynurenic acid are substrates of both OAT1 and OAT3 but exhibit lower sensitivity compared to PDA.<sup>161,186,187</sup>

Although the overlapping substrate specificity of OAT1 and OAT3 poses challenges for distinguishing individual transporter contributions *in vivo*, PDA remains the most robust and



reliable plasma biomarker currently available.<sup>161</sup> Its inclusion is recommended in early-phase clinical studies where renal transporter inhibition is anticipated.<sup>158,161,182</sup>

### **1.5.5.3 Renal P-gp activity**

#### **1.5.5.3.1 Probe drugs**

Digoxin is recommended by regulatory authorities as a probe substrate to evaluate P-gp activity in the intestinal tract and kidneys.<sup>19</sup> As a cardiac glycoside that inhibits Na<sup>+</sup>/K<sup>+</sup>-ATPase, digoxin is rapidly absorbed following oral administration, with an absolute bioavailability ranging from 60% to 80%.<sup>188</sup> It exhibits approximately 20% plasma protein binding and a large volume of distribution of around 510 liters in healthy individuals.<sup>3</sup> Digoxin undergoes minimal hepatic metabolism, accounting for approximately 10% and likely involving CYP3A enzymes, with additional contributions from gut microbial metabolism.<sup>3</sup> The majority of the drug, approximately 80%, is excreted unchanged by the kidneys through both glomerular filtration and active tubular secretion.<sup>3</sup> However, active secretion accounts for only one-third of renal clearance, limiting its sensitivity in detecting renal DDIs.<sup>3,189</sup> The elimination half-life of digoxin in individuals without renal impairment is approximately 2 days.<sup>3,188</sup>

The PK profile of digoxin is predominantly influenced by P-gp-mediated efflux at the apical membranes of enterocytes, hepatocytes, and renal tubular cells.<sup>3,91,190</sup> While uptake across the basolateral membrane may involve transporters such as OATP4C1, and possibly OATP1B3 to a lesser extent, intestinal P-gp remains the primary factor limiting digoxin absorption.<sup>3,190,191</sup> This is evidenced by clinical studies showing that rifampicin, a P-gp inducer, reduces digoxin's oral bioavailability by 30% and its C<sub>max</sub> by 52%.<sup>190,192</sup> In contrast, fostamatinib, a P-gp inhibitor, markedly increases C<sub>max</sub> by 70% and AUC by 37%.<sup>3,193</sup> Interestingly, rifampicin has little to no impact on P-gp-mediated transport in the liver or kidneys.<sup>3,192</sup> However, inhibitors such as verapamil and clarithromycin have been shown to reduce systemic clearance of digoxin, likely by affecting renal elimination pathways.<sup>3,97,194</sup> Emerging data suggest that OATP4C1 may also play a critical role in the renal handling of digoxin, potentially acting as a rate-limiting transporter in secretion.<sup>3,191,195,196</sup> This raises the possibility that some observed DDIs, previously attributed to P-gp inhibition, may involve OATP4C1, particularly in cases where the interacting drug lacks specificity, such as verapamil.<sup>3,194</sup>

The influence of genetic polymorphisms in P-gp on digoxin pharmacokinetics remains a topic of debate. Variants in the ABCB1 gene, which encodes P-gp, can affect its expression and function, thereby altering drug transport.<sup>197</sup> The most extensively studied SNPs include C1236T (rs1128503), G2677T/A (rs2032582), and C3435T (rs1045642).<sup>198,199</sup> While C1236T and C3435T are synonymous mutations, C3435T has been associated with reduced P-gp expression in the duodenum,<sup>200</sup> placenta,<sup>201</sup> and kidney,<sup>202</sup> potentially leading to increased plasma digoxin levels.<sup>154,200</sup> G2677T/A, a nonsynonymous variant, has been linked to reduced transporter activity and increased intracellular drug accumulation.<sup>203,204</sup> However, findings across studies remain inconsistent,<sup>199,205</sup> and strong linkage disequilibrium among these SNPs suggests that haplotype analysis may provide a more accurate assessment of their functional impact.<sup>197,206</sup>

A recent PopPK study highlighted the potential role of ABCB1 haplotypes in digoxin disposition.<sup>197</sup> Individuals carrying the TTT/TTT haplotype (homozygous for 1236T, 2677T, and 3435T) or CGC/CGT combinations exhibited approximately 35% higher apparent oral bioavailability compared to CGC/CGC carriers.<sup>197</sup> Notably, no significant differences in CL<sub>R</sub> were observed across genotypes, suggesting that while digoxin may serve as a useful probe for evaluating intestinal P-gp activity, it is likely suboptimal for assessing renal P-gp function.<sup>39,197</sup>

In conclusion, digoxin remains a valuable probe for assessing the impact of P-gp inducers and inhibitors on intestinal transport, especially at lower doses where P-gp saturation is less likely, as indicated by its relatively high oral bioavailability.<sup>3</sup> However, its specificity is limited, and the involvement of additional transporters such as OATP4C1 raises concerns about its reliability for evaluating renal P-gp activity.<sup>3,39</sup>

#### **1.5.5.3.2 Endogenous substrates**

To date, no endogenous probe for P-gp has been identified.<sup>162</sup>

#### **1.5.6 In vivo phenotyping for predicting renal TDDIs**

Assessing TDDIs in vivo is essential when in vitro studies suggest potential clinically significant or borderline effects.<sup>19</sup> This need stems from the often substantial discrepancies between in vitro-derived parameters and those observed in vivo, where drug pharmacokinetics are influenced by complex physiological factors.<sup>207</sup> Although wild-type and gene knockout animal

models have been used to study transport functions, their predictive value for human outcomes is limited due to interspecies differences in transporter expression, activity, and localization.<sup>208</sup>

To address these limitations, *in vivo* phenotyping in humans has become a key approach.<sup>49</sup> This approach involves the administration of selective probe substrates and the measurement of PK parameters that reflect the activity of specific transporter.<sup>49</sup> It enables quantitative assessment of how transporter function is modulated by external factors such as co-administered drugs, dietary influences, genetic polymorphisms, or disease states.<sup>49</sup> A key application of this methodology is the evaluation of TDDIs, particularly the inhibition or induction of specific transport pathways by candidate drugs.<sup>3,49</sup>

Given the wide range of transporters and the complexity of their interactions, conducting individual DDI studies for each transporter is time-consuming and labor-intensive.<sup>3,49</sup> To address this challenge, the cocktail approach has been increasingly adopted.<sup>3,208</sup> This method involves the simultaneous administration of multiple probe drugs, each selective for a particular enzyme or transporter, allowing for the concurrent evaluation of several pathways within a single study.<sup>208,209</sup> Analytical techniques such as high-performance liquid chromatography coupled with tandem mass spectrometry (HPLC–MS/MS) allow for the simultaneous quantification of plasma concentrations and urinary excretion of each probe, thereby reducing the overall burden of clinical studies.<sup>49</sup> Accordingly, the cocktail approach enhances efficiency, reduces the number of required clinical studies, and provides a more integrated view of transporter activity, including possible interactions and cooperation among different transporters.<sup>208</sup> However, it comes with challenges: probe substrates must not interfere with each other, as mutual interactions can lead to misleading PK results. Additionally, the broad substrate specificity and overlapping functions of many transporters make the identification of truly selective probes difficult.<sup>208</sup>

#### **1.5.6.1 Established renal transporter cocktails and their limitations**

Several transporter cocktails including renal transporters have been developed, with varying degrees of success.

- the “Boehringer” cocktail

Stopfer et al. introduced a transporter phenotyping cocktail (the “Boehringer cocktail”) comprising 0.25 mg digoxin (P-gp), 10 mg rosuvastatin (OATP1Bs, BCRP), 500 mg metformin (OCTs, MATEs), and 5 mg furosemide (OATs).<sup>210</sup> However, when tested in healthy volunteers, the plasma AUC of rosuvastatin increased by 43%,<sup>210</sup> an effect not predicted by in vitro studies.<sup>211</sup> Further investigation identified metformin (500 mg) and furosemide (5 mg) as contributors to this increase,<sup>212</sup> prompting a revised cocktail with reduced doses (digoxin 0.25 mg, furosemide 1 mg, metformin 10 mg, rosuvastatin 10 mg).<sup>213</sup> While the modified cocktail was validated for sensitivity and specificity using transporter inhibitors,<sup>214</sup> concerns remain regarding the selectivity of its probe drugs and the appropriateness of its PK parameters for characterizing transporter function.

- the “Cologne” cocktail

To address concerns regarding the “Boehringer” cocktail, Trueck et al. proposed an alternative transporter phenotyping cocktail comprising 10 mg adefovir-dipivoxil (OAT1; CL<sub>R</sub>), 100 mg sitagliptin (OAT3; CL<sub>R</sub>), 500 mg metformin (multiple renal transporters; CL<sub>R</sub>), 2 mg pitavastatin (OATP1B1; clearance/F), and 0.5 mg digoxin (intestinal and renal P-gp, OATP4C1; C<sub>max</sub> and CL<sub>R</sub>). This cocktail exhibited minimal mutual interactions, with only minor effects observed on adefovir and OAT1 activity.<sup>39</sup> Compared to the “Boehringer” cocktail,<sup>210,212-214</sup> it offered enhanced PK sensitivity by prioritizing renal clearance and secretion over AUC or C<sub>max</sub>, thereby reducing confounding effects from absorption, distribution, and non-renal elimination.<sup>39</sup> Additionally, it incorporated more selective probe drugs, replacing furosemide with adefovir for OAT1 and sitagliptin for OAT3.<sup>39</sup>

However, several limitations should be acknowledged regarding the proposed “Cologne” cocktail. In vitro studies have shown that sitagliptin significantly inhibits OCT1- and OCT2-mediated metformin uptake by more than 70% and 80%, respectively, as well as MATE2-K-mediated MPP<sup>+</sup> uptake by over 30%.<sup>149</sup> These interactions may confound the interpretation of transporter activity and distort estimates of metformin disposition.<sup>149</sup> Furthermore, as discussed in the previous sections, using CL<sub>R</sub> or eGFR-based renal secretion as surrogate metrics for renal transporter function can introduce bias and may not reliably detect TDDIs.<sup>39</sup> The cocktail also suffers from the lack of highly specific probe substrates, particularly for OCT2 and P-gp, where metformin and digoxin serve as imperfect substitutes due to the absence of better alternatives.<sup>39</sup> Finally, the cocktail has not yet been validated in clinical DDI studies,

especially for adefovir dipivoxil (OAT1) and sitagliptin (OAT3), both of which lack robust data on transporter specificity.<sup>39</sup> These limitations underscore the need for further refinement of the cocktail and clinical validation to support its use in assessing TDDIs.<sup>39</sup>

- Microdosing as a better alternative

To minimize unexpected DDIs, probe drug doses should be as low as possible, as potent transporter inhibition in clinical DDI studies can substantially elevate plasma drug concentrations, increasing the risk of unintended pharmacological or toxicological effects, particularly in vulnerable populations such as patients with renal impairment, elderly individuals, and children. A microdosing approach, where probe drugs are administered at 1% of their therapeutic dose, with a maximum dose of 100 mg, offers a safer alternative, and advances in HPLC-MS/MS allow for accurate PK profiling even at these low doses.<sup>215-218</sup>

Prueksaritanont et al. developed a microdosing cocktail to assess CYP3A and transporter function, which includes 10 µg midazolam (CYP3A), 375 µg dabigatran etexilate (intestinal P-gp), 10 µg pitavastatin (OATP1Bs), 25 µg rosuvastatin (BCRP, OATP1Bs, P-gp), and 50 µg atorvastatin (OATP1Bs, BCRP, P-gp, CYP3A).<sup>51,219</sup> This cocktail was successfully validated using known inhibitors.<sup>219</sup> However, microdosing strategies for renal transporters remain underdeveloped.<sup>51</sup>

- Challenges in renal transporter cocktail studies

Despite advancements in *in vivo* phenotyping technologies, particularly cocktail-based approaches, several challenges remain in predicting renal TDDIs.<sup>208</sup> Existing cocktails, such as the “Boehringer”<sup>210,212-214</sup> and “Cologne”<sup>39</sup> cocktails, have improved transporter phenotyping, but some limitations hinder their broader applicability. In addition to the specific issues previously discussed for each approach, one major limitation is the lack of clinical validation, particularly in populations with immature (developing) renal function, such as pediatric patients, and in those with impaired renal function, including elderly and critically ill individuals. Addressing these challenges is essential to enhance the clinical relevance of renal transporter phenotyping.

### 1.5.7 Understanding probe PK in phenotyping cocktails using PopPK modeling

In transporter and enzyme phenotyping studies, DDI assessments commonly rely on evaluating changes in phenotyping metrics such as  $C_{\max}$  and AUC of probe substrates administered as part of a cocktail approach.<sup>3</sup> These metrics are typically analyzed using noncompartmental analysis (NCA) and compared across study periods using the standard average bioequivalence method, with predefined acceptance boundaries for the geometric mean ratio (0.80 to 1.25).<sup>19,39</sup> Although this approach can be sufficient for ruling out clinically significant interactions involving specific probe drugs and transporters when performed under well-controlled conditions, it provides limited mechanistic insight.<sup>197</sup> In particular, it does not reveal the specific site or process affected by a perpetrator drug, which limits its usefulness in accurately predicting DDIs or explaining the mechanisms underlying altered drug exposure.<sup>197</sup>

To better understand the mechanisms underlying observed PK changes in DDI studies, especially in the context of complex or multi-site interactions, a detailed PK assessment is essential and can be effectively supported by modeling and simulation approaches.<sup>3,197</sup> This is especially important when a single enzyme or transporter, such as CYP3A4<sup>189,220</sup> or P-glycoprotein,<sup>197</sup> is expressed across multiple tissues, resulting in variable DDI effects.<sup>3</sup> Similarly, different probe substrates for the same enzyme (e.g., tizanidine vs. caffeine for CYP1A2, or dextromethorphan vs. desipramine for CYP2D6),<sup>189</sup> may exhibit different interaction profiles.<sup>3</sup> These differences may be better explained by a more detailed PK characterization of each probe.

Model-based PK approaches allow for a dynamic and mechanistic interpretation of drug interactions by capturing the full concentration–time profiles of both probe and perpetrator drugs.<sup>3</sup> Among available modeling strategies, semi-physiological PopPK models and physiologically based pharmacokinetic (PBPK) models are widely used.<sup>3</sup> This thesis focuses on the application of PopPK modeling as a flexible and data-driven approach to characterize the pharmacokinetics of probe substrates within phenotyping cocktails and to identify potential interactions.

PopPK modeling estimates typical PK parameters and characterizes their variability across individuals.<sup>221</sup> By analyzing concentration-time data from healthy volunteers or patients,

PopPK models quantify sources of variability, including inter-individual variability (IIV), inter-occasion variability (IOV), and residual error, which may arise from assay imprecision or inconsistencies in sampling. Incorporating clinical and demographic covariates into the model helps explain part of this variability and improves the model's predictive performance.<sup>221</sup>

In the context of DDI studies, PopPK modeling offers several advantages over NCA. It allows for the identification of parameters associated with specific PK processes, such as absorption, metabolism, and renal elimination.<sup>197</sup> This enables localization of interactions to physiological sites like the intestine, liver, or kidney.<sup>197</sup> Moreover, PopPK models can account for nonlinear processes, including saturable metabolism or transporter-mediated clearance,<sup>6</sup> and can integrate pharmacogenomic variability.<sup>197</sup> These features provide mechanistic insights into the underlying causes of observed interactions and support a more detailed understanding of how DDIs influence drug exposure.

Furthermore, PopPK modelling and simulation techniques are powerful tools for optimizing clinical trial design. They inform decisions on dosing regimens, sampling schedules, and sample sizes, ultimately improving the efficiency and interpretability of DDI investigations.<sup>222</sup> Overall, PopPK modeling enhances both the mechanistic understanding and clinical utility of assessing DDIs through phenotyping approaches.

## **2. Aims and objectives**

The overarching aim of the projects presented in this dissertation is to enhance the evaluation of renal PK processes by improving methods for the accurate quantification of GFR and renal transporter activity. The work is structured around the following key objectives:

1. To establish a practical method for estimating iohexol clearance after administration of a standard dose. This involves the use of optimized correction formulas and simplified PK models to improve accuracy and feasibility in GFR assessment. (Publication I)
2. To validate low-dose iohexol as a reliable GFR marker through comprehensive in vitro and in vivo studies. These investigations support its potential integration into standard clinical protocols to improve patient safety, and enable its use as a selective GFR probe in renal transporter phenotyping studies for more precise assessment of renal secretion and TDDIs in vivo. (Publication II)
3. To re-evaluate the suitability of adefovir as a phenotyping probe for OAT1 within a clinical drug transporter phenotyping cocktail. This objective includes a detailed assessment of potential DDIs between adefovir and other cocktail components, including sitagliptin, metformin, pitavastatin, and digoxin, using a PopPK modeling approach. (Publication III)



### **3. Relevant publications and contributions**

#### **3.1 Publication I**

**Title:** Improved correction formulas to estimate iohexol clearance from simple models

**Author:** Qian Dong<sup>1</sup>, Uwe Fuhr<sup>1</sup>, Elke Schaeffner<sup>2</sup>, Markus van der Giet<sup>3</sup>, Natalie Ebert<sup>2</sup>, Max Taubert<sup>1</sup>

**Institution:**

1. Department I of Pharmacology, Center for Pharmacology, Faculty of Medicine and University Hospital Cologne, University of Cologne, Gleueler Straße 24, Cologne 50931, Germany

2. Institute of Public Health, Charité Universitätsmedizin Berlin, Berlin, Germany

3. Department of Nephrology, Charité Universitätsmedizin Berlin, Berlin, Germany

**Published in:** European Journal of Clinical Pharmacology, 2023; 79(9):1215–1217.  
doi:10.1007/s00228-023-03535-y

**Qian Dong contributed to this publication as follows:**

**Qian Dong** conceived and designed the study in collaboration with Max Taubert. **Qian Dong** analyzed and interpreted the data together with Max Taubert. Additionally, **Qian Dong** drafted the initial manuscript and finalized it with substantial input and support from Max Taubert and Uwe Fuhr. All authors contributed to the revision and final approval of the manuscript.

**Cooperation:**

**Cooperation Partners:**

- Institute of Public Health, Charité Universitätsmedizin Berlin, Berlin, Germany
- Department of Nephrology, Charité Universitätsmedizin Berlin, Berlin, Germany

**Scope of Cooperation:**

Univ.-Prof. Dr. Elke Schaeffner and PD Dr. med. Natalie Ebert from the Institute of Public Health, along with Prof. Prof. h.c. Dr. med. Markus van der Giet from the Department of Nephrology at Charité Universitätsmedizin Berlin, contributed to data acquisition.

## Background and objectives

Iohexol plasma clearance has emerged as a preferred method for accurately measuring GFR in both clinical practice and research.<sup>116</sup> However, the choice of the most suitable PK model for analyzing iohexol concentrations remains under debate. Previous analyses using BIS data<sup>132</sup> indicated that a three-compartment PK model provides more accurate clearance estimates than the conventional two-compartment model, particularly in elderly individuals.<sup>117</sup> Although this model improves precision, its application in routine practice is limited by the complexity of Bayesian software and the technical expertise required.<sup>117</sup>

An alternative approach to mitigate bias arising from model simplifications is the use of correction formulas applied to clearance estimates derived from simpler one- or two-compartment models. Established correction methods, such as the Bröchner-Mortensen (BM)<sup>223</sup> and Chantler (Ch)<sup>224</sup> equations, have shown good performance in adjusting iohexol plasma clearance estimates based on a one-compartment approximation, using the full two-compartment clearance as the reference.<sup>225</sup> However, their ability to correct both one- and two-compartment iohexol clearance estimates when compared against a three-compartment clearance reference has not yet been evaluated. This study addresses this gap by examining the extent to which these correction formulas can enhance the accuracy of simplified iohexol clearance estimates relative to a three-compartment standard.<sup>4</sup>

## Methods

Data from the BIS, including 546 individuals with data obtained up to 300 min post-injection, were evaluated.<sup>117,132</sup> One-, two-, and three-compartment models were used to estimate iohexol clearance (CL1, CL2, and CL3), respectively. CL1 was estimated based on the slow component of iohexol concentrations 120 to 300 min post-dose, CL2 was estimated based on the protocol by Schwartz et al.<sup>226</sup> as carried out in the BIS,<sup>132</sup> and CL3 was estimated using the empirical Bayes approach based on the three-compartment model.<sup>117</sup> Equations resembling the BM<sup>223</sup> and Ch<sup>224</sup> formulas were then fitted to correct CL1 and CL2 results, using CL3 as the reference. A leave-one-out cross-validation<sup>227</sup> was utilized to assess the bias and root mean squared error (RMSE), as well as to evaluate Lin's concordance correlation coefficient (CCC)<sup>228</sup> and the relative total deviation index (TDI) for a range of coverage probabilities (CP).<sup>229</sup> A TDI  $\leq 10\%$  for a CP of 90% (TDI<sub>90</sub>) and an at least substantial CCC of  $\geq 0.95$  were considered optimal.

R version 4.2.1 (R Foundation for Statistical Computing, Vienna, Austria), the nonlinear mixed-effects modeling program NONMEM version 7.5.0 (ICON plc, Dublin, Ireland), and Perl speaks NONMEM (PsN) version 5.2.6 (Uppsala University, Uppsala, Sweden)<sup>230</sup> were used as statistical software.

## **Results**

The correction formulas demonstrated good agreement with the reference clearance values (CL<sub>3</sub>), regardless of whether they were based on CL<sub>1</sub> or CL<sub>2</sub>.<sup>4</sup> All equations yielded an absolute bias of less than 1 mL/min, with RMSE values ranging from 2.92 to 4.08 mL/min, and showed substantial concordance.<sup>4</sup> Overall, CL<sub>2</sub>-based correction formulas consistently outperformed their CL<sub>1</sub>-based counterparts, as evidenced by lower bias, reduced RMSE, higher CCC, and smaller TDI<sub>90</sub> values.<sup>4</sup> Importantly, only the CL<sub>2</sub>-based equations achieved the predefined TDI<sub>90</sub> target.<sup>4</sup> While the choice between BM-like and Ch-like equations made little difference among CL<sub>2</sub>-based formulas, for CL<sub>1</sub>-based formulas, the BM-like equation showed a notably smaller absolute bias (−0.0949 mL/min) than the Ch-like equation (−0.357 mL/min).<sup>4</sup>

## **Conclusion**

In summary, our findings indicate that correction formulas applied to one- or two-compartment models can provide reliable iohexol clearance estimates while reducing the complexity of three-compartment modeling.<sup>4</sup> The selection of an appropriate correction formula should be guided by the available compartment model and clinical requirements, ensuring a balance between accuracy and practicality.<sup>4</sup>

### 3.2 Publication II

**Title:** Validating low-dose iohexol as a marker for glomerular filtration rate by in vitro and in vivo studies

**Author:** Qian Dong<sup>1</sup>, Zhendong Chen<sup>1</sup>, Jana Boland<sup>1</sup>, Charalambos Dokos<sup>1</sup>, Yohannes Hagos<sup>2</sup>, Annett Kühne<sup>2</sup>, Max Taubert<sup>1</sup>, Dirk Gründemann<sup>1</sup>, Uwe Fuhr<sup>1</sup>

**Institution:**

1. Department of Pharmacology, Center for Pharmacology, Faculty of Medicine and University Hospital Cologne, University of Cologne, Cologne, Germany.
2. PortaCellTec Biosciences GmbH, Göttingen, Germany.

**Published in:** Clinical and Translational Science, 2025; 18(2):e70141. doi:10.1111/cts.70141

**Qian Dong contributed to this publication as follows:**

**Qian Dong** conducted in vitro experiments for OCT1/2, OAT1/3, and MATE1/2-K under the guidance of Dirk Gründemann and Uwe Fuhr, with additional support from Yohannes Hagos and Annett Kühne for the OATP1B1/1B3 and MDR1 experiments. **Qian Dong** collaborated with Uwe Fuhr, Zhendong Chen, Jana Boland, and Charalambos Dokos in conducting the clinical trial. Additionally, **Qian Dong** analyzed the data from both in vitro and in vivo studies, with some support from Zhendong Chen, Max Taubert, Yohannes Hagos, and Annett Kühne. **Qian Dong** drafted the initial manuscript and finalized it with substantial input and support from Uwe Fuhr.

**Cooperation:**

**Cooperation Partners**

- Prof. Dr. rer. nat. Dirk Gründemann's Lab, Department of Pharmacology, Faculty of Medicine and University Hospital Cologne, University of Cologne, Gleueler Straße 24, Cologne 50931, Germany.
- PortaCellTec Biosciences GmbH, Göttingen, Germany.

**Scope of Cooperation**

- In vitro experiments for OCT1/2, OAT1/3, and MATE1/2-K were conducted by Qian Dong in Prof. Dr. rer. nat. Dirk Gründemann's lab. The work was carried out under the scientific guidance of Univ.-Prof. Dr. Uwe Fuhr and Prof. Dr. rer. nat. Dirk Gründemann.

- Due to limitations in available resources and methods for conducting in vitro experiments on OATP1B1/1B3 and MDR1, Prof. Dr. rer. nat. Yohannes Hagos and Dr. rer. nat. Annett Kühne from PortaCellTec Biosciences GmbH kindly supported this work by performing the experiments in their laboratory.

## Background and objectives

Accurate GFR estimation is essential for evaluating kidney function.<sup>40</sup> “Serum creatinine concentrations and/or creatinine clearance are commonly used to this end.<sup>40</sup> However, renal elimination of creatinine is not only mediated by glomerular filtration but also by renal transporters.”<sup>5</sup> “Therefore, creatinine-based GFR estimations may be biased and influenced by TDDIs<sup>116,119</sup>.”<sup>5</sup> Additionally, both creatinine and cystatin C are affected by non-GFR factors, potentially leading to inaccuracies.<sup>231</sup>

Iohexol plasma clearance following a single dose (typically 3,235 mg) has emerged as a reliable method for GFR quantification, as it is presumed to be eliminated exclusively via glomerular filtration.<sup>116</sup> However, its use remains limited, partly due to an incomplete understanding of its PK.<sup>5</sup> While iohexol elimination in humans is generally considered to occur solely through glomerular filtration, some evidence suggests a potential role for membrane transporters.<sup>3,141-143</sup> If iohexol interacts with transporters, it could introduce nonlinearity in its PK, particularly at low concentrations, making it susceptible to TDDIs.<sup>5</sup> Similar to creatinine, such interactions could lead to discrepancies between iohexol clearance and true GFR.<sup>5</sup>

These potential limitations also impact the integration of iohexol as a GFR marker in probe drug cocktails designed for renal transporter phenotyping.<sup>3,5</sup> Additionally, since ADRs of iohexol are dose-dependent, a lower dose would be preferable, especially for patients with impaired renal function or those requiring frequent GFR monitoring.<sup>5,137,138</sup>

This study aimed to: (i) Investigate potential interactions between iohexol and key drug transporters in vitro. (ii) Evaluate whether a 259 mg dose of iohexol could serve as an alternative to the standard dose in vivo.

## Methods

We assessed whether iohexol inhibits or is transported by renal transporters (OAT1/3, OCT2, and MATE1/2-K) or other transporters (OATP1B1/3, OCT1, and MDR1) utilizing both cell-based and vesicle-based in vitro methods.<sup>5</sup> In addition, we conducted an in vivo clinical study including 12 volunteers, administering single intravenous doses of 3235 mg ("reference") and 259 mg ("test") utilizing a crossover design.<sup>5</sup> Plasma and urine samples were obtained up to 24 hours following administration.<sup>5</sup> We evaluated dose linearity of iohexol pharmacokinetics

utilizing the standard bioequivalence methodology<sup>232</sup> and performed a PopPK analysis to characterize its profile.<sup>5</sup>

## **Results**

“Our in vitro findings indicate that iohexol is neither a substrate nor a significant inhibitor of the transporters, suggesting it is unlikely to participate in TDDIs in vivo.”<sup>5</sup> “Twelve healthy subjects (7 females) with a median body mass index of 24.4 kg/m<sup>2</sup> (range: 21.2 - 28.9 kg/m<sup>2</sup>) and a median age of 34 years (range: 23 - 48 years) participated in the relevant part of the trial.”<sup>5</sup> The 90% confidence intervals (CIs) for the test-to-reference ratios were 1.01 (0.968–1.05) for iohexol clearance, defined as dose divided by AUC, and 1.06 (0.960–1.17) for urinary recovery, respectively.<sup>5</sup> “These values fall within the standard bioequivalence range of 0.800–1.25, indicating that the AUC increased proportionally with the iohexol dose.”<sup>5</sup> PopPK analysis corroborated these results, demonstrating no significant impact of dose on CL<sub>R</sub> and negligible nonrenal elimination of iohexol.<sup>5</sup>

## **Conclusion**

Our research verifies that iohexol is exclusively eliminated via the kidneys, without significant interaction with key drug transporters, and adheres to a nonsaturable clearance mechanism.<sup>5</sup> Additionally, we confirmed its dose-proportional pharmacokinetics in vivo.<sup>5</sup> These data endorse the utilization of a 259 mg dosage as a precise marker for GFR, even when concomitant medications are provided.<sup>5</sup>

### 3.3 Publication III

**Title:** Understanding adefovir pharmacokinetics as a component of a transporter phenotyping cocktail

Qian Dong<sup>1</sup>, Chunli Chen<sup>1,2</sup>, Max Taubert<sup>1</sup>, Muhammad Bilal<sup>1,3</sup>, Martina Kinzig<sup>4</sup>, Fritz Sörgel<sup>4</sup>, Oliver Scherf-Clavel<sup>5</sup>, Uwe Fuhr<sup>1</sup>, Charalambos Dokos<sup>1</sup>

1. Department I of Pharmacology, Center for Pharmacology, Faculty of Medicine and University Hospital Cologne, University of Cologne, Gleueler Straße 24, Cologne 50931, Germany.

2. Heilongjiang Key Laboratory for Animal Disease Control and Pharmaceutical Development, College of Veterinary Medicine, Northeast Agricultural University, 600 Changjiang Road, Xiangfang District, Harbin 150030, People's Republic of China.

3. Department of Clinical Pharmacy, Institute of Pharmacy, University of Bonn, Bonn, Germany.

4. Institute for Biomedical and Pharmaceutical Research, Nürnberg-Heroldsberg, Germany.

5. Department Pharmazie, Ludwig-Maximilians-Universität München, Butenandtstr. 5, 81377 München, Germany.

**Published in:** European Journal of Clinical Pharmacology, 2024; 80(7):1069–1078. doi:10.1007/s00228-024-03673-x

**Qian Dong contributed to this publication as follows:**

**Qian Dong** organized the database and conducted data analyses in collaboration with Chunli Chen, Max Taubert, and Muhammad Bilal. **Qian Dong** drafted the initial manuscript and finalized it with substantial input and support from Max Taubert and Uwe Fuhr. Additionally, **Qian Dong** contributed to the conception and design of the research in collaboration with all authors. Uwe Fuhr provided the data and supervised the project, while all authors reviewed and approved the final submitted version of the manuscript.

**Cooperation:**

**Cooperation Partners:**

No external cooperation partners were involved in this project.



**Scope of Cooperation:**

This project was conducted independently without external collaborations.

## **Background and objective**

In an earlier transporter phenotyping study, adefovir (dipivoxil) was employed as a probe drug to evaluate the activity of renal OAT1, with  $CL_R$  serving as the primary metric for quantifying transporter function.<sup>3,39</sup> When administered alongside other cocktail components (metformin, sitagliptin, pitavastatin, and digoxin), adefovir exhibited an approximately 20% increase in systemic exposure compared to its administration alone.<sup>39</sup> To further investigate this observation, the present study applied a PopPK modeling approach for a more in-depth characterization of adefovir's pharmacokinetics within the cocktail.<sup>6</sup>

## **Methods:**

Data from 24 healthy participants were reanalyzed.<sup>39</sup> Following the establishment of a base model, the impacts of covariates, including the influence of co-administered medications, were evaluated using forward inclusion and a subsequent backward elimination strategy.<sup>6</sup>

## **Results:**

A one-compartment model with first-order absorption (including a lag time) and combined nonlinear renal and linear nonrenal elimination processes provided the best fit to the data.<sup>6</sup> Compared to single administration, co-administration resulted in a markedly higher apparent bioavailability (73.6% vs. 59.0%) and a lower apparent absorption rate constant ( $2.29\text{ h}^{-1}$  vs.  $5.18\text{ h}^{-1}$ ), while renal elimination parameters remained unaffected.<sup>6</sup> The  $K_m$  for nonlinear renal clearance was estimated at 170 nmol/L, exceeding the maximum observed plasma concentrations of adefovir, and the  $V_{\max}$  was 2.40  $\mu\text{mol/h}$ , corresponding to a median absolute estimated GFR of 105 mL/min.<sup>6</sup>

## **Conclusion:**

In summary, the PopPK modeling results suggest that the observed minor DDI for adefovir primarily stemmed from alterations in its apparent absorption and/or prodrug conversion, rather than changes in renal elimination.<sup>6</sup> The stability of renal elimination supports the continued use of  $CL_R$  as a reliable marker for evaluating renal OAT1 activity under the dosing conditions applied in the cocktail study.<sup>6</sup> Moreover, the elevated  $K_m$  value indicates minimal risk of mischaracterization.<sup>6</sup> These conclusions align well with the principles outlined in the ICH M12 Guideline.<sup>19</sup>

## **4. Summary**

This cumulative dissertation comprises three publications that collectively advance the assessment of individual renal PK processes by refining methods for the precise quantification of GFR and renal transporter-mediated active net secretion, as detailed in the previous section: “3. Relevant publications and contributions”. The following sections provide a summary of the key findings, discuss the limitations of the proposed approaches, and outline potential future directions.

### **4.1 Key findings**

By integrating three complementary studies, this cumulative dissertation demonstrates that:

1. Simple compartment models, when combined with appropriate correction formulas, may serve as practical alternatives to complex modeling approaches for estimating iohexol-based GFR (Publication I);
2. Low-dose iohexol exhibits linear and predictable pharmacokinetics, with negligible interaction with drug transporters, thereby supporting its use as a safe and reliable marker for GFR in both clinical and research settings (Publication II);
3. PopPK modeling provides mechanistic insight into PK alterations observed in transporter phenotyping studies, which may reflect underlying drug interactions, and supports the continued use of adefovir as a probe for OAT1 activity under appropriately controlled conditions (Publication III).

Collectively, these findings contribute to more mechanistically grounded and clinically feasible approaches for evaluating renal function and drug elimination. These methodological advancements may further enhance clinical decision-making, particularly in patient populations with altered kidney function, and support the design of DDI studies, including those focused on renal transporter phenotyping.

### **4.2 Limitations**

While the studies presented in this dissertation advance methodologies for GFR measurement and enhance the understanding of active renal secretion, several limitations should be acknowledged.

Publication I evaluated simplified correction formulas for estimating iohexol clearance. Although these models improved usability, they demonstrated a slight reduction in accuracy and precision relative to the three-compartment model, warranting caution in clinical application. Moreover, the current reliance on linear correction formulas may not adequately capture the PK complexities present in certain clinical scenarios.<sup>4,40</sup>

Publication II included both in vitro and in vivo evaluations of low-dose iohexol as a GFR marker.<sup>5</sup> The in vitro findings are limited by the experimental systems, which may not fully replicate renal physiological complexity.<sup>5</sup> Additionally, assay variability observed across experimental days, consistent with previous studies,<sup>149</sup> may be attributed to differences in cell density and transfection timing, which influence transporter expression on the plasma membrane. However, this variability does not affect the overall conclusions of the study.<sup>5</sup> In the clinical study, although the findings support the feasibility of low-dose iohexol for GFR assessment, the exclusive inclusion of healthy volunteers, as in Publication I, limits the generalizability of the results.<sup>41-44</sup> Furthermore, although dense sampling enabled precise PK profiling in a research context, such sampling protocols are not feasible in routine clinical practice. While limited sampling strategy (LSS) have been established in healthy individuals<sup>133</sup> and may also apply to critically ill patients, their suitability in such populations remains uncertain.<sup>5</sup>

Publication III presented a PopPK analysis of adefovir, revealing nonlinear renal elimination.<sup>6</sup> However, the study was conducted solely in healthy adults receiving a single standard dose, which restricts insights into dose-dependent nonlinearities and limits the applicability of the findings to patients with impaired renal function.<sup>6</sup> Furthermore, mechanistic modeling efforts to jointly characterize glomerular filtration and active tubular secretion resulted in unstable parameter estimates, thereby limiting the physiological interpretability of the model.<sup>6</sup>

In summary, the studies presented in this dissertation are limited by the lack of validation in diverse clinical populations and challenges in model stability and physiological interpretability. These limitations constrain the broader clinical relevance and translational potential of the current work.

### **4.3 Future directions**

#### **4.3.1 Advancing GFR assessment in diverse patient groups**

The iohexol-based GFR measurement approaches developed in this dissertation, including improved correction formulas and low-dose protocols, have demonstrated acceptable accuracy and precision.<sup>4,5</sup> However, their validation has been largely confined to controlled settings, as discussed in Section “4.2 Limitations”. Consequently, the applicability of these methods to broader clinical populations remains unclear.<sup>41-44</sup> To enhance clinical applicability, future research should prioritize validation of these methodologies across a diverse spectrum of patient groups, including individuals with moderate to severe kidney dysfunction, pediatric and geriatric populations, and patients with comorbid conditions such as diabetes mellitus, cardiovascular disease, or chronic inflammatory disorders.<sup>40</sup> These factors are known to influence drug disposition and may significantly affect iohexol kinetics.<sup>40</sup> Although dose proportionality has generally been preserved across renal function levels,<sup>5</sup> further confirmation is required, particularly in the context of low-dose protocols and limited sampling designs intended for clinical use.<sup>66</sup>

Moreover, accurately tracking changes in GFR during AKI remains a significant challenge.<sup>41,42</sup> Dixon et al. demonstrated that although continuous infusion of low-dose iohexol (CILDl) takes time to reach equilibrium in critically ill patients, it allows for real-time monitoring of GFR with high precision and sensitivity, providing advantages over the traditional single bolus injection (SBI) method.<sup>41,42</sup> However, both CILDl and SBI are too cumbersome for routine clinical use.<sup>41,42</sup> These drawbacks show the need for alternative strategies. One promising approach is the development of correction formulas to estimate iohexol clearance using simplified models.<sup>4</sup> As discussed in the “4.2 Limitations” section, exploring non-linear correction models, rather than relying solely on linear methods, may improve accuracy, especially in patients with atypical body composition, altered extracellular fluid volumes, or rapidly changing renal function.<sup>4</sup> Such conditions are common in acute and intensive care settings and may significantly influence iohexol pharmacokinetics, leading to inaccurate GFR estimates if standard assumptions are applied.<sup>4,43,44</sup>

Beyond traditional GFR measurement methods such as iohexol clearance, future studies should prioritize the development and clinical validation of non-invasive, real-time techniques for assessing renal function.<sup>233,234</sup> Among these, MB-102 has emerged as a promising tool,

enabling continuous, real-time GFR monitoring through transdermal fluorescence detection.<sup>234</sup> This approach minimizes patient burden and holds potential for point-of-care applications.<sup>234</sup> In parallel, rhodamine-based dual fluorescent tracers offer a non-invasive method for simultaneously assessing both GFR and plasma volume, typically using optical detection systems.<sup>234</sup> These innovative technologies provide dynamic and accurate monitoring of renal function and are particularly valuable in acute and perioperative care settings, where rapid changes in kidney function are common.<sup>234</sup> To support their clinical translation and broader adoption, it is essential not only to enhance their sensitivity and practical utility but also to establish standardized testing protocols and calibrate their performance against gold-standard reference methods.<sup>233,234</sup> In addition, a thorough understanding of the pharmacokinetics, safety profiles, and potential variability of these tracers in diverse patient populations, including critically ill individuals, neonates, and those with significant fluid imbalances, is essential to support their clinical application.<sup>234</sup> As these technologies continue to evolve, they have the potential to significantly advance renal diagnostics by enabling earlier detection of dysfunction, informing individualized treatment strategies, and ultimately improving patient outcomes.<sup>234</sup>

In parallel with mGFR methodologies explored in this dissertation, recent research has increasingly focused on enhancing eGFR through the use of multi-marker panels.<sup>115</sup> Traditional eGFR approaches that rely on single endogenous filtration markers, such as serum creatinine or cystatin C, are limited by the influence of non-GFR determinants, which can introduce bias and reduce accuracy.<sup>40</sup> Emerging strategies seek to address these limitations by incorporating panels of filtration markers, including low-molecular-weight proteins (such as  $\beta$ 2-microglobulin and  $\beta$ -trace protein) and metabolites (such as pseudouridine).<sup>115</sup> “Including more markers minimizes the impact of non-GFR determinants of each marker and lessens the need to use demographics and clinical characteristics as surrogates for the non-GFR determinants, with increasing precision as the number of markers increases.”<sup>115</sup> Furthermore, the application of machine learning methods has been proposed to refine panel-based eGFR by identifying and down-weighting discordant markers, facilitating more accurate and individualized GFR estimation.<sup>115</sup> While panel-based eGFR approaches remain in the developmental stage, they represent a complementary and non-invasive strategy for kidney function assessment, particularly where direct GFR measurement is not feasible.<sup>115</sup>

However, their clinical translation will require robust standardization of marker assays and validation against measured GFR.<sup>115</sup>

In summary, expanding validation to broader clinical scenarios and improving correction methods are key to establishing iohexol-based GFR measurement as a reliable tool for routine use.<sup>4,5,133</sup> Simultaneously, advancing complementary strategies such as non-invasive tracer-based methods and multi-marker eGFR estimation will enrich the clinical toolkit for renal function assessment, especially in settings where direct measurement is challenging.<sup>115,233</sup>

#### **4.3.2 Further improvement and validation of the current cocktail approach**

While current transporter phenotyping cocktails have demonstrated utility in assessing transporter function,<sup>146,208</sup> there remains substantial scope for enhancing both their design and practical application. The following directions outline potential avenues for advancing the field.

##### **4.3.2.1 Optimization of probe drug doses in phenotyping cocktails**

A critical aspect of refining transporter cocktails involves optimizing the doses of individual probe drugs. Appropriate dose adjustments can reduce the risk of unintended TDDIs within the cocktail and enhance overall safety, especially in populations at risk for toxicity. One well-documented example is the optimization of the “Boehringer” cocktail, where lowering the doses of metformin and furosemide led to a reduced impact on rosuvastatin exposure.<sup>210,212-214</sup> These modifications improved the reliability of the cocktail for assessing TDDIs during drug development.<sup>210,212-214</sup>

In this dissertation, adefovir data from the “Cologne” transporter cocktail study<sup>39</sup> were reanalyzed using PopPK modeling to investigate intra-cocktail DDIs.<sup>6</sup> The results indicated that while adefovir remains a promising probe for OAT1 phenotyping, a reduced dose could help minimize interactions with other cocktail components.<sup>6</sup> In addition, in vitro validation of the same cocktail study showed that sitagliptin, which serves as the OAT3 probe, substantially inhibits OCT2.<sup>149</sup> This finding aligns with a borderline inhibition of metformin CL<sub>R</sub> observed in the clinical study.<sup>39</sup> Together, these results support a reduction in the doses of sitagliptin and possibly metformin to improve the specificity and safety profile of the cocktail.<sup>39,149</sup>

Although minimizing probe drug doses is desirable to reduce ADRs and the risk of PK interactions caused by the probe as a perpetrator, reducing doses below established thresholds may compromise their ability to reliably reflect transporter or enzyme activity.<sup>3</sup> Therefore, any proposed lower dose requires independent validation to ensure the robustness of phenotyping results.<sup>3</sup> For example, at microdose levels, warfarin and dextromethorphan, typically used to assess CYP2C9 and CYP2D6 activity, respectively, failed to exhibit the expected genotype-dependent differences, likely due to their complex pharmacokinetics and involvement in multiple metabolic pathways.<sup>3,235-237</sup> This highlights the need for dose-specific validation to confirm the specificity and sensitivity of low-dose strategies in phenotyping applications.<sup>3</sup>

In summary, future studies should consider validating optimized probe doses in phenotyping cocktails, such as the “Cologne” cocktail,<sup>39</sup> to ensure that dose adjustments do not compromise the reliability of phenotyping performance.<sup>3</sup>

#### **4.3.2.2 Refining transporter phenotyping with selective metrics**

While the development of selective probe drugs remains essential for distinguishing closely related PK processes in key organs such as the intestine, liver, and kidney, relying exclusively on probe selection poses considerable challenges.<sup>3</sup> Future approaches to transporter phenotyping should therefore integrate more selective and physiologically relevant PK and pharmacodynamic (PD) endpoints, as well as emerging techniques that enhance the mechanistic understanding of TDDIs.<sup>3,158</sup>

For renal transporters, net renal secretion can serve as a more appropriate metric of transporter activity than overall CL<sub>R</sub>, as it more directly reflects active transport processes.<sup>39</sup> However, many transporters are expressed across multiple organs and mediate distinct processes in a tissue-specific manner. For example, P-gp limits drug absorption in the intestine, facilitates biliary excretion in the liver, and contributes to tubular secretion in the kidney.<sup>3</sup> These diverse functions collectively shape the systemic disposition of P-gp substrates like digoxin.<sup>3</sup> Therefore, assessing only renal or systemic PK parameters may not fully capture or localize TDDIs. A more informative strategy for transporter phenotyping involves integrating a wider array of PK metrics that reflect site-specific transporter activity. For intestinal P-gp, parameters such as C<sub>max</sub>, partial AUC, and absorption rate constants can serve as indirect but



informative indicators of its functional role.<sup>3</sup> Similarly, nonrenal clearance can provide insight into hepatic transporter activity.<sup>3</sup> These complementary PK parameters help disentangle the contributions of individual transporters across different organs and better explain changes in systemic exposure (e.g., AUC changes), which often reflect combined transporter effects.<sup>3</sup>

However, not all mechanistically informative metrics are feasible to obtain in routine clinical DDI studies. Some require invasive sampling, such as portal vein blood or bile collection, while others reflect intracellular processes or in vivo binding kinetics that are difficult to assess directly.<sup>3</sup> For example, inhibition of efflux transporters such as P-gp and BCRP may cause intracellular drug accumulation and toxicity in organs of elimination, even in the absence of changes in systemic PK profiles.<sup>158,238-240</sup> This limitation reduces the sensitivity of traditional probe substrate approaches in detecting such localized effects.<sup>158</sup> To overcome these limitations, modeling and simulation techniques are essential for predicting intracellular concentrations of transporter substrates and inhibitors, and for linking these to systemic or PD responses.<sup>158</sup> Such predictions can be validated in clinical settings, especially for scenarios where direct measurement in humans is not feasible.<sup>158,195,239,241</sup>

As a complementary approach in transporter phenotyping, incorporating an internal reference compound unaffected by transporter-mediated disposition can enhance the interpretability of probe substrate pharmacokinetics. In this context, low-dose iohexol, which is validated in this dissertation as a reliable marker of GFR,<sup>5</sup> offers distinct advantages. Its inclusion in renal transporter phenotyping studies may help differentiate passive glomerular filtration from active tubular secretion, thereby improving the specificity and accuracy of renal transporter activity assessments.<sup>3</sup>

Beyond its utility in GFR estimation, reference compounds such as iohexol, which have well-characterized PK profiles,<sup>5</sup> can also strengthen urinary PK analyses. Urine sampling, as a non-invasive and widely used method in renal transporter phenotyping, offers critical insights into renal excretory function.<sup>57,158,242,243</sup> Specifically, since alterations in transporter-mediated tubular secretion may not be readily detectable through plasma concentrations alone, the comparison of urinary excretion with systemic PK data provides a sensitive approach for identifying renal TDDIs.<sup>158</sup> Moreover, changes in urinary drug recovery can signal alterations in oral bioavailability,<sup>158,243</sup> and such integrated data are essential for refining model-based predictions of renal drug exposure.<sup>158</sup> However, urinary PK analyses are susceptible to sources

of error, such as incomplete urine collection, which may compromise data reliability. In this context, internal reference compounds like iohexol, particularly when used alongside modeling and simulation techniques, can help identify and correct such inconsistencies. This strategy enhances the robustness of urinary PK assessments for both endogenous and exogenous transporter substrates and has been successfully applied in recent studies.<sup>136</sup>

A broader challenge in phenotyping research is the insufficient validation of PK metrics against tissue-specific transporter or enzyme expression and activity.<sup>3</sup> To address this, future work should focus on linking PK parameters, such as clearance and AUC, with localized biological function at the organ level. This is especially important for proteins with widespread or overlapping tissue distribution, such as P-gp and CYP3A4.<sup>3</sup> In this regard, integrating quantitative proteomics data with PBPK modeling offers a promising path to better mechanistic interpretation of systemic PK profiles.

In selected cases, PD endpoints can provide complementary information to PK assessments. For example, the glucose-lowering effect of metformin indirectly reflects not only its systemic exposure but also its transporter-mediated distribution and elimination.<sup>244,245</sup> However, the broader application of PD markers remains constrained by an incomplete understanding of PK–PD relationships and the limited availability of reliable and quantifiable outcome measures.

Finally, advancing the field will require the development of novel biomarkers and imaging technologies, such as positron emission tomography (PET), to directly visualize transporter and enzyme activity in vivo.<sup>246–248</sup> Such advances could enhance the precision of phenotyping strategies and improve the prediction of transporter- and enzyme-mediated DDIs.

In summary, advancing the phenotyping approach requires the integration of more selective PK and PD metrics, the use of internal reference compounds, and the application of modeling and simulation techniques to improve the prediction of DDIs and ultimately support safer and more effective drug development.

#### **4.3.2.3 Integration of endogenous biomarkers and LSS**

To enhance the scalability of transporter phenotyping and minimize the clinical burden, future research could benefit from integrating endogenous biomarkers with LSS.<sup>3,158</sup> Endogenous biomarkers are naturally occurring compounds whose disposition reflects

transporter activity and can serve as indicators of altered transporter function in vivo.<sup>158</sup> This approach offers a potentially cost-effective means to evaluate the transporter-modulating properties of NMEs during early drug development.<sup>158</sup> When coupled with pharmacometric modeling, LSS enables the estimation of PK parameters using only a few strategically timed samples or even a single time point, streamlining clinical evaluations.<sup>3</sup>

This integrated approach is particularly valuable in clinical and epidemiological studies where frequent or intensive sampling is logistically challenging or ethically constrained.<sup>3</sup> A recent example demonstrated the utility of this methodology using a joint pharmacometric model for iohexol and creatinine.<sup>136</sup> Following low-dose iohexol administration (259 mg), accurate estimates of both GFR and net creatinine tubular secretion mediated by renal transporters were obtained from a single plasma sample at 5 hours post-dose, and a 0–5 hour urine collection.<sup>136</sup> These results highlight the potential for simplified protocols that simultaneously assess renal function and transporter activity through the combined use of endogenous biomarkers, LSS, and pharmacometric modeling.<sup>136</sup>

Despite these promising developments, several challenges remain. Progress in endogenous biomarker discovery has been concentrated on specific transporters such as hepatic OATP1B1 (e.g., coproporphyrin I [CPI]), renal OCT2/MATE1/2-K (e.g., creatinine, NMN), and renal OAT1/3 (e.g., PDA).<sup>158</sup> However, suitable biomarkers for intestinal efflux transporters, including P-gp, remain unavailable, and data on BCRP are limited.<sup>158</sup> Moreover, while CPI has been widely studied as a marker for OATP1B activity in populations with renal or hepatic impairment, hyperlipidemia, rheumatoid arthritis, and some cancers,<sup>249,250</sup> baseline values for CPI in other patient groups remain undefined.<sup>158</sup> Similarly, there is still a lack of validated endogenous biomarkers for non-hepatic transporters, particularly those expressed in the kidney and intestine.<sup>158</sup>

Another complicating factor is that disease states affect not only transporter function but also the synthesis and elimination of endogenous biomarkers, adding complexity to biomarker-based transporter phenotyping.<sup>158</sup> In particular, recent modeling of CPI in individuals with renal impairment has demonstrated that disease-related alterations extend beyond impaired renal clearance.<sup>251</sup> The analysis demonstrated substantial reductions in CPI synthesis, impaired hepatic uptake via OATP1B1, and a decline in plasma protein binding.<sup>251</sup> These overlapping physiological disturbances complicate the interpretation of biomarker data.<sup>158</sup>

Therefore, there is a critical need for refined PK models capable of deconvoluting these interacting effects to improve the accuracy, interpretability, and clinical applicability of transporter phenotyping across heterogeneous patient populations.<sup>158</sup>

Looking ahead, emerging technologies such as liquid biopsy using small extracellular vesicles (sEVs) hold promise for advancing transporter phenotyping.<sup>158</sup> sEVs can provide a minimally invasive means to assess the expression of drug-metabolizing enzymes (DMEs) and transporters in key disposition organs.<sup>184,252</sup> While liver-derived sEVs have been characterized, reliable biomarkers for other organs remain under active investigation.<sup>158</sup> Although sEVs offer insights into transporter abundance, their relationship to functional activity is not yet fully understood.<sup>253</sup> Integrating sEV-derived abundance data with functional assessments based on endogenous biomarkers could provide a more comprehensive understanding of transporter behavior in the context of disease and genetic variation.<sup>158</sup>

Together, combining endogenous biomarkers with LSS and pharmacometric modeling provides a streamlined, low-burden approach to transporter phenotyping. While this integrated framework shows promising potential for early drug development and special populations, broader validation and the incorporation of emerging tools like liquid biopsy are needed to fully establish its clinical utility.

#### **4.3.2.4 Inhibitor-based validation in diverse patient populations**

The inclusion of well-characterized transporter inhibitors in cocktail studies provides a powerful strategy to validate both probe drugs and endogenous biomarkers. Inhibitors such as cimetidine, dolutegravir, and pyrimethamine (targeting OCTs and MATEs); probenecid (for OAT1 and OAT3); and verapamil and cyclosporin A (for P-gp and OATP1B1) can be strategically utilized to assess the sensitivity and selectivity of each probe.<sup>19</sup> By comparing PK parameters with and without these inhibitors, the specific contribution of individual transporters can be more precisely elucidated.

To ensure the clinical applicability of these findings, it is crucial to extend evaluations to diverse patient populations and disease states. Physiological and pathological variability, such as alterations in transporter expression, organ function, or biomarker levels, may significantly impact transporter activity and probe performance. Broader clinical testing is therefore essential to confirm the robustness of these approaches in real-world settings.

## 5. Acknowledgment

I would like to express my deepest gratitude to all those who have supported me throughout my PhD studies and the preparation of this thesis.

First and foremost, I am profoundly grateful to Univ.-Prof. Dr. Uwe Fuhr for the opportunity to pursue my doctoral research within his group. His exceptional mentorship, unwavering support, and continuous encouragement have been invaluable at every stage of this journey.

I extend my sincere thanks to Prof. Dr. rer. nat. Dirk Gründemann for his guidance in the in vitro assays, and to PD Dr. med. Max Philipp Taubert for his insightful advice and continuous support during the pharmacokinetic analyses that formed a central part of this work.

I am also grateful to Prof. Dr. rer. nat. Yohannes Hagos and Dr. rer. nat. Annett Kühne from PortaCellTec Biosciences for their excellent collaboration and essential contributions to the in vitro experiment.

Special thanks go to Univ.-Prof. Dr. Elke Schäffner, MSc, Prof. Prof. h.c. Dr. med. Markus van der Giet, and PD Dr. med. Natalie Ebert, MPH for their collaboration and for providing the iohexol datasets that were crucial to the development of improved correction formulas in this research.

I would like to thank Dr. Martina Kinzig, Prof. Dr. Fritz Sörgel, and Prof. Dr. Oliver Scherf-Clavel for the productive collaboration on the population pharmacokinetic analysis of adefovir and their valuable contributions to the associated publication.

My heartfelt appreciation goes to Sylvia Goitzsch, Simone Kalis, Samira Boussettaoui, Kathi Krüsemann, and Iris Villani for their excellent technical support, which greatly facilitated my experimental work.

I am also thankful to all colleagues from Department I of Pharmacology, including Dr. Tobias Heinen, Dr. Charalambos Dokos, Dr. Sören Büsker, Dr. Muhammad Bilal, Jil Hennig, Maria Alejandra Acosta Serrano, Chiara Mandl, Dr. Chunli Chen, Zhendong Chen, Jiang Zhixin, Huiping Huang, and Wenyu Yang, for their collegiality and scientific discussions.

In particular, I wish to thank Svenja Flögel, Dr. Lea Hartmann, and Maurice Tust for their outstanding support during the in vitro studies.

Last but not least, I owe my deepest thanks to my parents, my husband Tom, and my friends for their unwavering love, patience, and encouragement. Their support has been a constant source of strength throughout this journey.

## Reference

1. Feng B, Varma MV. Evaluation and Quantitative Prediction of Renal Transporter-Mediated Drug-Drug Interactions. *J Clin Pharmacol*. Jul 2016;56 Suppl 7:S110-21. doi:10.1002/jcph.702
2. Morrissey KM, Stocker SL, Wittwer MB, Xu L, Giacomini KM. Renal transporters in drug development. *Annu Rev Pharmacol Toxicol*. 2013;53:503-29. doi:10.1146/annurev-pharmtox-011112-140317
3. Fuhr U, Hsin CH, Li X, Jabrane W, Sörgel F. Assessment of Pharmacokinetic Drug-Drug Interactions in Humans: In Vivo Probe Substrates for Drug Metabolism and Drug Transport Revisited. *Annu Rev Pharmacol Toxicol*. Jan 6 2019;59:507-536. doi:10.1146/annurev-pharmtox-010818-021909
4. Dong Q, Fuhr U, Schaeffner E, van der Giet M, Ebert N, Taubert M. Improved correction formulas to estimate iohexol clearance from simple models. *Eur J Clin Pharmacol*. Sep 2023;79(9):1215-1217. doi:10.1007/s00228-023-03535-y
5. Dong Q, Chen Z, Boland J, et al. Validating Low-Dose Iohexol as a Marker for Glomerular Filtration Rate by In Vitro and In Vivo Studies. *Clin Transl Sci*. Feb 2025;18(2):e70141. doi:10.1111/cts.70141
6. Dong Q, Chen C, Taubert M, et al. Understanding adefovir pharmacokinetics as a component of a transporter phenotyping cocktail. *Eur J Clin Pharmacol*. Jul 2024;80(7):1069-1078. doi:10.1007/s00228-024-03673-x
7. Haraldsson B, Nyström J, Deen WM. Properties of the glomerular barrier and mechanisms of proteinuria. *Physiol Rev*. Apr 2008;88(2):451-87. doi:10.1152/physrev.00055.2006
8. Arif E, Nihalani D. Glomerular Filtration Barrier Assembly: An insight. *Postdoc J*. Apr 2013;1(4):33-45.
9. Feng B, LaPerle JL, Chang G, Varma MV. Renal clearance in drug discovery and development: molecular descriptors, drug transporters and disease state. *Expert Opin Drug Metab Toxicol*. Aug 2010;6(8):939-52. doi:10.1517/17425255.2010.482930
10. Tett SE, Kirkpatrick CM, Gross AS, McLachlan AJ. Principles and clinical application of assessing alterations in renal elimination pathways. *Clin Pharmacokinet*. 2003;42(14):1193-211. doi:10.2165/00003088-200342140-00002
11. Kaufman DP BH, Knohl SJ. Physiology, Glomerular Filtration Rate. [Updated 2023 Jul 17]. In: StatPearls [Internet]. Treasure Island (FL): StatPearls Publishing; 2025 Jan-. Available from: <https://www.ncbi.nlm.nih.gov/books/NBK500032/>.
12. Inker LA, Titan S. Measurement and Estimation of GFR for Use in Clinical Practice: Core Curriculum 2021. *Am J Kidney Dis*. Nov 2021;78(5):736-749. doi:10.1053/j.ajkd.2021.04.016
13. Davies NM, Anderson KE. Clinical pharmacokinetics of naproxen. *Clin Pharmacokinet*. Apr 1997;32(4):268-93. doi:10.2165/00003088-199732040-00002
14. Ivanyuk A, Livio F, Biollaz J, Buclin T. Renal Drug Transporters and Drug Interactions. *Clin Pharmacokinet*. Aug 2017;56(8):825-892. doi:10.1007/s40262-017-0506-8

15. Pritchard JB, Miller DS. Mechanisms mediating renal secretion of organic anions and cations. *Physiol Rev.* Oct 1993;73(4):765-96. doi:10.1152/physrev.1993.73.4.765
16. Yin J, Wang J. Renal drug transporters and their significance in drug-drug interactions. *Acta Pharm Sin B.* Sep 2016;6(5):363-373. doi:10.1016/j.apsb.2016.07.013
17. König J, Müller F, Fromm MF. Transporters and drug-drug interactions: important determinants of drug disposition and effects. *Pharmacol Rev.* Jul 2013;65(3):944-66. doi:10.1124/pr.113.007518
18. European Medicines Agency. (2024). ICH M12 Guideline on Drug Interaction Studies. EMA/CHMP/ICH/652460/2022. Available from: [https://www.ema.europa.eu/en/documents/scientific-guideline/ich-m12-guideline-drug-interaction-studies-step-5\\_en.pdf](https://www.ema.europa.eu/en/documents/scientific-guideline/ich-m12-guideline-drug-interaction-studies-step-5_en.pdf). Accessed March 9, 2025.
19. U.S. Food and Drug Administration. (2024). M12 Drug Interaction Studies: Guidance for Industry. Available from: <https://www.fda.gov/media/161199/download> Accessed December 8, 2024.
20. European Medicines Agency. (2012). Guideline on the Investigation of Drug Interactions. Available from: [https://www.ema.europa.eu/en/documents/scientific-guideline/guideline-investigation-drug-interactions-revision-1\\_en.pdf](https://www.ema.europa.eu/en/documents/scientific-guideline/guideline-investigation-drug-interactions-revision-1_en.pdf). Accessed September 8, 2024.
21. Koepsell H. Role of organic cation transporters in drug-drug interaction. *Expert Opin Drug Metab Toxicol.* 2015;11(10):1619-33. doi:10.1517/17425255.2015.1069274
22. Gorboulev V, Ulzheimer JC, Akhoundova A, et al. Cloning and Characterization of Two Human Polyspecific Organic Cation Transporters. *DNA and Cell Biology.* 1997/07/01 1997;16(7):871-881. doi:10.1089/dna.1997.16.871
23. Gründemann D, Schechinger B, Rappold GA, Schömig E. Molecular identification of the corticosterone-sensitive extraneuronal catecholamine transporter. *Nat Neurosci.* Sep 1998;1(5):349-51. doi:10.1038/1557
24. *Drug transporters: Molecular characterization and role in drug disposition (3rd ed.)*. Wiley; 2022.
25. Koepsell H, Lips K, Volk C. Polyspecific organic cation transporters: structure, function, physiological roles, and biopharmaceutical implications. *Pharm Res.* Jul 2007;24(7):1227-51. doi:10.1007/s11095-007-9254-z
26. Tzvetkov MV, Vormfelde SV, Balen D, et al. The effects of genetic polymorphisms in the organic cation transporters OCT1, OCT2, and OCT3 on the renal clearance of metformin. *Clin Pharmacol Ther.* Sep 2009;86(3):299-306. doi:10.1038/clpt.2009.92
27. Graham GG, Punt J, Arora M, et al. Clinical pharmacokinetics of metformin. *Clin Pharmacokinet.* Feb 2011;50(2):81-98. doi:10.2165/11534750-000000000-00000
28. Nies AT, Koepsell H, Damme K, Schwab M. Organic cation transporters (OCTs, MATEs), in vitro and in vivo evidence for the importance in drug therapy. *Handb Exp Pharmacol.* 2011;(201):105-67. doi:10.1007/978-3-642-14541-4\_3

29. Zhang X, He X, Baker J, Tama F, Chang G, Wright SH. Twelve transmembrane helices form the functional core of mammalian MATE1 (multidrug and toxin extruder 1) protein. *J Biol Chem*. Aug 10 2012;287(33):27971-82. doi:10.1074/jbc.M112.386979
30. Nies AT, Damme K, Kruck S, Schaeffeler E, Schwab M. Structure and function of multidrug and toxin extrusion proteins (MATEs) and their relevance to drug therapy and personalized medicine. *Arch Toxicol*. Jul 2016;90(7):1555-84. doi:10.1007/s00204-016-1728-5
31. Komatsu T, Hiasa M, Miyaji T, et al. Characterization of the human MATE2 proton-coupled polyspecific organic cation exporter. *Int J Biochem Cell Biol*. Jun 2011;43(6):913-8. doi:10.1016/j.biocel.2011.03.005
32. Masuda S, Terada T, Yonezawa A, et al. Identification and functional characterization of a new human kidney-specific H<sup>+</sup>/organic cation antiporter, kidney-specific multidrug and toxin extrusion 2. *J Am Soc Nephrol*. Aug 2006;17(8):2127-35. doi:10.1681/asn.2006030205
33. Tanihara Y, Masuda S, Sato T, Katsura T, Ogawa O, Inui K. Substrate specificity of MATE1 and MATE2-K, human multidrug and toxin extrusions/H(+)-organic cation antiporters. *Biochem Pharmacol*. Jul 15 2007;74(2):359-71. doi:10.1016/j.bcp.2007.04.010
34. Ito S, Kusuhara H, Yokochi M, et al. Competitive inhibition of the luminal efflux by multidrug and toxin extrusions, but not basolateral uptake by organic cation transporter 2, is the likely mechanism underlying the pharmacokinetic drug-drug interactions caused by cimetidine in the kidney. *J Pharmacol Exp Ther*. Feb 2012;340(2):393-403. doi:10.1124/jpet.111.184986
35. Sakaeda T. MDR1 genotype-related pharmacokinetics: fact or fiction? *Drug Metab Pharmacokinet*. Dec 2005;20(6):391-414. doi:10.2133/dmpk.20.391
36. Burckhardt G. Drug transport by Organic Anion Transporters (OATs). *Pharmacol Ther*. Oct 2012;136(1):106-30. doi:10.1016/j.pharmthera.2012.07.010
37. Burckhardt G, Burckhardt BC. In vitro and in vivo evidence of the importance of organic anion transporters (OATs) in drug therapy. *Handb Exp Pharmacol*. 2011;(201):29-104. doi:10.1007/978-3-642-14541-4\_2
38. Roth M, Obaidat A, Hagenbuch B. OATPs, OATs and OCTs: the organic anion and cation transporters of the SLCO and SLC22A gene superfamilies. *Br J Pharmacol*. Mar 2012;165(5):1260-87. doi:10.1111/j.1476-5381.2011.01724.x
39. Trueck C, Hsin CH, Scherf-Clavel O, et al. A Clinical Drug-Drug Interaction Study Assessing a Novel Drug Transporter Phenotyping Cocktail With Adefovir, Sitagliptin, Metformin, Pitavastatin, and Digoxin. *Clin Pharmacol Ther*. Dec 2019;106(6):1398-1407. doi:10.1002/cpt.1564
40. Stevens LA, Levey AS. Measured GFR as a confirmatory test for estimated GFR. *J Am Soc Nephrol*. Nov 2009;20(11):2305-13. doi:10.1681/asn.2009020171
41. Dixon JJ, Lane K, Dalton RN, et al. Validation of a continuous infusion of low dose iohexol to measure glomerular filtration rate: randomised clinical trial. *J Transl Med*. Feb 12 2015;13:58. doi:10.1186/s12967-015-0414-3



42. Dixon JJ, Lane K, Dalton RN, et al. Continuous Infusion of Low-Dose Iohexol Measures Changing Glomerular Filtration Rate in Critically Ill Patients. *Crit Care Med*. Mar 2018;46(3):e190-e197. doi:10.1097/ccm.0000000000002870
43. Morales Castro D, Dresser L, Granton J, Fan E. Pharmacokinetic Alterations Associated with Critical Illness. *Clin Pharmacokinet*. Feb 2023;62(2):209-220. doi:10.1007/s40262-023-01213-x
44. Vilay AM, Churchwell MD, Mueller BA. Clinical review: Drug metabolism and nonrenal clearance in acute kidney injury. *Crit Care*. 2008;12(6):235. doi:10.1186/cc7093
45. Keddis MT, Amer H, Voskoboev N, Kremers WK, Rule AD, Lieske JC. Creatinine-Based and Cystatin C-Based GFR Estimating Equations and Their Non-GFR Determinants in Kidney Transplant Recipients. *Clin J Am Soc Nephrol*. Sep 7 2016;11(9):1640-1649. doi:10.2215/cjn.11741115
46. Shafi T, Levey AS. Measurement and Estimation of Residual Kidney Function in Patients on Dialysis. *Adv Chronic Kidney Dis*. Jan 2018;25(1):93-104. doi:10.1053/j.ackd.2017.09.001
47. Steubl D, Fan L, Michels WM, et al. Development and Validation of Residual Kidney Function Estimating Equations in Dialysis Patients. *Kidney Med*. May-Jun 2019;1(3):104-114. doi:10.1016/j.xkme.2019.04.002
48. Matzke GR, Aronoff GR, Atkinson AJ, Jr., et al. Drug dosing consideration in patients with acute and chronic kidney disease-a clinical update from Kidney Disease: Improving Global Outcomes (KDIGO). *Kidney Int*. Dec 2011;80(11):1122-37. doi:10.1038/ki.2011.322
49. Fuhr U, Jetter A, Kirchheiner J. Appropriate phenotyping procedures for drug metabolizing enzymes and transporters in humans and their simultaneous use in the "cocktail" approach. *Clin Pharmacol Ther*. Feb 2007;81(2):270-83. doi:10.1038/sj.clpt.6100050
50. Lepist EI, Ray AS. Renal Transporter-Mediated Drug-Drug Interactions: Are They Clinically Relevant? *J Clin Pharmacol*. Jul 2016;56 Suppl 7:S73-81. doi:10.1002/jcph.735
51. Kusuhara H, Ito S, Kumagai Y, et al. Effects of a MATE protein inhibitor, pyrimethamine, on the renal elimination of metformin at oral microdose and at therapeutic dose in healthy subjects. *Clin Pharmacol Ther*. Jun 2011;89(6):837-44. doi:10.1038/clpt.2011.36
52. Somogyi A, Muirhead M. Pharmacokinetic interactions of cimetidine 1987. *Clin Pharmacokinet*. May 1987;12(5):321-66. doi:10.2165/00003088-198712050-00002
53. Somogyi A, Stockley C, Keal J, Rolan P, Bochner F. Reduction of metformin renal tubular secretion by cimetidine in man. *Br J Clin Pharmacol*. May 1987;23(5):545-51. doi:10.1111/j.1365-2125.1987.tb03090.x
54. Wang ZJ, Yin OQ, Tomlinson B, Chow MS. OCT2 polymorphisms and in-vivo renal functional consequence: studies with metformin and cimetidine. *Pharmacogenet Genomics*. Jul 2008;18(7):637-45. doi:10.1097/FPC.0b013e328302cd41
55. Tahara H, Kusuhara H, Endou H, et al. A species difference in the transport activities of H<sub>2</sub> receptor antagonists by rat and human renal organic anion and cation transporters. *J Pharmacol Exp Ther*. Oct 2005;315(1):337-45. doi:10.1124/jpet.105.088104

56. Ito S, Kusuhashi H, Kuroiwa Y, et al. Potent and specific inhibition of mMate1-mediated efflux of type I organic cations in the liver and kidney by pyrimethamine. *J Pharmacol Exp Ther*. Apr 2010;333(1):341-50. doi:10.1124/jpet.109.163642
57. Song IH, Zong J, Borland J, et al. The Effect of Dolutegravir on the Pharmacokinetics of Metformin in Healthy Subjects. *J Acquir Immune Defic Syndr*. Aug 1 2016;72(4):400-7. doi:10.1097/qai.0000000000000983
58. Metsu D, Lanot T, Fraissinet F, et al. Comparing ultrafiltration and equilibrium dialysis to measure unbound plasma dolutegravir concentrations based on a design of experiment approach. *Sci Rep*. Jul 23 2020;10(1):12265. doi:10.1038/s41598-020-69102-y
59. Gelé T, Gouget H, Furlan V, et al. Characteristics of Dolutegravir and Bictegravir Plasma Protein Binding: a First Approach for the Study of Pharmacologic Sanctuaries. *Antimicrob Agents Chemother*. Oct 20 2020;64(11)doi:10.1128/aac.00895-20
60. Reese MJ, Savina PM, Generaux GT, et al. In vitro investigations into the roles of drug transporters and metabolizing enzymes in the disposition and drug interactions of dolutegravir, a HIV integrase inhibitor. *Drug Metab Dispos*. Feb 2013;41(2):353-61. doi:10.1124/dmd.112.048918
61. Arany I, Safirstein RL. Cisplatin nephrotoxicity. *Semin Nephrol*. Sep 2003;23(5):460-4. doi:10.1016/s0270-9295(03)00089-5
62. Pabla N, Dong Z. Cisplatin nephrotoxicity: mechanisms and renoprotective strategies. *Kidney Int*. May 2008;73(9):994-1007. doi:10.1038/sj.ki.5002786
63. Filipinski KK, Loos WJ, Verweij J, Sparreboom A. Interaction of Cisplatin with the human organic cation transporter 2. *Clin Cancer Res*. Jun 15 2008;14(12):3875-80. doi:10.1158/1078-0432.Ccr-07-4793
64. Tanihara Y, Masuda S, Katsura T, Inui K. Protective effect of concomitant administration of imatinib on cisplatin-induced nephrotoxicity focusing on renal organic cation transporter OCT2. *Biochem Pharmacol*. Nov 1 2009;78(9):1263-71. doi:10.1016/j.bcp.2009.06.014
65. Yonezawa A, Masuda S, Yokoo S, Katsura T, Inui K. Cisplatin and oxaliplatin, but not carboplatin and nedaplatin, are substrates for human organic cation transporters (SLC22A1-3 and multidrug and toxin extrusion family). *J Pharmacol Exp Ther*. Nov 2006;319(2):879-86. doi:10.1124/jpet.106.110346
66. Filipinski KK, Mathijssen RH, Mikkelsen TS, Schinkel AH, Sparreboom A. Contribution of organic cation transporter 2 (OCT2) to cisplatin-induced nephrotoxicity. *Clin Pharmacol Ther*. Oct 2009;86(4):396-402. doi:10.1038/clpt.2009.139
67. Ciarimboli G, Deuster D, Knief A, et al. Organic cation transporter 2 mediates cisplatin-induced oto- and nephrotoxicity and is a target for protective interventions. *Am J Pathol*. Mar 2010;176(3):1169-80. doi:10.2353/ajpath.2010.090610
68. Sprowl JA, van Doorn L, Hu S, et al. Conjunctive therapy of cisplatin with the OCT2 inhibitor cimetidine: influence on antitumor efficacy and systemic clearance. *Clin Pharmacol Ther*. Nov 2013;94(5):585-92. doi:10.1038/clpt.2013.145

69. Nakamura T, Yonezawa A, Hashimoto S, Katsura T, Inui K. Disruption of multidrug and toxin extrusion MATE1 potentiates cisplatin-induced nephrotoxicity. *Biochem Pharmacol.* Dec 1 2010;80(11):1762-7. doi:10.1016/j.bcp.2010.08.019
70. Li Q, Guo D, Dong Z, et al. Ondansetron can enhance cisplatin-induced nephrotoxicity via inhibition of multiple toxin and extrusion proteins (MATEs). *Toxicol Appl Pharmacol.* Nov 15 2013;273(1):100-9. doi:10.1016/j.taap.2013.08.024
71. Emanuelsson BM, Beermann B, Paalzow LK. Non-linear elimination and protein binding of probenecid. *Eur J Clin Pharmacol.* 1987;32(4):395-401. doi:10.1007/bf00543976
72. Brown GR. Cephalosporin-probenecid drug interactions. *Clin Pharmacokinet.* Apr 1993;24(4):289-300. doi:10.2165/00003088-199324040-00003
73. Griffith RS, Black HR, Brier GL, Wolny JD. Effect of probenecid on the blood levels and urinary excretion of cefamandole. *Antimicrob Agents Chemother.* May 1977;11(5):809-12. doi:10.1128/aac.11.5.809
74. Ho ES, Lin DC, Mendel DB, Cihlar T. Cytotoxicity of antiviral nucleotides adefovir and cidofovir is induced by the expression of human renal organic anion transporter 1. *J Am Soc Nephrol.* Mar 2000;11(3):383-393. doi:10.1681/asn.V113383
75. Servais A, Lechat P, Zahr N, et al. Tubular transporters and clearance of adefovir. *Eur J Pharmacol.* Jul 1 2006;540(1-3):168-74. doi:10.1016/j.ejphar.2006.04.047
76. Gilead Sciences Ltd. Vistide (cidofovir) 75 mg/ml concentrate for solution for infusion: Summary of Product Characteristics. European Medicines Agency; 2024. Accessed March 20, 2025. [https://www.ema.europa.eu/en/documents/product-information/vistide-epar-product-information\\_en.pdf](https://www.ema.europa.eu/en/documents/product-information/vistide-epar-product-information_en.pdf).
77. Gessner A, König J, Fromm MF. Clinical Aspects of Transporter-Mediated Drug-Drug Interactions. *Clin Pharmacol Ther.* Jun 2019;105(6):1386-1394. doi:10.1002/cpt.1360
78. Shen DD, Azarnoff DL. Clinical pharmacokinetics of methotrexate. *Clin Pharmacokinet.* Jan-Feb 1978;3(1):1-13. doi:10.2165/00003088-197803010-00001
79. Kremer JM, Hamilton RA. The effects of nonsteroidal antiinflammatory drugs on methotrexate (MTX) pharmacokinetics: impairment of renal clearance of MTX at weekly maintenance doses but not at 7.5 mg. *J Rheumatol.* Nov 1995;22(11):2072-7.
80. Frenia ML, Long KS. Methotrexate and nonsteroidal antiinflammatory drug interactions. *Ann Pharmacother.* Feb 1992;26(2):234-7. doi:10.1177/106002809202600219
81. Aherne GW, Piall E, Marks V, Mould G, White WF. Prolongation and enhancement of serum methotrexate concentrations by probenecid. *Br Med J.* Apr 29 1978;1(6120):1097-9. doi:10.1136/bmj.1.6120.1097
82. Frain JB. Methotrexate toxicity in a patient receiving trimethoprim-sulfamethoxazole. *J Rheumatol.* Feb 1987;14(1):176-7.
83. Thomas MH, Gutterman LA. Methotrexate toxicity in a patient receiving trimethoprim-sulfamethoxazole. *J Rheumatol.* Apr 1986;13(2):440-1.
84. Steuer A, Gumpel JM. Methotrexate and trimethoprim: a fatal interaction. *Br J Rheumatol.* Jan 1998;37(1):105-6. doi:10.1093/rheumatology/37.1.105

85. Yang CH, Yang LJ, Jaing TH, Chan HL. Toxic epidermal necrolysis following combination of methotrexate and trimethoprim-sulfamethoxazole. *Int J Dermatol*. Aug 2000;39(8):621-3. doi:10.1046/j.1365-4362.2000.00022-3.x
86. Basin KS, Escalante A, Beardmore TD. Severe pancytopenia in a patient taking low dose methotrexate and probenecid. *J Rheumatol*. Apr 1991;18(4):609-10.
87. Ferrazzini G, Klein J, Sulh H, Chung D, Griesbrecht E, Koren G. Interaction between trimethoprim-sulfamethoxazole and methotrexate in children with leukemia. *J Pediatr*. Nov 1990;117(5):823-6. doi:10.1016/s0022-3476(05)83351-7
88. Bourré-Tessier J, Haraoui B. Methotrexate drug interactions in the treatment of rheumatoid arthritis: a systematic review. *J Rheumatol*. Jul 2010;37(7):1416-21. doi:10.3899/jrheum.090153
89. Li M, Anderson GD, Wang J. Drug-drug interactions involving membrane transporters in the human kidney. *Expert Opin Drug Metab Toxicol*. Aug 2006;2(4):505-32. doi:10.1517/17425255.2.4.505
90. Giacomini KM, Huang SM, Tweedie DJ, et al. Membrane transporters in drug development. *Nat Rev Drug Discov*. Mar 2010;9(3):215-36. doi:10.1038/nrd3028
91. Ma JD, Tsunoda SM, Bertino JS, Jr., Trivedi M, Beale KK, Nafziger AN. Evaluation of in vivo P-glycoprotein phenotyping probes: a need for validation. *Clin Pharmacokinet*. Apr 2010;49(4):223-37. doi:10.2165/11318000-000000000-00000
92. Bauman JL, Didomenico RJ, Galanter WL. Mechanisms, manifestations, and management of digoxin toxicity in the modern era. *Am J Cardiovasc Drugs*. 2006;6(2):77-86. doi:10.2165/00129784-200606020-00002
93. Feng B, Mills JB, Davidson RE, et al. In vitro P-glycoprotein assays to predict the in vivo interactions of P-glycoprotein with drugs in the central nervous system. *Drug Metab Dispos*. Feb 2008;36(2):268-75. doi:10.1124/dmd.107.017434
94. Ochs HR, Bodem G, Greenblatt DJ. Impairment of digoxin clearance by coadministration of quinidine. *J Clin Pharmacol*. Oct 1981;21(10):396-400. doi:10.1002/j.1552-4604.1981.tb01739.x
95. Fromm MF, Kim RB, Stein CM, Wilkinson GR, Roden DM. Inhibition of P-glycoprotein-mediated drug transport: A unifying mechanism to explain the interaction between digoxin and quinidine [see comments]. *Circulation*. Feb 2 1999;99(4):552-7. doi:10.1161/01.cir.99.4.552
96. Pedersen KE, Dorph-Pedersen A, Hvidt S, Klitgaard NA, Nielsen-Kudsk F. Digoxin-verapamil interaction. *Clin Pharmacol Ther*. Sep 1981;30(3):311-6. doi:10.1038/clpt.1981.165
97. Rengelshausen J, Göggelmann C, Burhenne J, et al. Contribution of increased oral bioavailability and reduced nonglomerular renal clearance of digoxin to the digoxin-clarithromycin interaction. *Br J Clin Pharmacol*. Jul 2003;56(1):32-8. doi:10.1046/j.1365-2125.2003.01824.x
98. Okamura N, Hirai M, Tanigawara Y, et al. Digoxin-cyclosporin A interaction: modulation of the multidrug transporter P-glycoprotein in the kidney. *J Pharmacol Exp Ther*. Sep 1993;266(3):1614-9.

99. Jalava KM, Partanen J, Neuvonen PJ. Itraconazole decreases renal clearance of digoxin. *Ther Drug Monit.* Dec 1997;19(6):609-13. doi:10.1097/00007691-199712000-00001
100. Ding R, Tayrouz Y, Riedel KD, et al. Substantial pharmacokinetic interaction between digoxin and ritonavir in healthy volunteers. *Clin Pharmacol Ther.* Jul 2004;76(1):73-84. doi:10.1016/j.clpt.2004.02.008
101. Penzak SR, Shen JM, Alfaro RM, Remaley AT, Natarajan V, Falloon J. Ritonavir decreases the nonrenal clearance of digoxin in healthy volunteers with known MDR1 genotypes. *Ther Drug Monit.* Jun 2004;26(3):322-30. doi:10.1097/00007691-200406000-00018
102. Shemesh O, Golbetz H, Kriss JP, Myers BD. Limitations of creatinine as a filtration marker in glomerulopathic patients. *Kidney Int.* Nov 1985;28(5):830-8. doi:10.1038/ki.1985.205
103. Zou W, Shi B, Zeng T, et al. Drug Transporters in the Kidney: Perspectives on Species Differences, Disease Status, and Molecular Docking. *Front Pharmacol.* 2021;12:746208. doi:10.3389/fphar.2021.746208
104. Deguchi T, Kusuhara H, Takadate A, Endou H, Otagiri M, Sugiyama Y. Characterization of uremic toxin transport by organic anion transporters in the kidney. *Kidney Int.* Jan 2004;65(1):162-74. doi:10.1111/j.1523-1755.2004.00354.x
105. Sun H, Frassetto L, Benet LZ. Effects of renal failure on drug transport and metabolism. *Pharmacol Ther.* Jan 2006;109(1-2):1-11. doi:10.1016/j.pharmthera.2005.05.010
106. Zhong K, Li X, Xie C, Zhang Y, Zhong D, Chen X. Effects of renal impairment on the pharmacokinetics of morinidazole: uptake transporter-mediated renal clearance of the conjugated metabolites. *Antimicrob Agents Chemother.* Jul 2014;58(7):4153-61. doi:10.1128/aac.02414-14
107. Kong F, Pang X, Zhong K, et al. Increased Plasma Exposures of Conjugated Metabolites of Morinidazole in Renal Failure Patients: A Critical Role of Uremic Toxins. *Drug Metab Dispos.* Jun 2017;45(6):593-603. doi:10.1124/dmd.116.074492
108. Nishizawa K, Yoda N, Morokado F, Komori H, Nakanishi T, Tamai I. Changes of drug pharmacokinetics mediated by downregulation of kidney organic cation transporters Mate1 and Oct2 in a rat model of hyperuricemia. *PLoS One.* 2019;14(4):e0214862. doi:10.1371/journal.pone.0214862
109. Koepsell H. Polyspecific organic cation transporters and their biomedical relevance in kidney. *Curr Opin Nephrol Hypertens.* Sep 2013;22(5):533-8. doi:10.1097/MNH.0b013e328363ffaf
110. Chu XY, Bleasby K, Yabut J, et al. Transport of the dipeptidyl peptidase-4 inhibitor sitagliptin by human organic anion transporter 3, organic anion transporting polypeptide 4C1, and multidrug resistance P-glycoprotein. *J Pharmacol Exp Ther.* May 2007;321(2):673-83. doi:10.1124/jpet.106.116517
111. Musso CG, Belloso WH, Scibona P, Bellizzi V, Macías Núñez JF. Impact of renal aging on drug therapy. *Postgrad Med.* Aug 2015;127(6):623-9. doi:10.1080/00325481.2015.1063957

112. Glasscock RJ, Rule AD. The implications of anatomical and functional changes of the aging kidney: with an emphasis on the glomeruli. *Kidney Int.* Aug 2012;82(3):270-7. doi:10.1038/ki.2012.65
113. Cheung KWK, van Groen BD, Spaans E, et al. A Comprehensive Analysis of Ontogeny of Renal Drug Transporters: mRNA Analyses, Quantitative Proteomics, and Localization. *Clin Pharmacol Ther.* Nov 2019;106(5):1083-1092. doi:10.1002/cpt.1516
114. Joseph S, Nicolson TJ, Hammons G, Word B, Green-Knox B, Lyn-Cook B. Expression of drug transporters in human kidney: impact of sex, age, and ethnicity. *Biol Sex Differ.* 2015;6:4. doi:10.1186/s13293-015-0020-3
115. Levey AS, Coresh J, Tighiouart H, Greene T, Inker LA. Measured and estimated glomerular filtration rate: current status and future directions. *Nat Rev Nephrol.* Jan 2020;16(1):51-64. doi:10.1038/s41581-019-0191-y
116. Delanaye P, Melsom T, Ebert N, et al. Iohexol plasma clearance for measuring glomerular filtration rate in clinical practice and research: a review. Part 2: Why to measure glomerular filtration rate with iohexol? *Clin Kidney J.* Oct 2016;9(5):700-4. doi:10.1093/ckj/sfw071
117. Taubert M, Ebert N, Martus P, van der Giet M, Fuhr U, Schaeffner E. Using a three-compartment model improves the estimation of iohexol clearance to assess glomerular filtration rate. *Sci Rep.* Dec 7 2018;8(1):17723. doi:10.1038/s41598-018-35989-x
118. KDIGO 2012 Clinical Practice Guideline for the Evaluation and Management of Chronic Kidney Disease. *Kidney Int Suppl.* January 2013;3(1):1–150.
119. Mathialagan S, Rodrigues AD, Feng B. Evaluation of Renal Transporter Inhibition Using Creatinine as a Substrate In Vitro to Assess the Clinical Risk of Elevated Serum Creatinine. *J Pharm Sci.* Sep 2017;106(9):2535-2541. doi:10.1016/j.xphs.2017.04.009
120. Lepist EI, Zhang X, Hao J, et al. Contribution of the organic anion transporter OAT2 to the renal active tubular secretion of creatinine and mechanism for serum creatinine elevations caused by cobicistat. *Kidney Int.* Aug 2014;86(2):350-7. doi:10.1038/ki.2014.66
121. Stehlé T, Delanaye P. Which is the best glomerular filtration marker: Creatinine, cystatin C or both? *Eur J Clin Invest.* Oct 2024;54(10):e14278. doi:10.1111/eci.14278
122. Levey AS, Stevens LA, Schmid CH, et al. A new equation to estimate glomerular filtration rate. *Ann Intern Med.* May 5 2009;150(9):604-12. doi:10.7326/0003-4819-150-9-200905050-00006
123. Levey AS, Bosch JP, Lewis JB, Greene T, Rogers N, Roth D. A more accurate method to estimate glomerular filtration rate from serum creatinine: a new prediction equation. Modification of Diet in Renal Disease Study Group. *Ann Intern Med.* Mar 16 1999;130(6):461-70. doi:10.7326/0003-4819-130-6-199903160-00002
124. Matsushita K, Mahmoodi BK, Woodward M, et al. Comparison of risk prediction using the CKD-EPI equation and the MDRD study equation for estimated glomerular filtration rate. *Jama.* May 9 2012;307(18):1941-51. doi:10.1001/jama.2012.3954

125. Chen DC, Potok OA, Rifkin D, Estrella MM. Advantages, Limitations, and Clinical Considerations in Using Cystatin C to Estimate GFR. *Kidney360*. Oct 27 2022;3(10):1807-1814. doi:10.34067/kid.0003202022
126. Inker LA, Schmid CH, Tighiouart H, et al. Estimating glomerular filtration rate from serum creatinine and cystatin C. *N Engl J Med*. Jul 5 2012;367(1):20-9. doi:10.1056/NEJMoa1114248
127. Delanaye P, Cavalier E, Pottel H, Stehlé T. New and old GFR equations: a European perspective. *Clin Kidney J*. Sep 2023;16(9):1375-1383. doi:10.1093/ckj/sfad039
128. KDIGO 2024 Clinical Practice Guideline for the Evaluation and Management of Chronic Kidney Disease. *Kidney Int*. Apr 2024;105(4s):S117-s314. doi:10.1016/j.kint.2023.10.018
129. Inker LA, Eneanya ND, Coresh J, et al. New Creatinine- and Cystatin C-Based Equations to Estimate GFR without Race. *N Engl J Med*. Nov 4 2021;385(19):1737-1749. doi:10.1056/NEJMoa2102953
130. Pottel H, Björk J, Courbebaisse M, et al. Development and Validation of a Modified Full Age Spectrum Creatinine-Based Equation to Estimate Glomerular Filtration Rate : A Cross-sectional Analysis of Pooled Data. *Ann Intern Med*. Feb 2021;174(2):183-191. doi:10.7326/m20-4366
131. Björk J, Grubb A, Sterner G, Nyman U. Revised equations for estimating glomerular filtration rate based on the Lund-Malmö Study cohort. *Scand J Clin Lab Invest*. May 2011;71(3):232-9. doi:10.3109/00365513.2011.557086
132. Schaeffner ES, Ebert N, Delanaye P, et al. Two novel equations to estimate kidney function in persons aged 70 years or older. *Ann Intern Med*. Oct 2 2012;157(7):471-81. doi:10.7326/0003-4819-157-7-201210020-00003
133. Ebert N, Schaeffner E, Seegmiller JC, et al. Iohexol plasma clearance measurement protocol standardization for adults: a consensus paper of the European Kidney Function Consortium. *Kidney Int*. Oct 2024;106(4):583-596. doi:10.1016/j.kint.2024.06.029
134. Salmon-Gandonnière C, Benz-de Bretagne I, Mercier E, et al. Iohexol clearance in unstable critically ill patients: a tool to assess glomerular filtration rate. *Clin Chem Lab Med*. Nov 1 2016;54(11):1777-1786. doi:10.1515/cclm-2015-1202
135. Levey AS, Inker LA. GFR Evaluation in Living Kidney Donor Candidates. *J Am Soc Nephrol*. Apr 2017;28(4):1062-1071. doi:10.1681/asn.2016070790
136. Chen Z, Dong Q, Dokos C, Boland J, Fuhr U, Taubert M. A Joint Pharmacometric Model of Iohexol and Creatinine Administered through a Meat Meal to Assess GFR and Renal OCT2/MATE Activity. *Clin Pharmacol Ther*. Feb 25 2025;doi:10.1002/cpt.3612
137. GE Healthcare. OMNIPAQUE (iohexol) injection and oral solution [package insert]. Food and Drug Administration. Revised October 2024. Available at: [https://www.accessdata.fda.gov/drugsatfda\\_docs/label/2024/018956Orig1s119,020608Orig1s047lbl.pdf](https://www.accessdata.fda.gov/drugsatfda_docs/label/2024/018956Orig1s119,020608Orig1s047lbl.pdf). Accessed December 13, 2024.
138. McDonald JS, Larson NB, Schmitz JJ, et al. Acute Adverse Events After Iodinated Contrast Agent Administration of 359,977 Injections: A Single-Center Retrospective Study. *Mayo Clin Proc*. Dec 2023;98(12):1820-1830. doi:10.1016/j.mayocp.2023.02.032

139. Khwaja A. KDIGO clinical practice guidelines for acute kidney injury. *Nephron Clin Pract.* 2012;120(4):c179-84. doi:10.1159/000339789
140. Kane GC, Doyle BJ, Lerman A, Barsness GW, Best PJ, Rihal CS. Ultra-low contrast volumes reduce rates of contrast-induced nephropathy in patients with chronic kidney disease undergoing coronary angiography. *J Am Coll Cardiol.* Jan 1 2008;51(1):89-90. doi:10.1016/j.jacc.2007.09.019
141. Masereeuw R, Moons MM, Smits P, Russel FG. Glomerular filtration and saturable absorption of iohexol in the rat isolated perfused kidney. *Br J Pharmacol.* Sep 1996;119(1):57-64. doi:10.1111/j.1476-5381.1996.tb15677.x
142. Yang S, Dai Y, Liu Z, et al. Involvement of organic cation transporter 2 in the metformin-associated increased lactate levels caused by contrast-induced nephropathy. *Biomed Pharmacother.* Oct 2018;106:1760-1766. doi:10.1016/j.biopha.2018.07.068
143. Supawat B, Udomtanakunchai C, Kothan S, Tungjai M. The Effects of Iodinated Radiographic Contrast Media on Multidrug-resistant K562/Dox Cells: Mitochondria Impairment and P-glycoprotein Inhibition. *Cell Biochem Biophys.* Jun 2019;77(2):157-163. doi:10.1007/s12013-019-00868-3
144. Shannon JA, Smith HW. THE EXCRETION OF INULIN, XYLOSE AND UREA BY NORMAL AND PHLORIZINIZED MAN. *J Clin Invest.* Jul 1935;14(4):393-401. doi:10.1172/jci100690
145. Lin K, Kong X, Tao X, et al. Research Methods and New Advances in Drug-Drug Interactions Mediated by Renal Transporters. *Molecules.* Jul 6 2023;28(13)doi:10.3390/molecules28135252
146. Russell LE, Yadav J, Maldonado BJ, et al. Transporter-mediated drug-drug interactions: regulatory guidelines, in vitro and in vivo methodologies and translation, special populations, and the blood-brain barrier. *Drug Metab Rev.* Jul 5 2024;1-28. doi:10.1080/03602532.2024.2364591
147. Brouwer KL, Keppler D, Hoffmaster KA, et al. In vitro methods to support transporter evaluation in drug discovery and development. *Clin Pharmacol Ther.* Jul 2013;94(1):95-112. doi:10.1038/clpt.2013.81
148. Bach M, Grigat S, Pawlik B, et al. Fast set-up of doxycycline-inducible protein expression in human cell lines with a single plasmid based on Epstein-Barr virus replication and the simple tetracycline repressor. *Febs j.* Feb 2007;274(3):783-90. doi:10.1111/j.1742-4658.2006.05623.x
149. Hsin CH, Kuehne A, Gu Y, et al. In vitro validation of an in vivo phenotyping drug cocktail for major drug transporters in humans. *Eur J Pharm Sci.* Jul 1 2023;186:106459. doi:10.1016/j.ejps.2023.106459
150. Tucker GT, Casey C, Phillips PJ, Connor H, Ward JD, Woods HF. Metformin kinetics in healthy subjects and in patients with diabetes mellitus. *Br J Clin Pharmacol.* Aug 1981;12(2):235-46. doi:10.1111/j.1365-2125.1981.tb01206.x
151. Krishnan S, Ramsden D, Ferguson D, et al. Challenges and Opportunities for Improved Drug-Drug Interaction Predictions for Renal OCT2 and MATE1/2-K Transporters. *Clin Pharmacol Ther.* Sep 2022;112(3):562-572. doi:10.1002/cpt.2666



152. Mathialagan S, Feng B, Rodrigues AD, Varma MVS. Drug-Drug Interactions Involving Renal OCT2/MATE Transporters: Clinical Risk Assessment May Require Endogenous Biomarker-Informed Approach. *Clin Pharmacol Ther.* Oct 2021;110(4):855-859. doi:10.1002/cpt.2089
153. Terada T, Inui K. Physiological and pharmacokinetic roles of H<sup>+</sup>/organic cation antiporters (MATE/SLC47A). *Biochem Pharmacol.* May 1 2008;75(9):1689-96. doi:10.1016/j.bcp.2007.12.008
154. Yee SW, Brackman DJ, Ennis EA, et al. Influence of Transporter Polymorphisms on Drug Disposition and Response: A Perspective From the International Transporter Consortium. *Clin Pharmacol Ther.* Nov 2018;104(5):803-817. doi:10.1002/cpt.1098
155. Zong J, Borland J, Jerva F, Wynne B, Choukour M, Song I. The effect of dolutegravir on the pharmacokinetics of metformin in healthy subjects. *J Int AIDS Soc.* 2014;17(4 Suppl 3):19584. doi:10.7448/IAS.17.4.19584
156. Zamek-Gliszczynski MJ, Chu X, Cook JA, et al. ITC Commentary on Metformin Clinical Drug-Drug Interaction Study Design That Enables an Efficacy- and Safety-Based Dose Adjustment Decision. *Clin Pharmacol Ther.* Nov 2018;104(5):781-784. doi:10.1002/cpt.1082
157. Levey AS, Perrone RD, Madias NE. Serum creatinine and renal function. *Annu Rev Med.* 1988;39:465-90. doi:10.1146/annurev.me.39.020188.002341
158. Galetin A, Brouwer KLR, Tweedie D, et al. Membrane transporters in drug development and as determinants of precision medicine. *Nat Rev Drug Discov.* Apr 2024;23(4):255-280. doi:10.1038/s41573-023-00877-1
159. Türk D, Müller F, Fromm MF, Selzer D, Dallmann R, Lehr T. Renal Transporter-Mediated Drug-Biomarker Interactions of the Endogenous Substrates Creatinine and N(1) -Methylnicotinamide: A PBPK Modeling Approach. *Clin Pharmacol Ther.* Sep 2022;112(3):687-698. doi:10.1002/cpt.2636
160. Chu X, Bleasby K, Chan GH, Nunes I, Evers R. The Complexities of Interpreting Reversible Elevated Serum Creatinine Levels in Drug Development: Does a Correlation with Inhibition of Renal Transporters Exist? *Drug Metab Dispos.* Sep 2016;44(9):1498-509. doi:10.1124/dmd.115.067694
161. Choi HJ, Madari S, Huang F. Utilising Endogenous Biomarkers in Drug Development to Streamline the Assessment of Drug-Drug Interactions Mediated by Renal Transporters: A Pharmaceutical Industry Perspective. *Clin Pharmacokinet.* Jun 2024;63(6):735-749. doi:10.1007/s40262-024-01385-0
162. Chu X, Liao M, Shen H, et al. Clinical Probes and Endogenous Biomarkers as Substrates for Transporter Drug-Drug Interaction Evaluation: Perspectives From the International Transporter Consortium. *Clin Pharmacol Ther.* Nov 2018;104(5):836-864. doi:10.1002/cpt.1216
163. Ito S, Kusuhara H, Kumagai Y, et al. N-methylnicotinamide is an endogenous probe for evaluation of drug-drug interactions involving multidrug and toxin extrusions (MATE1 and MATE2-K). *Clin Pharmacol Ther.* Nov 2012;92(5):635-41. doi:10.1038/clpt.2012.138
164. Müller F, Pontones CA, Renner B, et al. N(1)-methylnicotinamide as an endogenous probe for drug interactions by renal cation transporters: studies on the metformin-

trimethoprim interaction. *Eur J Clin Pharmacol*. Jan 2015;71(1):85-94. doi:10.1007/s00228-014-1770-2

165. Weber W, Toussaint S, Looby M, Nitz M, Kewitz H. System analysis in multiple dose kinetics: evidence for saturable tubular reabsorption of the organic cation N1-methylnicotinamide in humans. *J Pharmacokinet Biopharm*. Oct 1991;19(5):553-74. doi:10.1007/bf01062963

166. Miyake T, Kimoto E, Luo L, et al. Identification of Appropriate Endogenous Biomarker for Risk Assessment of Multidrug and Toxin Extrusion Protein-Mediated Drug-Drug Interactions in Healthy Volunteers. *Clin Pharmacol Ther*. Feb 2021;109(2):507-516. doi:10.1002/cpt.2022

167. Müller F, Hohl K, Keller S, et al. N(1) -Methylnicotinamide as Biomarker for MATE-Mediated Renal Drug-Drug Interactions: Impact of Cimetidine, Rifampin, Verapamil, and Probenecid. *Clin Pharmacol Ther*. May 2023;113(5):1070-1079. doi:10.1002/cpt.2849

168. Vourvahis M, Byon W, Chang C, et al. Evaluation of the Effect of Abrocitinib on Drug Transporters by Integrated Use of Probe Drugs and Endogenous Biomarkers. *Clin Pharmacol Ther*. Sep 2022;112(3):665-675. doi:10.1002/cpt.2594

169. Choi H, Huang F, Flack M. The Effect of BI 730357 (Retinoic Acid-Related Orphan Receptor Gamma t Antagonist, Bevuogant) on the Pharmacokinetics of a Transporter Probe Cocktail, Including Digoxin, Furosemide, Metformin, and Rosuvastatin: An Open-Label, Non-randomized, 2-Period Fixed-Sequence Trial in Healthy Subjects. *Clin Pharmacol Drug Dev*. Feb 2024;13(2):197-207. doi:10.1002/cpdd.1344

170. Dutta S, Shah RB, Singhal S, et al. Metformin: A Review of Potential Mechanism and Therapeutic Utility Beyond Diabetes. *Drug Des Devel Ther*. 2023;17:1907-1932. doi:10.2147/dddt.S409373

171. Gilead Sciences International Limited. Fachinformation (Summary of Product Characteristics, SPC): Hepsera 10 mg Tabletten. December 2018. Accessed April 25, 2025. [https://www.gilead.com/-/media/files/pdfs/medicines/liver-disease/hepsera/hepsera\\_pi.pdf](https://www.gilead.com/-/media/files/pdfs/medicines/liver-disease/hepsera/hepsera_pi.pdf).

172. Maeda K, Tian Y, Fujita T, et al. Inhibitory effects of p-aminohippurate and probenecid on the renal clearance of adefovir and benzylpenicillin as probe drugs for organic anion transporter (OAT) 1 and OAT3 in humans. *Eur J Pharm Sci*. Aug 1 2014;59:94-103. doi:10.1016/j.ejps.2014.04.004

173. Mathialagan S, Piotrowski MA, Tess DA, Feng B, Litchfield J, Varma MV. Quantitative Prediction of Human Renal Clearance and Drug-Drug Interactions of Organic Anion Transporter Substrates Using In Vitro Transport Data: A Relative Activity Factor Approach. *Drug Metab Dispos*. Apr 2017;45(4):409-417. doi:10.1124/dmd.116.074294

174. Cundy KC, Barditch-Crovo P, Walker RE, et al. Clinical pharmacokinetics of adefovir in human immunodeficiency virus type 1-infected patients. *Antimicrob Agents Chemother*. Nov 1995;39(11):2401-5. doi:10.1128/aac.39.11.2401

175. Imaoka T, Kusuhara H, Adachi M, Schuetz JD, Takeuchi K, Sugiyama Y. Functional involvement of multidrug resistance-associated protein 4 (MRP4/ABCC4) in the renal

elimination of the antiviral drugs adefovir and tenofovir. *Mol Pharmacol*. Feb 2007;71(2):619-27. doi:10.1124/mol.106.028233

176. MSD Sharp & Dohme GmbH. Fachinformation (Summary of Product Characteristics, SPC) Januvia. September 2023. Accessed April 6, 2025. <https://www.fachinfo.de/fi/detail/010175/januvia>.

177. Krishna R, Bergman A, Larson P, et al. Effect of a single cyclosporine dose on the single-dose pharmacokinetics of sitagliptin (MK-0431), a dipeptidyl peptidase-4 inhibitor, in healthy male subjects. *J Clin Pharmacol*. Feb 2007;47(2):165-74. doi:10.1177/0091270006296523

178. K PA, Meda VS, Kucherlapati VS, et al. Pharmacokinetic drug interaction between gemfibrozil and sitagliptin in healthy Indian male volunteers. *Eur J Clin Pharmacol*. May 2012;68(5):709-14. doi:10.1007/s00228-011-1177-2

179. Shen H, Nelson DM, Oliveira RV, et al. Discovery and Validation of Pyridoxic Acid and Homovanillic Acid as Novel Endogenous Plasma Biomarkers of Organic Anion Transporter (OAT) 1 and OAT3 in Cynomolgus Monkeys. *Drug Metab Dispos*. Feb 2018;46(2):178-188. doi:10.1124/dmd.117.077586

180. Shen H, Holenarsipur VK, Mariappan TT, et al. Evidence for the Validity of Pyridoxic Acid (PDA) as a Plasma-Based Endogenous Probe for OAT1 and OAT3 Function in Healthy Subjects. *J Pharmacol Exp Ther*. Jan 2019;368(1):136-145. doi:10.1124/jpet.118.252643

181. Willemin ME, Van Der Made TK, Pijpers I, et al. Clinical Investigation on Endogenous Biomarkers to Predict Strong OAT-Mediated Drug-Drug Interactions. *Clin Pharmacokinet*. Sep 2021;60(9):1187-1199. doi:10.1007/s40262-021-01004-2

182. Rodrigues D, Wezalis S. Clinical Assessment of Drug Transporter Inhibition Using Biomarkers: Review of the Literature (2015-2024). *J Clin Pharmacol*. Jan 19 2025;doi:10.1002/jcph.6183

183. Chu X, Chan GH, Evers R. Identification of Endogenous Biomarkers to Predict the Propensity of Drug Candidates to Cause Hepatic or Renal Transporter-Mediated Drug-Drug Interactions. *J Pharm Sci*. Sep 2017;106(9):2357-2367. doi:10.1016/j.xphs.2017.04.007

184. Rodrigues D, Rowland A. From Endogenous Compounds as Biomarkers to Plasma-Derived Nanovesicles as Liquid Biopsy; Has the Golden Age of Translational Pharmacokinetics-Absorption, Distribution, Metabolism, Excretion-Drug-Drug Interaction Science Finally Arrived? *Clin Pharmacol Ther*. Jun 2019;105(6):1407-1420. doi:10.1002/cpt.1328

185. Mori D, Kimoto E, Rago B, et al. Dose-Dependent Inhibition of OATP1B by Rifampicin in Healthy Volunteers: Comprehensive Evaluation of Candidate Biomarkers and OATP1B Probe Drugs. *Clin Pharmacol Ther*. Apr 2020;107(4):1004-1013. doi:10.1002/cpt.1695

186. Liu R, Hao J, Zhao X, Lai Y. Characterization of Elimination Pathways and the Feasibility of Endogenous Metabolites as Biomarkers of Organic Anion Transporter 1/3 Inhibition in Cynomolgus Monkeys. *Drug Metab Dispos*. Jul 2023;51(7):844-850. doi:10.1124/dmd.123.001277

187. Tang J, Shen H, Zhao X, et al. Endogenous Plasma Kynurenic Acid in Human: A Newly Discovered Biomarker for Drug-Drug Interactions Involving Organic Anion Transporter 1 and 3 Inhibition. *Drug Metab Dispos*. Dec 2021;49(12):1063-1069. doi:10.1124/dmd.121.000486

188. Greiner B, Eichelbaum M, Fritz P, et al. The role of intestinal P-glycoprotein in the interaction of digoxin and rifampin. *The Journal of clinical investigation*. 1999;104(2):147-153.
189. Gazzaz M, Kinzig M, Schaeffeler E, et al. Drinking Ethanol Has Few Acute Effects on CYP2C9, CYP2C19, NAT2, and P-Glycoprotein Activities but Somewhat Inhibits CYP1A2, CYP2D6, and Intestinal CYP3A: So What? *Clin Pharmacol Ther*. Dec 2018;104(6):1249-1259. doi:10.1002/cpt.1083
190. Oswald S, Terhaag B, Siegmund W. In vivo probes of drug transport: commonly used probe drugs to assess function of intestinal P-glycoprotein (ABCB1) in humans. *Handb Exp Pharmacol*. 2011;(201):403-47. doi:10.1007/978-3-642-14541-4\_11
191. He J, Yu Y, Prasad B, Chen X, Unadkat JD. Mechanism of an unusual, but clinically significant, digoxin-bupropion drug interaction. *Biopharm Drug Dispos*. Jul 2014;35(5):253-63. doi:10.1002/bdd.1890
192. Greiner B, Eichelbaum M, Fritz P, et al. The role of intestinal P-glycoprotein in the interaction of digoxin and rifampin. *J Clin Invest*. Jul 1999;104(2):147-53. doi:10.1172/jci6663
193. Martin P, Gillen M, Millson D, et al. Effects of Fostamatinib on the Pharmacokinetics of Digoxin (a P-Glycoprotein Substrate): Results From in Vitro and Phase I Clinical Studies. *Clin Ther*. Dec 1 2015;37(12):2811-22. doi:10.1016/j.clinthera.2015.09.018
194. Pedersen KE, Dorph-Pedersen A, Hvidt S, Klitgaard NA, Pedersen KK. The long-term effect of verapamil on plasma digoxin concentration and renal digoxin clearance in healthy subjects. *Eur J Clin Pharmacol*. 1982;22(2):123-7. doi:10.1007/bf00542456
195. Scotcher D, Jones CR, Galetin A, Rostami-Hodjegan A. Delineating the Role of Various Factors in Renal Disposition of Digoxin through Application of Physiologically Based Kidney Model to Renal Impairment Populations. *J Pharmacol Exp Ther*. Mar 2017;360(3):484-495. doi:10.1124/jpet.116.237438
196. Kirby BJ, Collier AC, Kharasch ED, Whittington D, Thummel KE, Unadkat JD. Complex drug interactions of the HIV protease inhibitors 3: effect of simultaneous or staggered dosing of digoxin and ritonavir, nelfinavir, rifampin, or bupropion. *Drug Metab Dispos*. Mar 2012;40(3):610-6. doi:10.1124/dmd.111.042705
197. Hsin CH, Stoffel MS, Gazzaz M, et al. Combinations of common SNPs of the transporter gene ABCB1 influence apparent bioavailability, but not renal elimination of oral digoxin. *Sci Rep*. Jul 27 2020;10(1):12457. doi:10.1038/s41598-020-69326-y
198. Fung KL, Gottesman MM. A synonymous polymorphism in a common MDR1 (ABCB1) haplotype shapes protein function. *Biochim Biophys Acta*. May 2009;1794(5):860-71. doi:10.1016/j.bbapap.2009.02.014
199. Hodges LM, Markova SM, Chinn LW, et al. Very important pharmacogene summary: ABCB1 (MDR1, P-glycoprotein). *Pharmacogenet Genomics*. Mar 2011;21(3):152-61. doi:10.1097/FPC.0b013e3283385a1c
200. Hoffmeyer S, Burk O, von Richter O, et al. Functional polymorphisms of the human multidrug-resistance gene: multiple sequence variations and correlation of one allele with P-glycoprotein expression and activity in vivo. *Proc Natl Acad Sci U S A*. Mar 28 2000;97(7):3473-8. doi:10.1073/pnas.97.7.3473

201. Hitzl M, Schaeffeler E, Hochar B, et al. Variable expression of P-glycoprotein in the human placenta and its association with mutations of the multidrug resistance 1 gene (MDR1, ABCB1). *Pharmacogenetics*. May 2004;14(5):309-18. doi:10.1097/00008571-200405000-00006
202. Siegsmond M, Brinkmann U, Schäffeler E, et al. Association of the P-glycoprotein transporter MDR1(C3435T) polymorphism with the susceptibility to renal epithelial tumors. *J Am Soc Nephrol*. Jul 2002;13(7):1847-54. doi:10.1097/01.asn.0000019412.87412.bc
203. Gow JM, Hodges LM, Chinn LW, Kroetz DL. Substrate-dependent effects of human ABCB1 coding polymorphisms. *J Pharmacol Exp Ther*. May 2008;325(2):435-42. doi:10.1124/jpet.107.135194
204. Schaefer M, Roots I, Gerloff T. In-vitro transport characteristics discriminate wild-type ABCB1 (MDR1) from ALA893SER and ALA893THR polymorphisms. *Pharmacogenet Genomics*. Dec 2006;16(12):855-61. doi:10.1097/01.fpc.0000230113.03710.34
205. Chinn LW, Kroetz DL. ABCB1 pharmacogenetics: progress, pitfalls, and promise. *Clin Pharmacol Ther*. Feb 2007;81(2):265-9. doi:10.1038/sj.clpt.6100052
206. Leschziner G, Zabaneh D, Pirmohamed M, et al. Exon sequencing and high resolution haplotype analysis of ABC transporter genes implicated in drug resistance. *Pharmacogenet Genomics*. Jun 2006;16(6):439-50. doi:10.1097/01.fpc.0000197467.21964.67
207. Lee SC, Arya V, Yang X, Volpe DA, Zhang L. Evaluation of transporters in drug development: Current status and contemporary issues. *Adv Drug Deliv Rev*. Jul 1 2017;116:100-118. doi:10.1016/j.addr.2017.07.020
208. Maeda K. Recent progress in in vivo phenotyping technologies for better prediction of transporter-mediated drug-drug interactions. *Drug Metab Pharmacokinet*. Feb 2020;35(1):76-88. doi:10.1016/j.dmpk.2019.12.004
209. Zhang L, Sparreboom A. Predicting transporter-mediated drug interactions: Commentary on: "Pharmacokinetic evaluation of a drug transporter cocktail consisting of digoxin, furosemide, metformin and rosuvastatin" and "Validation of a microdose probe drug cocktail for clinical drug interaction assessments for drug transporters and CYP3A". *Clin Pharmacol Ther*. Apr 2017;101(4):447-449. doi:10.1002/cpt.588
210. Stopfer P, Giessmann T, Hohl K, et al. Pharmacokinetic Evaluation of a Drug Transporter Cocktail Consisting of Digoxin, Furosemide, Metformin, and Rosuvastatin. *Clin Pharmacol Ther*. Sep 2016;100(3):259-67. doi:10.1002/cpt.406
211. Ebner T, Ishiguro N, Taub ME. The Use of Transporter Probe Drug Cocktails for the Assessment of Transporter-Based Drug-Drug Interactions in a Clinical Setting-Proposal of a Four Component Transporter Cocktail. *J Pharm Sci*. Sep 2015;104(9):3220-8. doi:10.1002/jps.24489
212. Stopfer P, Giessmann T, Hohl K, et al. Effects of Metformin and Furosemide on Rosuvastatin Pharmacokinetics in Healthy Volunteers: Implications for Their Use as Probe Drugs in a Transporter Cocktail. *Eur J Drug Metab Pharmacokinet*. Feb 2018;43(1):69-80. doi:10.1007/s13318-017-0427-9

213. Stopfer P, Giessmann T, Hohl K, et al. Optimization of a drug transporter probe cocktail: potential screening tool for transporter-mediated drug-drug interactions. *Br J Clin Pharmacol*. Sep 2018;84(9):1941-1949. doi:10.1111/bcp.13609
214. Wiebe ST, Giessmann T, Hohl K, et al. Validation of a Drug Transporter Probe Cocktail Using the Prototypical Inhibitors Rifampin, Probenecid, Verapamil, and Cimetidine. *Clin Pharmacokinet*. Dec 2020;59(12):1627-1639. doi:10.1007/s40262-020-00907-w
215. Yamane N, Tozuka Z, Kusama M, Maeda K, Ikeda T, Sugiyama Y. Clinical relevance of liquid chromatography tandem mass spectrometry as an analytical method in microdose clinical studies. *Pharm Res*. Aug 2011;28(8):1963-72. doi:10.1007/s11095-011-0423-8
216. Burt T, John CS, Ruckle JL, Vuong LT. Phase-0/microdosing studies using PET, AMS, and LC-MS/MS: a range of study methodologies and conduct considerations. Accelerating development of novel pharmaceuticals through safe testing in humans - a practical guide. *Expert Opin Drug Deliv*. May 2017;14(5):657-672. doi:10.1080/17425247.2016.1227786
217. Burt T, Yoshida K, Lappin G, et al. Microdosing and Other Phase 0 Clinical Trials: Facilitating Translation in Drug Development. *Clin Transl Sci*. Apr 2016;9(2):74-88. doi:10.1111/cts.12390
218. Maeda K, Sugiyama Y. Novel strategies for microdose studies using non-radiolabeled compounds. *Adv Drug Deliv Rev*. Jun 19 2011;63(7):532-8. doi:10.1016/j.addr.2011.02.004
219. Prueksaritanont T, Tatosian DA, Chu X, et al. Validation of a microdose probe drug cocktail for clinical drug interaction assessments for drug transporters and CYP3A. *Clin Pharmacol Ther*. Apr 2017;101(4):519-530. doi:10.1002/cpt.525
220. Frechen S, Junge L, Saari TI, et al. A semiphysiological population pharmacokinetic model for dynamic inhibition of liver and gut wall cytochrome P450 3A by voriconazole. *Clin Pharmacokinet*. Sep 2013;52(9):763-81. doi:10.1007/s40262-013-0070-9
221. Mould DR, Upton RN. Basic concepts in population modeling, simulation, and model-based drug development-part 2: introduction to pharmacokinetic modeling methods. *CPT Pharmacometrics Syst Pharmacol*. Apr 17 2013;2(4):e38. doi:10.1038/psp.2013.14
222. Mould DR, Upton RN. Basic concepts in population modeling, simulation, and model-based drug development. *CPT Pharmacometrics Syst Pharmacol*. Sep 26 2012;1(9):e6. doi:10.1038/psp.2012.4
223. Bröchner-Mortensen J. A simple method for the determination of glomerular filtration rate. *Scand J Clin Lab Invest*. Nov 1972;30(3):271-4. doi:10.3109/00365517209084290
224. Chantler C, Barratt TM. Estimation of glomerular filtration rate from plasma clearance of 51-chromium edetic acid. *Arch Dis Child*. Aug 1972;47(254):613-7. doi:10.1136/ad.47.254.613
225. Pottel H, Schaeffner E, Ebert N, van der Giet M, Delanaye P. Iohexol plasma clearance for measuring glomerular filtration rate: effect of different ways to calculate the area under the curve. *BMC Nephrol*. May 5 2021;22(1):166. doi:10.1186/s12882-021-02376-0
226. Schwartz GJ, Furth S, Cole SR, Warady B, Muñoz A. Glomerular filtration rate via plasma iohexol disappearance: pilot study for chronic kidney disease in children. *Kidney Int*. Jun 2006;69(11):2070-7. doi:10.1038/sj.ki.5000385

227. Gareth James DW, Trevor Hastie, Robert Tibshirani. *An introduction to statistical learning*. Springer; 2013.
228. Lin LI. A concordance correlation coefficient to evaluate reproducibility. *Biometrics*. Mar 1989;45(1):255-68.
229. Lin LI. Total deviation index for measuring individual agreement with applications in laboratory performance and bioequivalence. *Stat Med*. Jan 30 2000;19(2):255-70. doi:10.1002/(sici)1097-0258(20000130)19:2<255::aid-sim293>3.0.co;2-8
230. Lindbom L, Pihlgren P, Jonsson EN. PsN-Toolkit--a collection of computer intensive statistical methods for non-linear mixed effect modeling using NONMEM. *Comput Methods Programs Biomed*. Sep 2005;79(3):241-57. doi:10.1016/j.cmpb.2005.04.005
231. Stevens LA, Schmid CH, Greene T, et al. Factors other than glomerular filtration rate affect serum cystatin C levels. *Kidney Int*. Mar 2009;75(6):652-60. doi:10.1038/ki.2008.638
232. European Medicines Agency. (2010). Committee for Medicinal Products for Human Use (CHMP) Guideline on the Investigation of Bioequivalence. CPMP/EWP/QWP/1401/98 Rev 1/Corr. Available from: [https://www.ema.europa.eu/en/documents/scientific-guideline/guideline-investigation-bioequivalence-rev1\\_en.pdf](https://www.ema.europa.eu/en/documents/scientific-guideline/guideline-investigation-bioequivalence-rev1_en.pdf). Accessed May 16, 2024.
233. Tuttle M, Levey AS. Relmapirazin, a new exogenous filtration marker, and more widespread use of measured GFR. *Kidney Int*. Oct 2024;106(4):562-565. doi:10.1016/j.kint.2024.07.019
234. Sheikh MS, Kashani KB. Beyond creatinine: New methods to measure renal function? *Eur J Intern Med*. Apr 2025;134:17-24. doi:10.1016/j.ejim.2025.01.015
235. Ieiri I, Fukae M, Maeda K, et al. Pharmacogenomic/pharmacokinetic assessment of a four-probe cocktail for CYPs and OATPs following oral microdosing. *Int J Clin Pharmacol Ther*. Oct 2012;50(10):689-700. doi:10.5414/cp201763
236. Frank D, Jaehde U, Fuhr U. Evaluation of probe drugs and pharmacokinetic metrics for CYP2D6 phenotyping. *Eur J Clin Pharmacol*. Apr 2007;63(4):321-33. doi:10.1007/s00228-006-0250-8
237. Stehle S, Kirchheiner J, Lazar A, Fuhr U. Pharmacogenetics of oral anticoagulants: a basis for dose individualization. *Clin Pharmacokinet*. 2008;47(9):565-94. doi:10.2165/00003088-200847090-00002
238. Chu X, Korzekwa K, Elsby R, et al. Intracellular drug concentrations and transporters: measurement, modeling, and implications for the liver. *Clin Pharmacol Ther*. Jul 2013;94(1):126-41. doi:10.1038/clpt.2013.78
239. Guo Y, Chu X, Parrott NJ, et al. Advancing Predictions of Tissue and Intracellular Drug Concentrations Using In Vitro, Imaging and Physiologically Based Pharmacokinetic Modeling Approaches. *Clin Pharmacol Ther*. Nov 2018;104(5):865-889. doi:10.1002/cpt.1183
240. Watanabe T, Kusuhara H, Maeda K, Shitara Y, Sugiyama Y. Physiologically based pharmacokinetic modeling to predict transporter-mediated clearance and distribution of pravastatin in humans. *J Pharmacol Exp Ther*. Feb 2009;328(2):652-62. doi:10.1124/jpet.108.146647

241. Lang J, Vincent L, Chenel M, Ogungbenro K, Galetin A. Reduced physiologically-based pharmacokinetic model of dabigatran etexilate-dabigatran and its application for prediction of intestinal P-gp-mediated drug-drug interactions. *Eur J Pharm Sci.* Oct 1 2021;165:105932. doi:10.1016/j.ejps.2021.105932
242. Barth A, Perry CR, Shabbir S, et al. Clinical assessment of gepotidacin (GSK2140944) as a victim and perpetrator of drug-drug interactions via CYP3A metabolism and transporters. *Clin Transl Sci.* Apr 2023;16(4):647-661. doi:10.1111/cts.13477
243. Hibma JE, Zur AA, Castro RA, et al. The Effect of Famotidine, a MATE1-Selective Inhibitor, on the Pharmacokinetics and Pharmacodynamics of Metformin. *Clin Pharmacokinet.* Jun 2016;55(6):711-21. doi:10.1007/s40262-015-0346-3
244. Zamek-Gliszczynski MJ, Giacomini KM, Zhang L. Emerging Clinical Importance of Hepatic Organic Cation Transporter 1 (OCT1) in Drug Pharmacokinetics, Dynamics, Pharmacogenetic Variability, and Drug Interactions. *Clin Pharmacol Ther.* May 2018;103(5):758-760. doi:10.1002/cpt.941
245. Cho SK, Kim CO, Park ES, Chung JY. Verapamil decreases the glucose-lowering effect of metformin in healthy volunteers. *Br J Clin Pharmacol.* Dec 2014;78(6):1426-32. doi:10.1111/bcp.12476
246. Toyohara J. Importance of P-gp PET Imaging in Pharmacology. *Curr Pharm Des.* 2016;22(38):5830-5836. doi:10.2174/1381612822666160804092258
247. Bauer M, Tournier N, Langer O. Imaging P-Glycoprotein Function at the Blood-Brain Barrier as a Determinant of the Variability in Response to Central Nervous System Drugs. *Clin Pharmacol Ther.* May 2019;105(5):1061-1064. doi:10.1002/cpt.1402
248. Hsin CH, Fuhr U, Trueck C. Response to "Impact of Acute Alcohol Exposure on P-Glycoprotein Function at the Blood-Brain Barrier Assessed Using (11) C-Metoclopramide PET Imaging". *Clin Pharmacol Ther.* Apr 2019;105(4):814. doi:10.1002/cpt.1265
249. Chu X, Prasad B, Neuhoff S, et al. Clinical Implications of Altered Drug Transporter Abundance/Function and PBPK Modeling in Specific Populations: An ITC Perspective. *Clin Pharmacol Ther.* Sep 2022;112(3):501-526. doi:10.1002/cpt.2643
250. Lin J, Kimoto E, Yamazaki S, et al. Effect of Hepatic Impairment on OATP1B Activity: Quantitative Pharmacokinetic Analysis of Endogenous Biomarker and Substrate Drugs. *Clin Pharmacol Ther.* May 2023;113(5):1058-1069. doi:10.1002/cpt.2829
251. Takita H, Scotcher D, Chu X, Yee KL, Ogungbenro K, Galetin A. Coproporphyrin I as an Endogenous Biomarker to Detect Reduced OATP1B Activity and Shift in Elimination Route in Chronic Kidney Disease. *Clin Pharmacol Ther.* Sep 2022;112(3):615-626. doi:10.1002/cpt.2672
252. Rowland A, Ruanglertboon W, van Dyk M, et al. Plasma extracellular nanovesicle (exosome)-derived biomarkers for drug metabolism pathways: a novel approach to characterize variability in drug exposure. *Br J Clin Pharmacol.* Jan 2019;85(1):216-226. doi:10.1111/bcp.13793
253. Achour B, Gosselin P, Terrier J, et al. Liquid Biopsy for Patient Characterization in Cardiovascular Disease: Verification against Markers of Cytochrome P450 and P-Glycoprotein Activities. *Clin Pharmacol Ther.* Jun 2022;111(6):1268-1277. doi:10.1002/cpt.2576



254. Bradford MM. A rapid and sensitive method for the quantitation of microgram quantities of protein utilizing the principle of protein-dye binding. *Anal Biochem*. May 7 1976;72:248-54. doi:10.1006/abio.1976.9999
255. Toutain PL, Bousquet-Mélou A. Volumes of distribution. *J Vet Pharmacol Ther*. Dec 2004;27(6):441-53. doi:10.1111/j.1365-2885.2004.00602.x
256. Delanaye P, Ebert N, Melsom T, et al. Iohexol plasma clearance for measuring glomerular filtration rate in clinical practice and research: a review. Part 1: How to measure glomerular filtration rate with iohexol? *Clinical kidney journal*. 2016;9(5):682-699.
257. U.S. Department of Health and Human Services; Food and Drug Administration; Center for Drug Evaluation and Research (CDER). (2018). Bioanalytical Method Validation: Guidance for Industry. Available from: <https://www.fda.gov/files/drugs/published/Bioanalytical-Method-Validation-Guidance-for-Industry.pdf>. Accessed July 30, 2024.
258. European Medicines Agency, Committee for Medicinal Products for Human Use. (2022). ICH Guideline M10 on Bioanalytical Method Validation and Study Sample Analysis. EMA/CHMP/ICH/172948/2019. Available from: [https://www.ema.europa.eu/en/documents/scientific-guideline/ich-guideline-m10-bioanalytical-method-validation-step-5\\_en.pdf](https://www.ema.europa.eu/en/documents/scientific-guideline/ich-guideline-m10-bioanalytical-method-validation-step-5_en.pdf). Accessed July 30, 2024
259. Mosteller R. Simplified calculation of body surface area. *New Engl J Med*. 1987;317:1098. doi:10.1056/NEJM198710223171717



## Improved correction formulas to estimate iohexol clearance from simple models

Qian Dong<sup>1</sup> · Uwe Fuhr<sup>1</sup> · Elke Schaeffner<sup>2</sup> · Markus van der Giet<sup>3</sup> · Natalie Ebert<sup>2</sup> · Max Taubert<sup>1</sup>

Received: 21 April 2023 / Accepted: 27 June 2023 / Published online: 8 July 2023  
 © The Author(s) 2023

**Keywords** Correction formula · Iohexol plasma clearance · Measured glomerular filtration rate · Three-compartment model

To the editor,

Measuring glomerular filtration rate by iohexol plasma clearance has become a preferred method in clinical practice and research [1–9], but ambiguities remain regarding the choice of pharmacokinetic modeling when evaluating iohexol concentration. We recently showed that a three-compartment pharmacokinetic model provides better iohexol clearance estimates than the two-compartment approach in elderly subjects in the Berlin Initiative Study (BIS) [7, 8]. However, implementation of the presented model in clinical and research practice is complicated by the required technical expertise and the complexity of Bayesian software [7]. A viable alternative could be the use of correction formulas which rely on traditional one- or two-compartment models and correct the obtained clearance estimates for the bias introduced by the omission of compartments [9–14]. Well-known examples for established correction formulas are the Bröchner-Mortensen (BM) equation [12] and the further simplified Chantler (Ch) formula [14] based on a one-compartment model, which have recently been shown to perform well in iohexol data from the BIS [9]. Such an evaluation remains to be carried out based on a three-compartment model, which is the subject of this letter.

Data from the BIS, including 546 individuals with data obtained up to 300 min post-injection, were evaluated [7, 8]. One-, two-, and three-compartment models were used to estimate iohexol clearance (CL1, CL2, and CL3), respectively. CL1 was estimated based on the slow component of iohexol concentrations 120 to 300 min post-dose, CL2 was estimated based on the protocol by Schwartz et al. [11] as carried out in the BIS [8], and CL3 was estimated using the empirical Bayes approach based on the three-compartment model [7]. Equations resembling the BM and Ch formulas were then fitted to correct CL1 and CL2 results, using CL3 as the reference (Table 1) [12, 14]. A leave-one-out cross-validation [15] was utilized to assess the bias and root mean squared error (RMSE), as well as to evaluate Lin's concordance correlation coefficient (CCC) [16] and the relative total deviation index (TDI) for a range of coverage probabilities (CP) [17]. A TDI ≤ 10% for a CP of 90% (TDI<sub>90</sub>) and an at least substantial CCC of ≥ 0.95 were considered optimal. R 4.2.1 [18] and NONMEM 7.4.2 [19] were used as statistical software.

BM- and Ch-like equations performed similarly well (Table 1), with an absolute bias < 1 mL/min, an RMSE between 2.92 and 4.08 mL/min, and a substantial concordance for all equations. The TDI<sub>90</sub> goal was achieved with Eqs. 3 and 4 based on two compartments, while it was missed with Eqs. 1 and 2 based on one compartment. Differences between BM-like and Ch-like equations were negligible with equations based on two compartments, while the BM-like equation provided a notably lower absolute bias than the Ch-like equation in the case of one compartment (−0.0949 versus −0.357 mL/min). In summary, our evaluation demonstrates that correction formulas in conjunction with one- or two-compartment models can provide adequate clearance estimates with only a minimal loss in accuracy and precision compared to a three-compartment model. When one-compartment estimates are available, the BM-like correction formula might be a good choice, while the simple

✉ Qian Dong  
[qian.dong@uk-koeln.de](mailto:qian.dong@uk-koeln.de)

<sup>1</sup> Department I of Pharmacology, Center for Pharmacology, Faculty of Medicine and University Hospital Cologne, University of Cologne, Gleueler Straße 24, Cologne 50931, Germany

<sup>2</sup> Institute of Public Health, Charité Universitätsmedizin Berlin, Berlin, Germany

<sup>3</sup> Department of Nephrology, Charité Universitätsmedizin Berlin, Berlin, Germany

**Table 1** Performance of correction formulas based on leave-one-out cross-validation, comparing iohexol clearance estimates obtained from different correction formulas to reference clearance values from three-compartment model

Nr.	Equation	Bias (mL/min) mean (95% CI)	Relative bias (%) mean (95% CI)	RMSE (mL/min)	CCC	$TDI_{90}$ (%)
1 (BM)	$CL = 0.872 \times CL1 - 0.000560 \times CL1^2$	-0.0949 (-0.428 to 0.238)	-0.103 (-0.616 to 0.411)	3.97	0.974	10.6
2 (Ch)	$CL = 0.824 \times CL1$	-0.357 (-0.698 to -0.016)	-0.953 (-1.50 to -0.409)	4.08	0.974	11.5
3 (BM)	$CL = 0.894 \times CL2 + 0.000246 \times CL2^2$	-0.0415 (-0.288 to 0.205)	-0.0331 (-0.411 to 0.344)	2.94	0.986	7.71
4 (Ch)	$CL = 0.896 \times CL2$	-0.0313 (-0.277 to 0.214)	-0.0022 (-0.378 to 0.374)	2.92	0.986	7.68

*CL* iohexol clearance estimates obtained from different correction formulas, *CL1* one-compartment clearance estimates, *CL2* two-compartment clearance estimates, *BM* Bröchner-Mortensen-like equation, *Ch* Chantler-like equation, *CI* confidence interval, *RMSE* root mean square error, *CCC* Lin's concordance correlation coefficient,  $TDI_{90}$  total deviation index for a coverage probability of 90%

Ch-like formula might be sufficient if two-compartment estimates are available. This provides the means to efficiently estimate iohexol clearance in settings where complexities and costs associated with the implementation of a Bayesian model are prohibitive. Whether the slight loss of accuracy and precision compared to the three-compartment model is acceptable depends on the clinical context and should therefore be judged on a case-by-case basis. Further validation in diverse patient populations is required, and the evaluation of additional, potentially non-linear correction formulas might provide further improvements.

**Author contribution** Conception and design: MT, QD. Acquisition of data: ES, NE, MvdG. Analysis and/or interpretation of data: QD, MT. Manuscript drafting: QD, MT, UF. Revision and final approval of manuscript: all authors.

**Funding** Open Access funding enabled and organized by Projekt DEAL. Qian Dong received a scholarship from the China Scholarship Council (CSC) for support of her PhD studies (scholarship number 202008320388).

**Availability of data and materials** The data that support the findings of this study are available from the corresponding author upon reasonable request.

## Declarations

**Competing interests** The authors declare no competing interests.

**Disclaimer** The funder had no role in design, collection, analysis, and interpretation of data, and writing and publication of the manuscript.

**Open Access** This article is licensed under a Creative Commons Attribution 4.0 International License, which permits use, sharing, adaptation, distribution and reproduction in any medium or format, as long as you give appropriate credit to the original author(s) and the source, provide a link to the Creative Commons licence, and indicate if changes were made. The images or other third party material in this article are included in the article's Creative Commons licence, unless indicated otherwise in a credit line to the material. If material is not included in the article's Creative Commons licence and your intended use is not permitted by statutory regulation or exceeds the permitted use, you will

need to obtain permission directly from the copyright holder. To view a copy of this licence, visit <http://creativecommons.org/licenses/by/4.0/>.

## References

1. Stolz A, Hoizey G, Toupance O, Lavaud S, Vitry F, Chanard J, Rieu P (2010) Evaluation of sample bias for measuring plasma iohexol clearance in kidney transplantation. *Transplantation* 89(4):440–445. <https://doi.org/10.1097/TP.0b013e3181ca7d1b>
2. Dixon JJ, Lane K, Dalton RN, Turner C, Grounds RM, MacPhee IA, Philips BJ (2015) Validation of a continuous infusion of low dose Iohexol to measure glomerular filtration rate: randomised clinical trial. *J Transl Med* 13:58. <https://doi.org/10.1186/s12967-015-0414-3>
3. Martus P, Ebert N, van der Giet M, Jakob O, Schaeffner ES (2014) An efficient approach for glomerular filtration rate assessment in older adults. *Br J Clin Pharmacol* 78(2):384–392. <https://doi.org/10.1111/bcp.12331>
4. Delanaye P, Melsom T, Ebert N, Bäck S-E, Mariat C, Cavalier E, Björk J, Christensson A, Nyman U, Porrini E, Remuzzi G, Ruggenenti P, Schaeffner E, Soveri I, Sterner G, Eriksen BO, Gaspari F (2016) Iohexol plasma clearance for measuring glomerular filtration rate in clinical practice and research: a review. Part 2: why to measure glomerular filtration rate with iohexol? *Clin Kidney J* 9(5):700–704. <https://doi.org/10.1093/ckj/sfw071>
5. Sterner G, Frennby B, Mansson S, Nyman U, Van Westen D, Almén T (2008) Determining 'true' glomerular filtration rate in healthy adults using infusion of inulin and comparing it with values obtained using other clearance techniques or prediction equations. *Scand J Urol Nephrol* 42(3):278–285. <https://doi.org/10.1080/00365590701701806>
6. Taubert M, Schaeffner E, Martus P, van der Giet M, Fuhr U, Lösment A, Ebert N (2021) Advancement of pharmacokinetic models of iohexol in patients aged 70 years or older with impaired kidney function. *Sci Rep* 11(1):22656. <https://doi.org/10.1038/s41598-021-01892-1>
7. Taubert M, Ebert N, Martus P, van der Giet M, Fuhr U, Schaeffner E (2018) Using a three-compartment model improves the estimation of iohexol clearance to assess glomerular filtration rate. *Sci Rep* 8(1):17723. <https://doi.org/10.1038/s41598-018-35989-x>
8. Schaeffner ES, Ebert N, Delanaye P, Frei U, Gaedeke J, Jakob O, Kuhlmann MK, Schuchardt M, Tölle M, Ziebig R, van der Giet M, Martus P (2012) Two novel equations to estimate kidney function in persons aged 70 years or older. *Ann Intern Med* 157(7):471–481. <https://doi.org/10.7326/0003-4819-157-7-201210020-00003>
9. Pottel H, Schaeffner E, Ebert N, van der Giet M, Delanaye P (2021) Iohexol plasma clearance for measuring glomerular filtration rate: effect of different ways to calculate the area under

- the curve. *BMC Nephrol* 22(1):166. <https://doi.org/10.1186/s12882-021-02376-0>
10. Fleming JS (2007) An improved equation for correcting slope-intercept measurements of glomerular filtration rate for the single exponential approximation. *Nucl Med Commun* 28(4):315–320. <https://doi.org/10.1097/MNM.0b013e328014a14a>
  11. Schwartz GJ, Furth S, Cole SR, Warady B, Muñoz A (2006) Glomerular filtration rate via plasma iothexol disappearance: pilot study for chronic kidney disease in children. *Kidney Int* 69(11):2070–2077. <https://doi.org/10.1038/sj.ki.5000385>
  12. Bröchner-Mortensen J (1972) A simple method for the determination of glomerular filtration rate. *Scand J Clin Lab Invest* 30(3):271–274. <https://doi.org/10.3109/00365517209084290>
  13. Bröchner-Mortensen J, Haahr J, Christoffersen J (1974) A simple method for accurate assessment of the glomerular filtration rate in children. *Scand J Clin Lab Invest* 33(2):140–143
  14. Chantler C, Barratt TM (1972) Estimation of glomerular filtration rate from plasma clearance of 51-chromium edetic acid. *Arch Dis Child* 47(254):613–617. <https://doi.org/10.1136/adc.47.254.613>
  15. Games G, Witten D, Hastie T, Tibshirani R (2013) An introduction to statistical learning. Springer. <https://doi.org/10.1007/978-1-4614-7138-7>
  16. Lin LI (1989) A concordance correlation coefficient to evaluate reproducibility. *Biometrics* 45(1):255–268
  17. Lin LI (2000) Total deviation index for measuring individual agreement with applications in laboratory performance and bioequivalence. *Stat Med* 19(2):255–270. [https://doi.org/10.1002/\(sici\)1097-0258\(20000130\)19:2%3c255::aid-sim293%3e3.0.co;2-8](https://doi.org/10.1002/(sici)1097-0258(20000130)19:2%3c255::aid-sim293%3e3.0.co;2-8)
  18. R Core Team (2022) R: A language and environment for statistical computing. R Foundation for Statistical Computing, Vienna, Austria. <https://www.R-project.org/>. Accessed 25 June 2023
  19. Beal SL, Sheiner LB, Boeckmann A, Bauer RJ (1992) NONMEM users guides. University of California, San Francisco, NONMEM Project Group

**Publisher's Note** Springer Nature remains neutral with regard to jurisdictional claims in published maps and institutional affiliations.



## ARTICLE OPEN ACCESS

## Validating Low-Dose Iohexol as a Marker for Glomerular Filtration Rate by In Vitro and In Vivo Studies

Qian Dong<sup>1</sup> | Zhendong Chen<sup>1</sup> | Jana Boland<sup>1</sup> | Charalambos Dokos<sup>1</sup> | Yohannes Hagos<sup>2</sup> | Annett Kühne<sup>2</sup> | Max Taubert<sup>1</sup> | Dirk Gründemann<sup>1</sup> | Uwe Fuhr<sup>1</sup>

<sup>1</sup>Department of Pharmacology, Center for Pharmacology, Faculty of Medicine and University Hospital Cologne, University of Cologne, Cologne, Germany | <sup>2</sup>PortaCellTec Biosciences GmbH, Göttingen, Germany

**Correspondence:** Qian Dong (qdong2@smail.uni-koeln.de)

**Received:** 15 December 2024 | **Revised:** 9 January 2025 | **Accepted:** 10 January 2025

**Funding:** The authors received no specific funding for this work.

**Keywords:** clinical trial | glomerular filtration rate | Iohexol | transporter-mediated drug–drug interactions

## ABSTRACT

Clearance of an intravenous iohexol dose of 3235 mg is used to assess glomerular filtration rate (GFR), although systematic assessment of its pharmacokinetic (PK) properties is incomplete. The objectives of the present investigations were (i) to assess potential interactions of iohexol with important drug transporters, and (ii) whether a 259 mg dose could replace the current standard dose. In vitro, we evaluated whether iohexol inhibits or is transported by renal transporters (hOAT1/3, hOCT2, and hMATE1/2K) or other transporters (hOATP1B1/3, hOCT1, and hMDR1) using cell-based and vesicle-based systems. In vivo, we conducted a clinical trial with 12 volunteers with the administration of single intravenous doses of 3235 mg (“reference”) and 259 mg (“test”) using a changeover design. Plasma and urine samples were collected up to 24 h postdose. We assessed the dose linearity of iohexol pharmacokinetics using the standard bioequivalence approach and conducted a population PK analysis to characterize its profile. Our in vitro findings indicate that iohexol is neither a substrate nor a significant inhibitor of the transporters, suggesting it is unlikely to participate in transporter-mediated drug–drug interactions in vivo. In the clinical trial, the test/reference ratio for plasma clearance, calculated as dose divided by the area under the plasma concentration–time curve, was 1.01 (90% confidence interval 0.968–1.05), confirming dose linearity. Population PK analysis further supported these results, showing no significant effect of dose on renal clearance and negligible nonrenal clearance of iohexol. Low-dose iohexol is a suitable marker for precise GFR measurement, even when coadministered with other drugs.

**JEL Classification:** Biomarkers

## 1 | Introduction

Reliable quantification of renal function, specifically glomerular filtration rate (GFR) is essential for optimizing drug dosing in patients and evaluating drug pharmacokinetic (PK) properties in clinical research [1]. Serum creatinine concentrations and/or creatinine clearance are commonly used to this end [2]. However, renal elimination of creatinine is not only mediated by glomerular filtration but also by renal transporters, including human organic cation transporter (hOCT)2, 2 forms of human multidrug

and toxin extrusion proteins (hMATE1 and hMATE2K), and human organic anion transporter (hOAT)2 [3]. Therefore, creatinine-based GFR estimations may be biased and influenced by transporter-mediated drug–drug interactions (TDDIs) [1, 3]. Cystatin C is less affected by renal tubular processes compared to creatinine, potentially making it a more reliable GFR marker [4]. However, both markers are affected by non-GFR factors: serum creatinine concentrations are influenced by muscle mass, physical activity, and diet [5], while cystatin C is impacted by inflammation, metabolic disorders, and steroid use [6].

This is an open access article under the terms of the [Creative Commons Attribution License](#), which permits use, distribution and reproduction in any medium, provided the original work is properly cited.

© 2025 The Author(s). *Clinical and Translational Science* published by Wiley Periodicals LLC on behalf of American Society for Clinical Pharmacology and Therapeutics.

## Summary

- What is the current knowledge on the topic?
  - Estimating glomerular filtration rate (GFR) to assess kidney function is a key aspect of medical practice. While serum creatinine concentration is typically used for this purpose, results are error-prone. Iohexol clearance of a standard 3235 mg intravenous bolus dose is more reliable in estimating GFR, but it is rarely used, partly due to limited research.
- What question did this study address?
  - This study investigated whether iohexol interacts with key drug transporters using in vitro methods and whether the iohexol dose to estimate GFR could be reduced to 259 mg in a clinical trial with healthy volunteers.
- What does this study add to our knowledge?
  - Iohexol is neither a substrate nor a significant inhibitor for transporters, suggesting that it is unlikely to interfere with other medications, and our clinical trial provided equivalent clearance values for both iohexol doses. Thus, a 259 mg iohexol bolus dose enables accurate GFR measurement, even when coadministered with other drugs.
- How might this change clinical pharmacology or translational science?
  - Clinically, the low iohexol dose enables accurate GFR measurement even in patients with fluctuating renal function and those with significant differences in non-GFR determinants of creatinine clearance compared to the population used to develop the creatinine-based GFR estimation equations. For the evaluation of renal transporter activity in clinical studies, the low iohexol dose fulfills the requirements for integration into a probe drug cocktail.

Alternatively, iohexol plasma clearance following a single dose (typically 3235 mg of iohexol) has become a robust GFR quantification method owing to its favorable PK properties [1]. Unlike endogenous filtration markers, iohexol-based assessments are unaffected by variations in body composition or disease [2]. It is used in clinical settings, where precise GFR assessment is required, such as in patients with fluctuating kidney function [7, 8], and in clinical trials evaluating the role of GFR in drug pharmacokinetics [1, 9]. Iodinated contrast media (ICM), including iohexol, are generally well tolerated; however, adverse drug reactions (ADRs) occur in up to 3% of cases, with acute and prolonged effects [10]. Acute ADRs, including allergic-like and physiologic responses, are dose-dependent [10, 11]. Contrast-induced acute kidney injury (CI-AKI) is the primary serious ADR associated with ICM, with a low (1%–2%) in patients with normal renal function but increases to 25% in those with chronic kidney disease (CKD) or other risk factors, such as comorbidities, aging, or nephrotoxic drugs [12]. The volume of ICM injected is a critical determinant of CI-AKI risk, with the risk doubling for every additional 20 mL in CKD patients [13]. Given the dose dependency of ADRs, it is desirable to validate and use iohexol at the lowest possible dose for GFR assessment, particularly in patients with impaired renal function or those requiring repeated GFR monitoring.

While iohexol elimination in humans is considered to be mediated exclusively by glomerular filtration, there is limited evidence suggesting that iohexol may interact with membrane transporters [9, 14–16]. Minor inconsistencies have been observed when comparing iohexol clearance to that of inulin, which is regarded as an ideal GFR marker [9], though inulin is no longer preferred due to practical limitations [17]. Additionally, beyond glomerular filtration iohexol might be reabsorbed through a saturable mechanism in rats [14]. Moreover, iohexol downregulated the expression of OCT2 in both rat kidneys and HK-2 cells [15]. It also exerted a mild inhibitory effect on P-glycoprotein in human cancer cell lines [16]. The involvement of membrane transporters in iohexol pharmacokinetics may lead to nonlinearity in its pharmacokinetics, particularly at low concentrations. Similar to creatinine, this can make iohexol susceptible to TDDIs when coadministered with drugs that affect transporter activity [3]. Both nonlinearity and TDDIs with iohexol as a victim could cause discrepancies between iohexol clearance and GFR.

TDDIs with iohexol as a perpetrator may affect drug therapy in patients. Furthermore, it could also influence the pharmacokinetics of probe drugs to assess the activity of renal transporters when integrated into “cocktail” studies. Cocktail studies are established approaches to quantify the activity of transporters (and enzymes) in vivo by simultaneous administration of several drugs, each of which is a substrate of a specific enzyme or transporter of interest [9]. Enzyme or transporter activities are quantified based on PK parameters representative of specific transporter activity. Several such cocktails have been developed specifically to assess the activity of renal transporters [18–21]. Renal clearance of a probe drug depends on the activity of the respective transporter(s) and glomerular filtration. Evaluating net renal secretion, a primary metric for quantifying renal transporter activity, therefore requires an accurate assessment of GFR, for which iohexol plasma clearance may be a valuable tool [9]. However, to incorporate iohexol into future transporter cocktail approaches, it is essential to ensure that iohexol is not involved in relevant TDDIs. Furthermore, to minimize potential TDDIs, reduce the risk of adverse effects associated with iohexol exposure [11, 13], and lower iohexol consumption, a reduction in the standard dose is desirable. However, PK information on low-dose iohexol is limited [7, 22].

This study, therefore, comprised two parts: The first part focused on assessing potential TDDIs of iohexol, including in vitro characterization of iohexol as a potential substrate and/or inhibitor of major drug transporters [23, 24]. The second part was a clinical study in healthy volunteers to assess the dose linearity of iohexol pharmacokinetics.

## 2 | Materials and Methods

### 2.1 | Part 1: In Vitro Study

#### 2.1.1 | Study Design

We characterized the inhibitory potential of iohexol on major drug transporters recommended by regulatory agencies [23, 24], which were previously assessed in a clinical transporter phenotyping cocktail study [18]. These



transporters include hOAT1, hOAT3, hOCT1, hOCT2, hMATE1, hMATE2K, human organic anion transporter polypeptides (hOATP)1B1, hOATP1B3, and human multidrug resistance protein (hMDR)1. Additionally, we investigated whether iohexol is a substrate for any of the renal transporters among these, including hOAT1/3, hOCT1/2, and hMATE1/2K. Cell-based uptake assays were used to assess the activities of hOAT1/3, hOCT1/2, hMATE1/2K, and hOATP1B1/1B3. Inside-out membrane vesicle uptake assays were used to evaluate the activity of hMDR1.

For substrate assessments, iohexol was incubated with stably transfected HEK-293 cells expressing one of the following transporters: hOAT1, hOAT3, hOCT1, hOCT2, hMATE1, or hMATE2K, as well as with control cells lacking transporter expression. Stably transfected cell lines containing pEBTetD plasmids [25] with wild-type human transporter cDNAs were generated as previously described [26]. Transporter expression was induced by adding 1 µg/mL doxycycline to the growth medium for at least 20 h [26]. Iohexol would be considered a substrate for these transporters if: (1) the ratio of iohexol uptake in cells expressing the transporter to that in control cells was  $\geq 2$ , and (2) a known inhibitor of the transporter reduced iohexol uptake to  $\leq 50\%$  at concentrations  $\geq 10$  times its inhibition constant or half-maximal inhibitory concentration [23, 24].

Inhibition experiments were conducted to investigate whether iohexol exhibits inhibitory effects on hOAT1/3, hOCT1/2, hMATE1/2K, hOATP1B1/3, and hMDR1 [18], potentially leading to TDDIs in vivo. To determine the maximal inhibitory potential of iohexol, intracellular accumulation of a standard substrate was measured with and without the clinically relevant highest concentrations of iohexol. Control inhibitors were tested in each experiment.

According to guidelines for assessing TDDIs after intravenous administration, the highest test concentration should be up to 50 times the unbound maximal plasma concentration ( $C_{max}$ ) [23, 24]. Given the minimal plasma protein binding of iohexol (1.5%) [27], we assumed an unbound fraction of 1 for the experiments. Typically, iohexol is administered as a 5 or 10 mL intravenous bolus (300 or 240 mg iodine/mL) for GFR measurement [27]. Based on prior clinical trials in patients aged  $\geq 70$  years with impaired kidney function (median GFR: 60.7 [interquartile range: 48.9–71.5] mL/min/1.73 m<sup>2</sup>), the  $C_{max}$  was considered to correspond to the initial plasma concentration following a 3235 mg iohexol injection, which was approximately 0.37 mM [28, 29]. Therefore, we selected a concentration range of 1–20 mM for the in vitro TDDI assessment to evaluate its maximum inhibitory potential.

In all subsequent in vitro studies, control experiments were conducted to validate the results. These included positive controls for substrates and inhibitors, as well as cells either without transporter expression or transfected with an empty vector, and control vesicles. Each condition, including cells or vesicles with the transporter and their respective controls, was analyzed in at least three replicates. For detailed information on materials, methods, and data analysis techniques used, refer to the [Supporting Information](#). Additional details on the

cell lines and culturing conditions are available in the related publication [26].

## 2.2 | Part 2: In Vivo Study

### 2.2.1 | Study Design

The clinical trial was registered with the German Clinical Trials Register under the identification code DRKS00029908 and approved by the Ethics Committee of the Medical Faculty of the University of Cologne, Germany, on November 21, 2022 (number 22-1347\_1). The study adhered to Good Clinical Practice guidelines and the Declaration of Helsinki. All participants provided written informed consent before any study-related procedures and were confirmed to be healthy through a standard screening examination (See also [Supporting Information](#)).

The trial had two separate objectives, that is, (i) to assess dose linearity of iohexol pharmacokinetics for a lower dose (reported here) and (ii) to improve the assessment of creatinine volume of distribution by oral administration of creatinine in beef meat (will be reported separately). Building on the PK findings from a 3235 mg iohexol injection [28, 29], we determined that the current quantification method is sufficiently sensitive to measure iohexol plasma concentrations corresponding to doses over 10 times lower, up to at least 20 h postadministration. Therefore, a 259 mg iohexol dose was selected for this study. The pertinent part of the trial had an open-label, randomized, single-dose, three-period changeover design involving 12 volunteers. Each participant was randomly assigned to one of six sequences, receiving iohexol intravenously at different single doses on separate occasions: (1) 259 mg iohexol without beef ingestion (defined as “fasting,” “test”); (2) 3235 mg iohexol fasting (“reference”); and (3) 3235 mg iohexol with beef ingestion (not reported here). The washout interval between administrations was 7 to 14 days. Adverse events were surveyed until the completion of the study.

A total of 19 blood samples were drawn before iohexol administration and at 10, 20, 30, 45, 60, and 90 min, as well as at 2, 3, 4, 5, 6, 8, 10, 12, 14, 16, 20, and 24 h postdosing under fasting conditions. For urine, 11 samples were collected before dosing and at 0–2, 2–4, 4–6, 6–8, 8–10, 10–12, 12–14, 14–16, 16–20, and 20–24 h postdosing under fasting conditions. Iohexol concentrations in plasma and urine samples were quantified using validated high-performance liquid chromatography coupled with tandem mass spectrometry, as detailed in the [Supporting Information](#). Only data from the two fasting conditions were included in further analyses.

### 2.2.2 | Noncompartmental Analysis

The noncompartmental analysis (NCA) was conducted using PKanalix 2024R1 (Lixoft SAS, a Simulations Plus company, Paris, France) followed by comparing between doses using the bioequivalence module. To assess the potential nonlinear relationship between the dose and exposure of iohexol, plasma clearance (CL) estimates obtained from NCA were compared between doses using the standard bioequivalence approach [30]. Detailed information on the calculation of PK parameters

via NCA and the statistical methods used is provided in the [Supporting Information](#).

### 2.2.3 | Population Pharmacokinetic Analysis

A population PK model of iohexol was developed using the non-linear mixed-effects modeling program NONMEM version 7.5.0 (ICON plc, Dublin, Ireland), Perl speaks NONMEM (PsN) version 5.2.6 (Uppsala University, Uppsala, Sweden) [31], and Pirana version 3.0.0 (Certara, Princeton, New Jersey). R version 4.2.1 (R Foundation for Statistical Computing, Vienna, Austria) was used for data preparation, visualization, and statistical summaries.

The structural model was developed in a stepwise manner, as previously detailed [28]. After establishing a reasonable structural model, the impact of dose-related effects was assessed as a categorical covariate on PK parameters through forward and backward selection processes. Model improvement was evaluated using the change in the objective function value ( $\Delta\text{OFV}$ ), with significance levels of 0.05 ( $\Delta\text{OFV} \leq -3.84$ ) and 0.01 ( $\Delta\text{OFV} \leq -6.63$ ). The stability and performance of the final model were evaluated graphically and statistically, using goodness-of-fit plots, nonparametric bootstrap analysis [32], and the visual predictive check (VPC) technique [33], as described earlier [28].

## 3 | Results

### 3.1 | Part 1: In Vitro Study

#### 3.1.1 | Quality Assessment of In Vitro Systems

The in vitro systems for hOAT1/3, hOCT1/2, hMATE1/2K, hOATP1B1/3, and hMDR1 uptake assays demonstrated robust performance in this study. Reference substrate concentrations in cells or vesicles expressing the transporters were 3.3 to 250 times higher than in controls (Table S3). The median inhibitory effects of prototypical inhibitors on the uptake of their respective reference substrates across all transporters ranged from 49% to 99% (Table S3). These findings validate the functionality of the in vitro systems in our study.

#### 3.1.2 | Substrate Assessments

Transporter-expressing cells showed no significant increase in iohexol accumulation compared to control cells, with median values ranging from  $-0.67$  to  $1.5$  pmol/mg protein after incubation with  $10 \mu\text{M}$  iohexol for 10 and 30 min (Table S4, Figure S1). The median iohexol uptake ratio of transporter-expressing cells to control cells varied between 0.89 and 1.2 across all transporters (Figure 1, Figure S1, Table S4).

#### 3.1.3 | Inhibition Assays

As shown in Figure 2, iohexol exhibited no significant inhibitory effect on the transporter-mediated uptake of standard substrates at concentrations of 1 mM and 2 mM. At 20 mM, iohexol reduced hMATE2K-mediated MPP<sup>+</sup> uptake and hMDR1-mediated

[<sup>3</sup>H]-N-methyl-quinidine uptake by 26% and 21%, respectively, while no notable inhibitory effects were observed for hOCT1/2-, hOAT1/3-, hMATE1-, or hOATP1B1/3-mediated substrates uptake. Detailed results of the inhibition assays are shown in Figures S2 and S3 and Table S3.

### 3.2 | Part 2 in Vivo Study

#### 3.2.1 | Demographics and Dataset

Twelve healthy subjects (7 females) with a median body mass index of  $24.4 \text{ kg/m}^2$  (range:  $21.2$ – $28.9 \text{ kg/m}^2$ ) and a median age of 34 years (range: 23–48 years) participated in the relevant part of the trial. Detailed demographic characteristics are presented in Table 1.

A total of 432 postdose plasma and 238 postdose urine samples were collected for PK analysis of iohexol. Of these, 9 samples (1.34%) had concentrations below the lower limit of quantification (LLOQ) and were excluded from the analyses (for details see [Supporting Information](#)). The plasma concentration–time profiles of iohexol, and its cumulative urinary excretion following single reference or test doses, are depicted in Figure 3.

#### 3.2.2 | Noncompartmental Analysis

NCA was performed using plasma concentrations from 12 subjects and urine concentrations from 10 subjects who had no missing urine samples. The corresponding PK parameters of iohexol following test and reference doses are summarized in Table 2. The 90% confidence intervals (CIs) for the ratio of test to reference doses for CL, calculated as dose divided by the area under the plasma concentration–time curve (AUC), and for urinary recovery were 1.01 (0.968–1.05) and 1.06 (0.960–1.17), respectively. These values fall within the standard bioequivalence range of 0.800–1.25, indicating that the AUC increased proportionally with the iohexol dose.

#### 3.2.3 | Population Pharmacokinetic Analysis

**3.2.3.1 | Model Building.** The three-compartment model with first-order renal elimination best-described plasma and urine data, reducing the OFV by 225 points compared to the two-compartment model. Adding a nonrenal clearance did not improve the OFV (0.053-point increase) and its estimate was negligible ( $0.001 \text{ L/h}$ ). The data confirmed that iohexol is exclusively eliminated by the kidneys through linear kinetics, without requiring more complex models such as nonlinear elimination.

The model was parameterized with central ( $V_1$ ) and peripheral ( $V_2$ ,  $V_3$ ) volumes of distribution, intercompartment clearances ( $Q_1$ ,  $Q_2$ ), and renal clearance ( $\text{CL}_R$ ) of iohexol. Interindividual variability was estimated for  $\text{CL}_R$ ,  $V_1$ ,  $V_2$ , and  $V_3$  using an exponential model. Inter-occasion variability for  $\text{CL}_R$ ,  $V_1$ , and  $Q_2$  was linked to inter-individual variability through an additive model. The residual variability in plasma and urine data was best described by proportional error models.



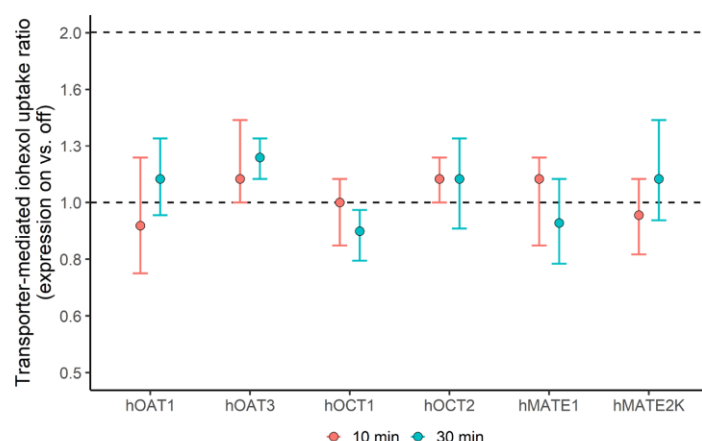


**FIGURE 1** | Ratio of iohexol uptake in transporter-expressing cells vs. nonexpressing cells. Stably transfected 293 cells, either expressing (expression on;  $n = 3$  or 4) or not expressing (expression off;  $n = 3$  or 4) hOAT1, hOAT3, hOCT1, hOCT2, hMATE1, or hMATE2K, were incubated with  $10 \mu\text{M}$  iohexol for 10 and 30 min, respectively. Each experiment was performed in triplicate, with each assay conducted on a separate day. In each assay, the ratio of iohexol uptake rates in transporter-expressing cells (expression on) compared with nonexpressing cells (expression off) was calculated through element-wise division within each experimental group. The dots and error bars represent the median values with 95% confidence intervals (CIs) of the log-scaled ratios across three independent experiments.

Based on the final model, median (range) individual empirical Bayesian estimates (EBEs) were 5.25 (4.74–8.05) L/h for  $\text{CL}_R$  and 15.1 (11.5–18.8) L for the volume of distribution (sum of  $V_1$ ,  $V_2$ , and  $V_3$ ). Bland–Altman plots indicated no significant differences in the individual EBEs of  $\text{CL}_R$  between the test and reference doses (Figure 4). Details of other PK parameters are presented in Table 3.

**3.2.3.2 | Evaluating Dose-Related Effects.** Dose levels were tested as a categorical covariate in the analysis of PK parameters. No significant reduction in the OFV was observed, confirming that the PK parameters did not differ significantly across the different dose levels.

**3.2.3.3 | Model Evaluation.** The final model showed good agreement between predicted and observed data, though a few outliers were noted. For more details, refer to the [Supporting Information](#).

## 4 | Discussion

In this study, we investigated whether iohexol inhibits renal transporters (hOAT1/3, hOCT2, and hMATE1/2K), hepatic transporters (hOATP1B1/3), and transporters in various tissues (hOCT1, hMDR1) and whether it is a substrate for these renal transporters through laboratory-based assays. Additionally, we assessed the PK characteristics of iohexol by comparing a low-test dose to the usual reference dose in a clinical trial with healthy volunteers.

### 4.1 | In Vitro Studies

In control experiments, the functional expression of each transporter was confirmed by the uptake of standard substrates. The use of specific inhibitors for each transporter effectively inhibited

substrate uptake as expected, consistent with our previous study [26]. Thus, the results of these experiments should be reliable.

The potential interactions between iohexol and key drug transporters were evaluated through a series of in vitro experiments, which had not been systematically investigated previously. The results indicate that iohexol is neither a substrate nor a significant inhibitor for the investigated transporters. At a concentration of 20 mM, iohexol slightly inhibited hMATE2K and hMDR1 activities (<30%). However, this concentration is far above the levels expected with the clinical dose (3235 mg) of iohexol used for GFR measurement or the reduced dose evaluated in this study. Thus, the mild inhibitory effect observed at this concentration is clinically irrelevant for using iohexol as a GFR probe. Similarly, Supawat et al. reported mild inhibitory effects of iohexol on P-glycoprotein in human cancer cell lines. However, this inhibition was not statistically significant, raising doubt about the existence of this effect [16]. These in vitro findings align with clinical evidence [35–38]. Studies have shown that iohexol clearance remains unaffected by OCT2 and MATE inhibitors, supporting the absence of significant interaction with these transporters [35, 36]. Furthermore, the low contribution of genetic polymorphisms to iohexol renal clearance variability suggests that genetically polymorphic transporters play a negligible role in its elimination [37]. Finally, iohexol does not induce metabolic drug–drug interactions, as it does not inhibit human Phase I or Phase II enzymes [38].

Our in vitro results, however, do not fully explain the minor discrepancies between iohexol-based GFR measurements and the unavailable “gold standard” inulin-based GFR [9, 39]. Furthermore, the discrepancy between our findings and those of Masereeuw et al., who proposed a saturable mechanism for iohexol elimination in the rat-isolated perfused kidney, may arise from methodological limitations [14]. Masereeuw et al. observed an increase in the ratio of renal clearance to GFR

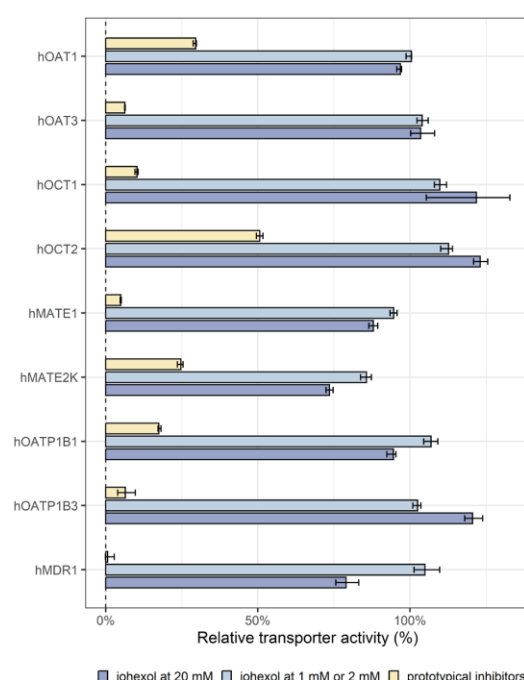


**FIGURE 2** | Inhibitory effects of prototypical inhibitors and iohexol on transporter-mediated transport of standard substrates. Relative transporter activity was calculated as the ratio of activity in the presence of inhibitors or iohexol to the activity in their absence, using element-wise division within each experiment. Transporter activity (net uptake rate) was derived by element-wise subtraction of the probe substrate concentrations under “expression off” conditions from those under “expression on” conditions for each transporter and study group. Columns and error bars represent the median values and 95% CIs of relative transporter activity across all respective experiments.

(from  $0.63 \pm 0.06$  to  $1.02 \pm 0.06$ , mean  $\pm$  standard deviation) as perfusate concentrations increased from  $5 \mu\text{g/mL}$  to  $20 \mu\text{g/mL}$ , suggesting saturable reabsorption [14]. However, their use of cyanocobalamin for GFR measurement, relying on colorimetric assay may be less accurate at low concentrations [40], and increasing protein binding further undermines its reliability [41]. These limitations warrant caution in interpreting their conclusions. Similarly, the downregulation of OCT2 expression in rat kidneys and HK-2 cells reported by Yang et al. also requires scrutiny [15]. Firstly, OCT2 expression is inconsistently observed in HK-2 cells across studies [42], suggesting that any observed downregulation might not be specific to iohexol but could result from other factors or experimental conditions. Moreover, decreased OCT2 expression in contrast-induced nephropathy rats may reflect nonspecific injury rather than a direct effect of iohexol [15]. Finally, relying on a single concentration of iohexol ( $6 \text{ mg/mL}$  iodine) limits the robustness of the findings [15].

The variability in uptake and inhibition assays across experiments on different days, consistent with previous investigations [26], may result from differences in cell density and transfection age, which affect the number of active transporters in the

**TABLE 1** | Demographic summary of enrolled subjects ( $n = 12$ , 5 men, 7 women).

Characteristic	Median (range)
Age (years)	34 (23–48)
Weight (kg)	77.3 (59.1–95.8)
Height (cm)	178 (163–196)
BMI ( $\text{kg/m}^2$ )	24.4 (21.2–28.9)
eGFR ( $\text{mL/min/1.73 m}^2$ )	100 (83.6–134)

Abbreviations: BMI, body mass index; eGFR, estimated glomerular filtration rate, estimated using the 2021 Chronic Kidney Disease Epidemiology Collaboration (CKD-EPI) creatinine–cystatin C equation [34], based on plasma creatinine and cystatin C concentrations from the screening examination.

plasma membrane. However, this variability does not compromise the pivotal results. Overall, our findings demonstrate that iohexol is neither a substrate nor a significant inhibitor of major drug transporters in vitro [23, 24].

## 4.2 | Clinical Trial

We conducted a clinical trial to evaluate the feasibility of using a lower iohexol dose for GFR assessment by investigating the dose linearity of iohexol pharmacokinetics. In this trial, dose proportionality was assessed using two methods. First, the standard average bioequivalence approach was applied, utilizing noncompartmental PK evaluation. This method compares dose-adjusted AUCs and employs well-established criteria to confirm the absence of significant differences between doses without additional assumptions. Second, a population PK analysis was performed to gain a more detailed understanding of iohexol pharmacokinetics. The population PK employed a three-compartment model that accurately described both plasma concentration profiles and urinary excretion of iohexol, consistent with prior findings in elderly individuals with impaired renal function based on plasma data alone [28]. Standard model evaluation and sensitivity analyses confirmed the stability and reliability of the final model. Iohexol PK parameters were unaffected by the dose, supporting the suitability of low-dose iohexol (e.g.,  $259 \text{ mg}$ ) for GFR measurement.

Our results are consistent with previous research indicating iohexol plasma clearance as a reliable GFR comparable to inulin clearance [27, 43]. The iohexol clearance estimates agree with those reported for healthy adults, including the median renal clearance of  $6.78 \text{ L/h/1.73 m}^2$  (interquartile range:  $6.36$ – $7.50 \text{ L/h/1.73 m}^2$ ) by Sterner et al. [39], and  $7.32 \text{ L/h}$  (95% CI:  $7.08$ – $7.68 \text{ L/h}$ ) by Olsson et al. [44]. The intraindividual coefficient of variation for iohexol plasma clearance in this study (5.29%) was within the reported range of 5.6%–11.4% [27]. Other PK parameters, such as the volume of distribution estimated using the population PK analysis approach, were consistent with the previous three-compartment model estimate (median  $15.09 \text{ L}$ ) [28] and comparable to the reported  $0.27 \text{ L/kg}$  in healthy volunteers [44]. Discrepancies between the volumes of distribution obtained from the population PK evaluation (representing the steady-state volume) and the pseudoequilibrium volume ( $V_d$ ) obtained by NCA are attributed to ongoing distribution processes during the apparent terminal elimination

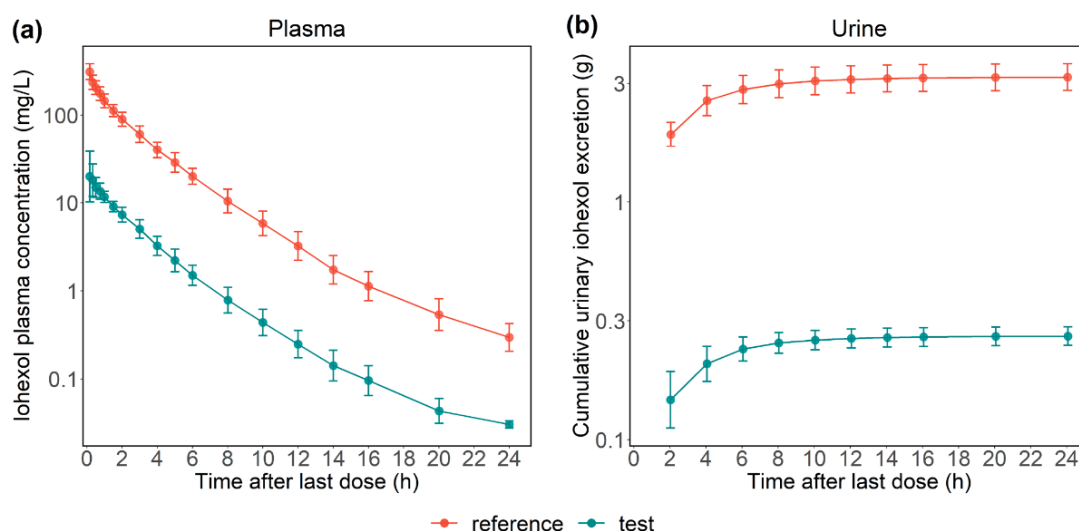


**FIGURE 3** | Semi-logarithmic plots of (a) plasma concentration–time profiles of iohexol and (b) cumulative urinary excretion following single reference or test doses. Symbols and error bars represent geometric means and geometric standard deviations, respectively. Data from 12 subjects are included: 10 completed all sample collections, providing both plasma and urine data for the reference and test periods. One provided complete plasma data for both periods and urine data only in the reference period, while another provided complete plasma data for both periods and urine data only in the test period.

**TABLE 2** | Plasma and urine pharmacokinetic parameters of iohexol for test and reference doses by noncompartmental analysis ( $n=12$ ).

Samples (number of subjects)	Parameters (unit)	Test		Reference		T/R ratio (90% CIs)	CV <sub>intra</sub> (%)
		Geomean (geoSD)	Geocv (%)	Geomean (geoSD)	Geocv (%)		
Plasma (12)	AUC <sub>0-t</sub> (mg·h/L)	46.5 (1.16)	14.8	598 (1.19)	17.4	—	—
	AUC <sub>0-∞</sub> (mg·h/L)	46.7 (1.16)	14.7	600 (1.19)	17.4	—	—
	$t_{1/2,\lambda z}$ (h)	3.32 (1.11)	10.2	4.14 (1.07)	6.97	—	—
	$V_z$ (L)	26.1 (1.14)	13.2	32.4 (1.20)	18.6	—	—
	CL (L/h)	5.46 (1.15)	14.2	5.43 (1.19)	17.3	1.01 (0.968–1.05)	5.29
Urine (10 <sup>a</sup> )	$R_{max}$ (mg/h)	73.7 (1.27)	24.1	951 (1.12)	11.7	—	—
	$\Delta e_{0-t}$ (mg)	273 (1.09)	8.96	3364 (1.14)	13.0	—	—
	Recovery (%)	106 (1.13)	11.8	103 (1.13)	12.7	1.06 (0.960–1.17)	11.9

Abbreviations:  $\Delta e_{0-t}$ , cumulative urinary excretion of unchanged iohexol from administration to the last time point; AUC, area under the plasma concentration–time curve; AUC from time zero to the last time point and AUC from time zero extrapolated to infinity are represented by AUC<sub>0-t</sub> and AUC<sub>0-∞</sub>, respectively; CI, confidence interval; CL, plasma clearance; CV<sub>intra</sub>, intraindividual coefficient of variation; geoCV, geometric coefficient of variation; Geomean, geometric mean; geoSD, geometric standard deviation; Recovery, percentage of the administered iohexol dose recovered in urine;  $R_{max}$ , maximum observed excretion rate; T/R ratio, test-to-reference ratio;  $t_{1/2,\lambda z}$ , apparent terminal plasma elimination half-life;  $V_z$ , volume of distribution during pseudoequilibrium.

<sup>a</sup>In two subjects, urine collection was not complete.

phase in iohexol plasma concentration–time profiles [45]. This also applies to differences in  $t_{1/2,\lambda z}$  and  $V_z$  between periods with different iohexol doses, which cannot be described properly by NCA.

Iohexol has many characteristics of an ideal GFR marker. Including minimal protein binding and exclusive elimination via glomerular filtration without tubular reabsorption or secretion

[27], as confirmed in this study. Using lower doses of iohexol to minimize potential toxicity may be of special interest for critically ill patients or those at risk of AKI, where frequent or even continuous monitoring of unstable GFR is crucial for understanding the impact of physiological and pathological changes on renal function. Continuous low-dose iohexol infusion has been shown to accurately track GFR changes, although further validation with

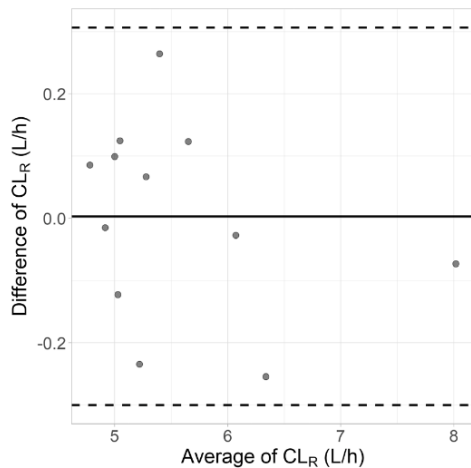


**FIGURE 4** | Bland-Altman plots comparing individual empirical Bayesian estimates (EBEs) of iohexol renal clearance following reference and test doses. The plot illustrates the difference between EBEs for renal clearance obtained after the test dose and those obtained after the reference dose. The mean bias of 0.00311 L/h is shown by the thin solid line, while the dashed lines denote the upper and lower limits of agreement.

larger sample sizes is needed [7, 22]. By improving the sensitivity of the previously reported analytical method [46], we decreased the LLOQ to 25 ng/mL, successfully measuring 91.7% of plasma iohexol concentrations 20 h after a single bolus dose of 259 mg. This method enables a tenfold reduction in iohexol doses compared with Dixon et al.'s study [7, 22], extending GFR monitoring periods while keeping total doses within safe limits.

The absence of transporter-mediated iohexol uptake in vitro, combined with the lack of nonrenal elimination pathways and the negligible impact of dose on iohexol pharmacokinetics in vivo, confirms that iohexol does not significantly interact with major drug transporters [23, 24]. This supports the conclusion that clinically relevant TDDIs with iohexol are highly unlikely. Therefore, iohexol meets the necessary criteria for inclusion as a GFR probe drug in our established transporter phenotyping cocktail [18], or in other respective cocktails [19–21]. Additionally, iohexol is not expected to interact with coadministered drugs during GFR measurements.

The study's main limitation is its exclusive focus on healthy volunteers and the use of dense sampling, which may not be directly applicable to patients. However, this sampling schedule is neither intended nor necessary for clinical practice, as established limited sampling strategies for reliable GFR assessment with iohexol are available [47], and can also be applied to low-dose iohexol. In critically ill patients, variations in GFR and the volume of distribution may impact iohexol pharmacokinetics [48, 49]. While there is no reason to believe that deviations from dose linearity would differ between healthy volunteers and patients with renal impairment, further validation studies are recommended to strengthen confidence in its clinical use in these populations.

**TABLE 3** | Population pharmacokinetic parameters of iohexol and bootstrap results ( $n = 12$ ).

Parameter (unit)	Point estimate	RSE%	Bootstrap median (95% CI)
Fixed effect			
$CL_R$ (L/h)	5.50	4.22	5.50 (5.13–6.02)
$V_1$ (L)	9.06	4.88	9.06 (8.18–10.1)
$Q_1$ (L/h)	0.221	14.7	0.219 (0.164–0.313)
$V_2$ (L)	1.56	7.74	1.57 (1.36–1.87)
$Q_2$ (L/h)	5.84	18.5	5.76 (4.11–8.23)
$V_3$ (L)	4.34	7.37	4.34 (3.81–4.99)
Interindividual variability (CV%)			
$CL_R$	14.0	29.5	13.5 (5.05–20.1)
$V_1$	16.6	24.0	15.5 (6.88–23.1)
$V_2$	14.0	21.3	13.4 (7.81–20.7)
$V_3$	15.5	18.8	13.7 (5.57–19.2)
Interoccasion variability (CV%)			
$CL_R$	2.51	29.1	2.44 (0.900–3.87)
$V_1$	6.23	39.2	6.06 (1.55–10.2)
$Q_2$	29.2	50.0	28.7 (6.99–65.8)
Residual unexplained variability (CV%)			
Plasma	11.3	17.9	11.2 (8.33–14.7)
Urine	25.0	20.7	24.8 (14.7–36.8)

Note: CV% for interindividual and interoccasion variability computed as  $\sqrt{\exp(\omega^2)} - 1$ , CV% for residual unexplained variability computed as  $\sqrt{\exp(\sigma^2)} - 1$ .

Abbreviations: CI, confidence interval;  $CL_R$ , renal clearance; CV%, coefficient of variation expressed as a percentage;  $Q_1$  and  $Q_2$ , intercompartmental clearances; RSE%, relative standard error expressed as a percentage;  $V_1$ , central volume of distribution;  $V_2$  and  $V_3$ , peripheral volumes of distribution.

### 4.3 | Overall Conclusion

Our results demonstrate that iohexol does not interact with major drug transporters and is eliminated exclusively by a nonsaturable renal elimination, and confirmed dose proportionality of iohexol pharmacokinetics in vivo. Based on these findings, a 259 mg dose of iohexol is suitable for precise GFR measurement in clinical settings and as part of a probe drug cocktail to enable the evaluation of renal transporter activity in clinical studies.

### Author Contributions

Q.D. and U.F. wrote the manuscript. U.F. and D.G. designed the research. Q.D., Z.C., J.B., C.D., Y.H., A.K., and U.F. performed the research. Q.D., Z.C., M.T., Y.H., and A.K. analyzed the data.



## Acknowledgments

We appreciate our colleagues from the Department of Pharmacology, Center for Pharmacology, Faculty of Medicine and University Hospital Cologne, University of Cologne, for their support during the study. We extend our gratitude to Muhammad Bilal, Yali Wu, Jil Hennig, Maria Alejandra Acosta Serrano, Svenja Flögel, Lea Hartman, Maurice Tust, Chiara Mandl, Sylvia Goitzsch, Samira Boussettaoui, Simone Kalis, and Kathi Krüsemann. We also thank the volunteers who participated in this study. Qian Dong and Zhendong Chen received scholarships from the China Scholarship Council to support their PhD studies. Open Access funding enabled and organized by Projekt DEAL.

## Conflicts of Interest

The authors declare no conflicts of interest.

## References

1. P. Delanaye, T. Melsom, N. Ebert, et al., "Iohexol Plasma Clearance for Measuring Glomerular Filtration Rate in Clinical Practice and Research: A Review. Part 2: Why to Measure Glomerular Filtration Rate With Iohexol?," *Clinical Kidney Journal* 9, no. 5 (2016): 700–704, <https://doi.org/10.1093/ckj/sfw071>.
2. L. A. Stevens and A. S. Levey, "Measured GFR as a Confirmatory Test for Estimated GFR," *Journal of the American Society of Nephrology* 20, no. 11 (2009): 2305–2313, <https://doi.org/10.1681/asn.2009020171>.
3. S. Mathialagan, A. D. Rodrigues, and B. Feng, "Evaluation of Renal Transporter Inhibition Using Creatinine as a Substrate in Vitro to Assess the Clinical Risk of Elevated Serum Creatinine," *Journal of Pharmaceutical Sciences* 106, no. 9 (2017): 2535–2541, <https://doi.org/10.1016/j.xphs.2017.04.009>.
4. D. C. Chen, O. A. Potok, D. Rifkin, and M. M. Estrella, "Advantages, Limitations, and Clinical Considerations in Using Cystatin C to Estimate GFR," *Kidney360* 3, no. 10 (2022): 1807–1814, <https://doi.org/10.34067/kid.0003202022>.
5. F. P. Wilson, J. M. Sheehan, L. H. Mariani, and J. S. Berns, "Creatinine Generation Is Reduced in Patients Requiring Continuous Venovenous Hemodialysis and Independently Predicts Mortality," *Nephrology, Dialysis, Transplantation* 27, no. 11 (2012): 4088–4094, <https://doi.org/10.1093/ndt/gfr809>.
6. L. A. Stevens, C. H. Schmid, T. Greene, et al., "Factors Other Than Glomerular Filtration Rate Affect Serum Cystatin C Levels," *Kidney International* 75, no. 6 (2009): 652–660, <https://doi.org/10.1038/KI.2008.638>.
7. J. J. Dixon, K. Lane, R. N. Dalton, et al., "Validation of a Continuous Infusion of Low Dose Iohexol to Measure Glomerular Filtration Rate: Randomised Clinical Trial," *Journal of Translational Medicine* 13 (2015): 58, <https://doi.org/10.1186/s12967-015-0414-3>.
8. C. Salmon-Gandonnière, I. Benz-de Bretagne, E. Mercier, et al., "Iohexol Clearance in Unstable Critically Ill Patients: A Tool to Assess Glomerular Filtration Rate," *Clinical Chemistry and Laboratory Medicine* 54, no. 11 (2016): 1777–1786, <https://doi.org/10.1515/cclm-2015-1202>.
9. U. Fuhr, C. H. Hsin, X. Li, W. Jabrane, and F. Sörgel, "Assessment of Pharmacokinetic Drug–Drug Interactions in Humans: In Vivo Probe Substrates for Drug Metabolism and Drug Transport Revisited," *Annual Review of Pharmacology and Toxicology* 59 (2019): 507–536, <https://doi.org/10.1146/annurev-pharmtox-010818-021909>.
10. GE Healthcare, "OMNIPAQUE (Iohexol) Injection and Oral Solution [Package Insert], Food and Drug Administration, Revised October (2024), accessed December 13, 2024, [https://www.accessdata.fda.gov/drugsatfda\\_docs/label/2024/018956Orig1s119,020608Orig1s0471bl.pdf](https://www.accessdata.fda.gov/drugsatfda_docs/label/2024/018956Orig1s119,020608Orig1s0471bl.pdf).
11. J. S. McDonald, N. B. Larson, J. J. Schmitz, et al., "Acute Adverse Events After Iodinated Contrast Agent Administration of 359,977 Injections: A Single-Center Retrospective Study," *Mayo Clinic Proceedings* 98, no. 12 (2023): 1820–1830, <https://doi.org/10.1016/j.mayocp.2023.02.032>.
12. A. Khwaja, "KDIGO Clinical Practice Guidelines for Acute Kidney Injury," *Nephron. Clinical Practice* 120, no. 4 (2012): c179–c184, <https://doi.org/10.1159/000339789>.
13. G. C. Kane, B. J. Doyle, A. Lerman, G. W. Barsness, P. J. Best, and C. S. Rihal, "Ultra-Low Contrast Volumes Reduce Rates of Contrast-Induced Nephropathy in Patients With Chronic Kidney Disease Undergoing Coronary Angiography," *Journal of the American College of Cardiology* 51, no. 1 (2008): 89–90, <https://doi.org/10.1016/j.jacc.2007.09.019>.
14. R. Masereeuw, M. M. Moons, P. Smits, and F. G. Russel, "Glomerular Filtration and Saturable Absorption of Iohexol in the Rat Isolated Perfused Kidney," *British Journal of Pharmacology* 119, no. 1 (1996): 57–64, <https://doi.org/10.1111/j.1476-5381.1996.tb15677.x>.
15. S. Yang, Y. Dai, Z. Liu, et al., "Involvement of Organic Cation Transporter 2 in the Metformin-Associated Increased Lactate Levels Caused by Contrast-Induced Nephropathy," *Biomedicine & Pharmacotherapy* 106 (2018): 1760–1766, <https://doi.org/10.1016/j.biopha.2018.07.068>.
16. B. Supawat, C. Udomtanakunchai, S. Kothan, and M. Tungjai, "The Effects of Iodinated Radiographic Contrast Media on Multidrug-Resistant K562/Dox Cells: Mitochondria Impairment and P-Glycoprotein Inhibition," *Cell Biochemistry and Biophysics* 77, no. 2 (2019): 157–163, <https://doi.org/10.1007/s12013-019-00868-3>.
17. J. A. Shannon and H. W. Smith, "The Excretion of Inulin, Xylose and Urea by Normal and PHLORIZINIZED Man," *Journal of Clinical Investigation* 14, no. 4 (1935): 393–401, <https://doi.org/10.1172/jci100690>.
18. C. Trueck, C. H. Hsin, O. Scherf-Clavel, et al., "A Clinical Drug–Drug Interaction Study Assessing a Novel Drug Transporter Phenotyping Cocktail With Adefovir, Sitagliptin, Metformin, Pitavastatin, and Digoxin," *Clinical Pharmacology and Therapeutics* 106, no. 6 (2019): 1398–1407, <https://doi.org/10.1002/cpt.1564>.
19. F. Müller, K. Hohl, S. Keller, et al., "N(1)-Methylnicotinamide as Biomarker for MATE-Mediated Renal Drug–Drug Interactions: Impact of Cimetidine, Rifampin, Verapamil, and Probenecid," *Clinical Pharmacology and Therapeutics* 113, no. 5 (2023): 1070–1079, <https://doi.org/10.1002/cpt.2849>.
20. D. A. Tatossian, K. L. Yee, Z. Zhang, et al., "A Microdose Cocktail to Evaluate Drug Interactions in Patients With Renal Impairment," *Clinical Pharmacology and Therapeutics* 109, no. 2 (2021): 403–415, <https://doi.org/10.1002/cpt.1998>.
21. S. T. Wiebe, T. Giessmann, K. Hohl, et al., "Validation of a Drug Transporter Probe Cocktail Using the Prototypical Inhibitors Rifampin, Probenecid, Verapamil, and Cimetidine," *Clinical Pharmacokinetics* 59, no. 12 (2020): 1627–1639, <https://doi.org/10.1007/s40262-020-00907-w>.
22. J. J. Dixon, K. Lane, R. N. Dalton, et al., "Continuous Infusion of Low-Dose Iohexol Measures Changing Glomerular Filtration Rate in Critically Ill Patients," *Critical Care Medicine* 46, no. 3 (2018): e190–e197, <https://doi.org/10.1097/ccm.0000000000002870>.
23. European Medicines Agency, "Guideline on the Investigation of Drug Interactions," (2012), accessed September 8, 2024, [https://www.ema.europa.eu/en/documents/scientific-guideline/guideline-investigation-drug-interactions-revision-1\\_en.pdf](https://www.ema.europa.eu/en/documents/scientific-guideline/guideline-investigation-drug-interactions-revision-1_en.pdf).
24. U.S. Food and Drug Administration, "M12 Drug Interaction Studies: Guidance for Industry," (2024), accessed December 8, 2024, <https://www.fda.gov/media/161199/download>.
25. M. Bach, S. Grigat, B. Pawlik, et al., "Fast Set-Up of Doxycycline-Inducible Protein Expression in Human Cell Lines With a Single Plasmid Based on Epstein-Barr Virus Replication and the Simple Tetra-cycline Repressor," *FEBS Journal* 274, no. 3 (2007): 783–790, <https://doi.org/10.1111/j.1742-4658.2006.05623.x>.
26. C. H. Hsin, A. Kuehne, Y. Gu, et al., "In Vitro Validation of an In Vivo Phenotyping Drug Cocktail for Major Drug Transporters in

- Humans,” *European Journal of Pharmaceutical Sciences* 186 (2023): 106459, <https://doi.org/10.1016/j.ejps.2023.106459>.
27. P. Delanaye, N. Ebert, T. Melsom, et al., “Iohexol Plasma Clearance for Measuring Glomerular Filtration Rate in Clinical Practice and Research: A Review. Part 1: How to Measure Glomerular Filtration Rate With Iohexol?,” *Clinical Kidney Journal* 9, no. 5 (2016): 682–699, <https://doi.org/10.1093/ckj/sfw070>.
28. M. Taubert, N. Ebert, P. Martus, M. van der Giet, U. Fuhr, and E. Schaeffner, “Using a Three-Compartment Model Improves the Estimation of Iohexol Clearance to Assess Glomerular Filtration Rate,” *Scientific Reports* 8 (2018): 17723, <https://doi.org/10.1038/s41598-018-35989-x>.
29. E. S. Schaeffner, N. Ebert, P. Delanaye, et al., “Two Novel Equations to Estimate Kidney Function in Persons Aged 70 Years or Older,” *Annals of Internal Medicine* 157, no. 7 (2012): 471–481, <https://doi.org/10.7326/0003-4819-157-7-201210020-00003>.
30. European Medicines Agency, “Committee for Medicinal Products for Human Use (CHMP) Guideline on the Investigation of Bioequivalence,” CPMP/EWP/QWP/1401/98 Rev 1/Corr, (2010), accessed May 16, 2024, [https://www.ema.europa.eu/en/documents/scientific-guideline/guideline-investigation-bioequivalence-rev1\\_en.pdf](https://www.ema.europa.eu/en/documents/scientific-guideline/guideline-investigation-bioequivalence-rev1_en.pdf).
31. L. Lindbom, P. Pihlgren, and E. N. Jonsson, “PsN-Toolkit—A Collection of Computer Intensive Statistical Methods for Non-Linear Mixed Effect Modeling Using NONMEM,” *Computer Methods and Programs in Biomedicine* 79, no. 3 (2005): 241–257, <https://doi.org/10.1016/j.cmpb.2005.04.005>.
32. J. Parke, N. H. Holford, and B. G. Charles, “A Procedure for Generating Bootstrap Samples for the Validation of Nonlinear Mixed-Effects Population Models,” *Computer Methods and Programs in Biomedicine* 59, no. 1 (1999): 19–29, [https://doi.org/10.1016/s0169-2607\(98\)00098-4](https://doi.org/10.1016/s0169-2607(98)00098-4).
33. T. M. Post, J. I. Freijer, B. A. Ploeger, and M. Danhof, “Extensions to the Visual Predictive Check to Facilitate Model Performance Evaluation,” *Journal of Pharmacokinetics and Pharmacodynamics* 35, no. 2 (2008): 185–202, <https://doi.org/10.1007/s10928-007-9081-1>.
34. L. A. Inker, N. D. Eneanya, J. Coresh, et al., “New Creatinine- and Cystatin C-Based Equations to Estimate GFR Without Race,” *New England Journal of Medicine* 385, no. 19 (2021): 1737–1749, <https://doi.org/10.1056/NEJMoa2102953>.
35. A. R. Topletz-Erickson, A. J. Lee, J. G. Mayor, et al., “Tucatinib Inhibits Renal Transporters OCT2 and MATE Without Impacting Renal Function in Healthy Subjects,” *Journal of Clinical Pharmacology* 61, no. 4 (2021): 461–471, <https://doi.org/10.1002/jcph.1750>.
36. J. C. Chappell, P. K. Turner, Y. A. Pak, et al., “Abemaciclib Inhibits Renal Tubular Secretion Without Changing Glomerular Filtration Rate,” *Clinical Pharmacology and Therapeutics* 105, no. 5 (2019): 1187–1195, <https://doi.org/10.1002/cpt.1296>.
37. M. K. Leabman and K. M. Giacomini, “Estimating the Contribution of Genes and Environment to Variation in Renal Drug Clearance,” *Pharmacogenetics* 13, no. 9 (2003): 581–584, <https://doi.org/10.1097/00008571-200309000-00007>.
38. A. Joshi, J. Guo, J. L. Holleran, et al., “Evaluation of the Pharmacokinetic Drug–Drug Interaction Potential of Iohexol, a Renal Filtration Marker,” *Cancer Chemotherapy and Pharmacology* 86, no. 4 (2020): 535–545, <https://doi.org/10.1007/s00280-020-04145-6>.
39. G. Sterner, B. Frennby, S. Mansson, U. Nyman, D. Van Westen, and T. Almén, “Determining ‘True’ Glomerular Filtration Rate in Healthy Adults Using Infusion of Inulin and Comparing It With Values Obtained Using Other Clearance Techniques or Prediction Equations,” *Scandinavian Journal of Urology and Nephrology* 42, no. 3 (2008): 278–285, <https://doi.org/10.1080/00365590701701806>.
40. H. M. Brink and J. F. Slegers, “Instantaneous Measurement of Glomerular Filtration Rate in the Isolated Perfused Rat Kidney,” *Pflügers Archiv* 383, no. 1 (1979): 71–73, <https://doi.org/10.1007/bf00584477>.
41. C. F. Anderson, T. K. Sawyer, and R. E. Cutler, “Iothalamate Sodium I 125 vs Cyanocobalamin co 57 as a Measure of Glomerular Filtration Rate in Man,” *Journal of the American Medical Association* 204, no. 8 (1968): 653–656.
42. S. E. Jenkinson, G. W. Chung, E. van Loon, N. S. Bakar, A. M. Dalzell, and C. D. Brown, “The Limitations of Renal Epithelial Cell Line HK-2 as a Model of Drug Transporter Expression and Function in the Proximal Tubule,” *Pflügers Archiv* 464, no. 6 (2012): 601–611, <https://doi.org/10.1007/s00424-012-1163-2>.
43. I. Soveri, U. B. Berg, J. Björk, et al., “Measuring GFR: A Systematic Review,” *American Journal of Kidney Diseases* 64, no. 3 (2014): 411–424, <https://doi.org/10.1053/j.ajkd.2014.04.010>.
44. B. Olsson, A. Aulie, K. Sveen, and E. Andrew, “Human Pharmacokinetics of Iohexol. A New Nonionic Contrast Medium,” *Investigative Radiology* 18, no. 2 (1983): 177–182, <https://doi.org/10.1097/00004424-198303000-00015>.
45. P. L. Toutain and A. Bousquet-Mélou, “Volumes of Distribution,” *Journal of Veterinary Pharmacology and Therapeutics* 27, no. 6 (2004): 441–453, <https://doi.org/10.1111/j.1365-2885.2004.00602.x>.
46. J. Stevens, M. A. Wessels, J. Roggeveeld, et al., “UHPLC-MS/MS Method for Iohexol Determination in Human EDTA and Lithium-Heparin Plasma, Human Urine and in Goat- and Pig EDTA Plasma,” *Bioanalysis* 12, no. 14 (2020): 981–990, <https://doi.org/10.4155/bio-2020-0122>.
47. N. Ebert, E. Schaeffner, J. C. Seegmiller, et al., “Iohexol Plasma Clearance Measurement Protocol Standardization for Adults: A Consensus Paper of the European Kidney Function Consortium,” *Kidney International* 106, no. 4 (2024): 583–596, <https://doi.org/10.1016/j.kint.2024.06.029>.
48. D. Morales Castro, L. Dresser, J. Granton, and E. Fan, “Pharmacokinetic Alterations Associated With Critical Illness,” *Clinical Pharmacokinetics* 62, no. 2 (2023): 209–220, <https://doi.org/10.1007/s40262-023-01213-x>.
49. A. M. Vilay, M. D. Churchwell, and B. A. Mueller, “Clinical Review: Drug Metabolism and Nonrenal Clearance in Acute Kidney Injury,” *Critical Care* 12, no. 6 (2008): 235, <https://doi.org/10.1186/cc7093>.

## Supporting Information

Additional supporting information can be found online in the Supporting Information section.

## Supplementary Material for Publication II

### MATERIALS

Iohexol, cimetidine, and para-aminohippuric acid (PAH) were purchased from Cayman Chemical (Ann Arbor, MI, USA), while Iohexol-d5 was purchased from Toronto Research Chemicals (Toronto, Ontario, Canada). Metformin, decynium-22, 1-methyl-4-phenylpyridinium (MPP+), Estrone 3-sulfate (E3S), Elacridar, cyclosporine A, and probenecid were acquired from Sigma-Aldrich (Darmstadt, Germany). [<sup>3</sup>H]Estrone sulfate, ammonium salt, [6,7-<sup>3</sup>H(N)] with a specific activity of 40 Ci/mmol was purchased from American Radiolabeled Chemicals (Saint Louis; MO, USA), [<sup>3</sup>H]BSP with a specific activity of 10.2 Ci/mmol was obtained from Hartmann Analytics (Braunschweig, Germany), and [<sup>3</sup>H]NMQ (N-methyl-quinidine) with a specific activity of 69 Ci/mmol was purchased from SOLVO (Hungary). All other chemicals were at least of analytical grade.

### METHODS

#### Part 1. In vitro study

##### Uptake assays for hOCT, hOAT, and hMATE transporters

Uptake assays were performed using stably transfected 293 cells, with or without the expression of one of the following transporters: hOAT1, hOAT3, hOCT1, hOCT2, hMATE1, or hMATE2K, as previously described.<sup>149</sup>

For the substrate assessment, cells were incubated with 10  $\mu$ M iohexol for 10 minutes and 30 minutes for each transporter. Inhibition assays were performed using specific standard substrates for each transporter: 10  $\mu$ M para-aminohippuric acid (PAH) for hOAT1, 3  $\mu$ M estrone-3-sulfate (E3S) for hOAT3, 50  $\mu$ M metformin for hOCT1, 5  $\mu$ M metformin for hOCT2, and 3  $\mu$ M 1-methyl-4-phenylpyridinium (MPP+) for hMATE1 and hMATE2K. These substrates were tested either alone or in combination with iohexol at concentrations of 1 mM and 20 mM, respectively, or with specific positive control inhibitors: 50  $\mu$ M probenecid for hOAT1, 100  $\mu$ M probenecid for hOAT3, 10  $\mu$ M decynium-22 for hOCT1, and 100  $\mu$ M cimetidine for hOCT2, hMATE1, and hMATE2K. To correct for the increased osmolarity due to the addition of 20 mM iohexol, 10 mM NaCl was removed from the uptake buffer, resulting in a final composition of 115 mM NaCl, 25 mM HEPES-NaOH (pH 7.4), 5.6 mM (+) glucose, 4.8 mM KCl,

1.2 mM  $\text{KH}_2\text{PO}_4$ , 1.2 mM  $\text{CaCl}_2$ , and 1.2 mM  $\text{MgSO}_4$ . Incubation times were 1 minute for hOAT1, hOAT3, and hOCT2, 20 minutes for hOCT1, and 0.5 minutes for hMATE1 and hMATE2K. The uptake was terminated by washing the cells with the ice-cold uptake buffer. The cells were then lysed with 1 mL of methanol for at least 20 minutes and stored at  $-20^\circ\text{C}$ . For substrate assessment, the methanol used for cell lysis included 2 ng/mL of iohexol-d5 as an internal standard.

The concentrations of probe drugs in cell lysate samples from uptake experiments were determined using liquid chromatography coupled with tandem mass spectrometry (LC-MS/MS), as detailed in the “LC-MS/MS analysis” section. Protein content in the mass spectrometry samples was estimated from three paired dishes using the BCA (bicinchoninic acid) assay (Pierce; Thermo Fisher 23225, Life Technologies, Darmstadt, Germany) with bovine serum albumin as the standard, following the previously described method.<sup>149</sup>

#### **Uptake assay for hOATP1B1 and hOATP1B3**

Uptake assays were carried out with stably transfected 293 cells expressing hOATP1B1 or hOATP1B3, as well as cells containing an empty vector, using the method described by Hsin CH, *et al.*<sup>149</sup> For the inhibition assays, cells were incubated with the radiolabeled standard substrates specific to each transporter:  $0.01\ \mu\text{M}$   $^3\text{H}$ -estrone sulfate for hOATP1B1, and  $0.02\ \mu\text{M}$   $^3\text{H}$ -bromosulphophthalein (BSP) for hOATP1B3. These substrates were incubated either alone or in the presence of iohexol (2 or 20 mM) or the respective positive control inhibitor ( $5\ \mu\text{M}$  cyclosporine A for hOATP1B1 and hOATP1B3). Incubation times were 1 minute for hOATP1B1 and 7 minutes for hOATP1B3. The accumulation of radio-labelled probe substrates ( $^3\text{H}$ ) in the cell lysate is determined using a Tri-Carb 2810 liquid scintillation counter (PerkinElmer, Waltham, MA, USA) as described previously.<sup>149</sup> Cellular protein amount was determined in parallel from 6 paired wells per cell line and experimental day, using the Bradford method.<sup>254</sup> The 1X lysis buffer (5X lysis buffer from Promega, diluted 1+4 [v/v] in ddH<sub>2</sub>O) was used as the lysis buffer. Protein was measured using 1X Bradford reagent (5X stock reagent from Carl Roth, Karlsruhe, Germany, diluted 1+4 [v/v] in ddH<sub>2</sub>O) and a Berthold Technologies TriStar2 LB942 spectrophotometer (Bad Wildbad, Germany) with bovine serum albumin as the standard.

#### **Uptake assay for hMDR1**



Inside-out membrane vesicles (1.5 mg/mL) from HEK293 cells, including both hMDR1-vesicles and control vesicles, were purchased from Pharm Tox, Netherlands. These vesicles were used to measure the ATP-dependent uptake of a radiolabeled probe substrate using the rapid filtration technique. The uptake was initiated by rapidly mixing the membrane suspension (7.5 µg protein) with the pre-warmed (37°C) vesicle buffer containing the radio-labeled substrate (0.01 µM <sup>3</sup>H-NMQ [N-methyl-quinidine]) either alone or in combination with iohexol (2 mM or 20 mM) or the respective positive control inhibitor (5 µM Elacridar) as well as 4 mM ATP and 10 mM MgCl<sub>2</sub>. After a 1 min incubation, the uptake was terminated by the addition of 500 µL of ice-cold Phosphate Buffered Saline (PBS) buffer. The mixture was immediately filtered through a glass fiber filter (Whatman GF/C) under vacuum. The filter was washed with ice-cold PBS buffer and dried under vacuum, before transferring the filter into a 6 mL scintillation vial. The measurement of the radiolabeled content was performed using the same technique employed in the uptake assays for hOATP1B1 and hOATP1B3.

### **Data analysis**

R version 4.2.1 (R Foundation for Statistical Computing, Vienna, Austria) was used for statistical evaluations and data visualization. The data analysis approach for the in vitro study was detailed by Hsin CH *et al.*<sup>149</sup> In brief, for transport assays, the initial uptake rate was calculated by normalizing the substrate concentration to both the protein concentration and the incubation time for each dish or well. The transporter-mediated uptake rate (net uptake) was determined by performing an element-wise subtraction of uptake rates from different conditions. First, all possible pairs of uptake rates were formed, with each pair consisting of one uptake rate from cells expressing the transporter or vesicles containing the transporter, and one uptake rate from control cells (vector-only or without transporter expression) or control vesicles within the same assay. Net uptake rates were determined by subtracting the uptake rate of the control cells or vesicles from that of the transporter-expressing cells or vesicles for each pair. The overall net uptake for a given transporter was then determined as the median, along with the 95% confidence intervals (CIs), of the net uptake rates across all assays.

## **Part 2. In vivo study**

### **Participants and assessment**

Twelve healthy volunteers, aged 18-60 years with a body mass index (BMI) between 18.5 and 30 kg/m<sup>2</sup>, were enrolled in the relevant part of the study once all screening results were available and the subjects were considered eligible. The screening process included a review of medical history, a physical examination, a 12-lead standard ECG, routine laboratory tests, serological blood tests for hepatitis B, hepatitis C, and HIV, a urine analysis for substances of abuse, an alcohol breath test, measurement of thyroid-stimulating hormone serum levels, and, for female volunteers, a pregnancy test. The main exclusion criteria included contraindications to iohexol, significant clinical or laboratory abnormalities, current medication use, smoking, drug addiction, pregnancy, or breastfeeding.

Adverse events were monitored at multiple time points: within 1 hour before the administration of iohexol, and then at 10 minutes, 30 minutes, 1 hour, and 2 hours post-dose, as well as at the end of hospitalization for each period and during the end-of-study evaluation. Vital signs were recorded at the same time points as adverse events. Overall health was reassessed at the end of the study.

### **Treatments**

Participants will be randomly assigned to one of six sequences (1-2-3, 2-3-1, 3-1-2, 3-2-1, 1-3-2, 2-1-3) with each sequence comprising three treatments administered on separate occasions:

- 1) a 259 mg dose of iohexol under fasting conditions ("test"),
- 2) a 3235 mg dose of iohexol under fasting conditions ("reference"),
- 3) a 3235 mg dose of iohexol with the ingestion of boiled beef (not reported here).

For each treatment, either 5 ml (containing 3235 mg) or 0.4 ml (containing 259 mg) of iohexol solution (ACCUPAQUE™ 300 Injektionslösung)<sup>137</sup> was injected intravenously as a single bolus over 1-2 minutes or 0.1-0.2 minutes, respectively. The syringes containing iohexol were weighed before and after injection to ensure accurate dosing. During the "fasting conditions", participants were hospitalized from 2 hours before to 24 hours after the administration of iohexol.

### **Non-compartmental analysis**

#### **Evaluation of pharmacokinetic parameters**

Plasma pharmacokinetic (PK) parameters were calculated, including the terminal elimination rate constant ( $\lambda_z$ ), terminal plasma elimination half-life ( $t_{1/2, \lambda_z}$ ), the volume of distribution ( $V_z$ ),<sup>255</sup> the area under the plasma concentration-time curve (AUC), which includes AUC from time zero to the last time point ( $AUC_{0-t}$ ) and AUC from time zero extrapolated to infinity ( $AUC_{0-\infty}$ ), and plasma clearance (CL). The  $\lambda_z$  value was determined by linear regression analysis of the terminal log-linear phase of individual concentration-time curves, using the last three concentration values above the lower limit of quantification (LLOQ). This approach ensures an accurate reflection of the terminal slope. The  $t_{1/2, \lambda_z}$  was calculated as  $\ln(2)/\lambda_z$ , and the  $V_z$  was calculated as  $Dose/(\lambda_z * AUC_{0-\infty})$ . AUC was determined using the linear log trapezoidal rule.  $AUC_{0-\infty}$  was calculated as  $AUC_{0-t} + C_{last}/\lambda_z$ , where the  $C_{last}$  is the concentration of the last time point with measurable concentration. CL was calculated as  $Dose/AUC_{0-\infty}$ . Urine iohexol PK parameters were also calculated, including the cumulative urinary excretion of unchanged iohexol from administration to the last time point ( $Ae_{0-t}$ ), the maximum observed excretion rate ( $R_{max}$ ), and the percentage of the administered iohexol dose recovered in urine, referred to as urinary recovery.

### Statistical methods

Statistical evaluations for non-compartmental analysis (NCA) and bioequivalence analysis were performed using PKanalix 2024R1 (Lixoft SAS, a Simulations Plus company, Paris, France). CL estimates and urinary recovery, derived from NCA, were compared between the reference and test doses using the standard bioequivalence approach.<sup>232</sup> Log-transformed values of CL and urinary recovery were evaluated using an analysis of variance model with fixed effects for sequence, subject within sequence, period, and dose (instead of “preparation” for bioequivalence assessment). The point estimate and 90% confidence interval (CI) for the test-to-reference ratio of CL and urinary recovery were calculated. The null hypothesis of “a relevant difference in CL between doses” was rejected, and CL was considered to be dose-linear if the 90 % CI was completely within the standard bioequivalence boundaries of 80–125%. The sample size calculation assumed that the intra-individual coefficient of variation ( $CV_{intra}$ ) for GFR measurement with iohexol would not exceed 11.4% in the general population.<sup>256</sup> With this assumed  $CV_{intra}$  and a true ratio of  $0.95 \leq \mu_{test}/\mu_{reference} \leq 1.05$ , a sample size of 8 subjects would be sufficient to reject the null hypothesis of a significant difference in CL between doses, with a two-sided alpha of 0.05 and a power of at

least 80%. However, since a minimum of 12 subjects is required for a bioequivalence study, we included 12 subjects.

### **Population pharmacokinetic analysis**

#### **Assessing the impact of implausible data**

We identified slight leakage during the injection of the test iohexol dose in one subject. To evaluate its impact on the final parameter estimates, we used two approaches: (i) conducting a sensitivity analysis by comparing parameter estimates across three models—the final model, a model excluding early post-dose plasma samples from the subject, and a model excluding all data from this period for the subject. (ii) expanding the model to describe absorption from an additional para-venous compartment for the administration of iohexol in this subject and period only.

#### **LC-MS/MS analysis**

For quantification, all drugs except for PAH were measured using an API 5000 device (AB Sciex Germany GmbH, Darmstadt, Germany), connected to an Agilent 1200 HPLC binary pump and an Agilent 1260 Infinity autosampler (Agilent Technologies Deutschland GmbH, Waldbronn, Germany). The concentrations of PAH in cell lysis samples were determined using an API 4000 QTRAP device (AB Sciex Germany GmbH, Darmstadt, Germany), connected to a Shimadzu LC-20AD HPLC pump and a Shimadzu SIL-20AC HT autosampler (Shimadzu Deutschland GmbH, Duisburg, Germany). For all measurements, the column temperature was maintained at 40°C, and the samples were stored at 4°C in an autosampler until injection. Instrument control and data acquisition were performed using Analyst 1.6.2 software (AB Sciex Germany GmbH, Darmstadt, Germany). Quantification was based on peak area, with calibration functions determined using weighted least-squares linear regression. Specific quantitation methods are detailed below, and the liquid chromatography conditions and tandem mass spectrometry parameters are provided in Tables S1 and S2, respectively.

#### **Quantitation of iohexol in plasma and urine**

For the preparation of plasma and urine samples, 50 µL of each plasma sample or 10 µL of each urine sample was dispensed into a 96-well plate. To each sample, 10 µL of an iohexol-d5 (internal standard) working solution (5 µg/mL) was added. Plasma samples were

deproteinized using 200  $\mu$ L of acetonitrile, while urine samples were deproteinized with 400  $\mu$ L of acetonitrile. After vortexing the mixture for 30 seconds, it was centrifuged at room temperature for 15 minutes at  $3000 \times g$ . A 150- $\mu$ L aliquot of the resulting supernatant was transferred to a 96-well plate for LC-MS/MS analysis. All assays for iohexol concentration in plasma and urine met the bioanalytical method validation criteria established by the US Food and Drug Administration (FDA)<sup>257</sup> and the European Medicines Agency (EMA)<sup>258</sup>. The LLOQs were 25 ng/mL for plasma and 125 ng/mL for urine. Accuracy for plasma and urine quality control (QC) samples, including LLOQ, low, medium, and high concentrations, ranged from 89.07% to 109.24% of the nominal values. Intra-day and inter-day precision, expressed as coefficients of variation, were below 6.08% for plasma samples and 6.76% for urine samples.

### **Quantitation of probe drugs in cell lysate**

For sample preparation, cell lysate samples from uptake experiments were vortexed and centrifuged at room temperature for 2 minutes at  $16,100 \times g$ . A 150- $\mu$ L aliquot of the resulting supernatant was then transferred to a 96-well plate for LC-MS/MS analysis.

## **RESULTS**

### **Part 2 In vivo study**

#### **Dataset**

##### **1. Missing data**

Urinary excretion data were unavailable for the 2–4 hour interval in Subject 8 following the reference dose and for the 14–16 hour interval in Subject 9 following the test dose (see Figure S4). Consequently, data from these two subjects were excluded from the NCA.

##### **2. Implausible data**

Figure S4 shows that the initial plasma concentrations of iohexol in Subject 6 after the test dose exhibited an absorption-like behavior, suggesting that at least part of the dose might have been administered paravenously.

#### **Safety**

In total, 7 of 12 subjects reported 9 adverse events. None of these were related to iohexol, while one rated as severe (syncope after venipuncture prior to scheduled iohexol

administration) was associated with study procedures. Four subjects used single doses of concomitant medications for the adverse events, including ibuprofen, paracetamol, and pantoprazole. Ibuprofen, as the only one of these drugs with a relevant effect on renal function, was taken between study periods and is therefore not expected to have influenced the results.

## **Population pharmacokinetic analysis**

### **Model evaluation**

The visual predictive check (VPC) results (Figure S5) indicated that the medians and 10<sup>th</sup> and 90<sup>th</sup> percentiles of the simulated data from the final model were in acceptable agreement with the observed data. The goodness-of-fit (GOF) plots (Figure S6) demonstrated that the final model accurately described the observed iohexol plasma concentrations and urinary excretion. There was good agreement between the observed and individual/population-predicted plasma concentrations and urinary amounts. Conditional weighted residuals (CWRES) were randomly scattered around zero, suggesting no systematic deviations in the model. However, several outliers in plasma concentrations during the early phase after administration of the test dose were observed in the GOF plots (Figure S6 (b)), primarily from Subject 6, who displayed an apparent absorption phase, as previously described. The final point estimates and bootstrap statistics of PK parameters are summarized in Table 3, with no indications of overparameterization in any of the model diagnostics or the bootstrap results.

### **Assessing the impact of implausible data**

The sensitivity analysis of parameter estimates from models using different datasets is presented in Table S5. The parameter estimates remained nearly unchanged across models developed using the entire dataset, the dataset excluding plasma samples taken within 45 minutes after the test dose for the subject with delayed absorption, and the dataset excluding the respective period. Modeling an absorption phase for this subject and period resulted in a first-order absorption rate constant of 0.876 h<sup>-1</sup>, a relative bioavailability of 93.6%, and an improvement in OFV by 185 points, while other parameters were almost identical (not shown).

# SUPPLEMENTARY TABLES

**Table S1 Liquid chromatography condition for analytes.**

Analyte (IS)	Matrix	Standard curve range	Injection volume (μL)	Flow rate (mL/min)	Gradient elution %B <sup>a</sup> (min)	Columns
Iohexol (Iohexol-d5)	Plasma	25 – 2500 ng/mL	10	0.3	90 (0.0) → 90 (0.2) → 15(1.0) → 15(3.5) → 90 (4.0) → 90 (6.0)	SeQuant® ZIC®-HILIC column (2.1 x 100 mm, 5 μm, 200Å, Merck KGaA, Darmstadt, Germany)
	Urine	0.125 – 12.5 μg/mL				
	Cell lysate	0.5 – 32 ng/mL				
metformin	Cell lysate	3.125 – 800 ng/mL (for hOCT1)	5	0.3	85 (0.0) → 85 (0.1) → 15(0.5) → 15(3.5) → 85 (4.0) → 85 (7.0)	SeQuant® ZIC®-HILIC column (2.1 x 100 mm, 5 μm, 200Å, Merck KGaA, Darmstadt, Germany)
		0.195 – 100 ng/mL (for hOCT2)				
PAH	Cell lysate	0.49 – 1000 ng/mL	20	0.4	80 (0.0) → 80 (0.25) → 20(2.0) → 20(3.0) → 80 (4.0) → 80 (5.0)	Waters Atlantis HILIC Silica Column 3.0 x 50 mm 5 μm, combined with Altantis®HILIC, 5μM VanGuard® Cartridge (Waters Chromatography Ireland Limited, Dublin, Ireland)
E3S	Cell lysate	0.78 – 100 ng/mL	10	0.2	35 (0.0) → 35 (0.25) → 90(3.0) → 90(3.5) → 35 (5.5) → 35 (9.0)	Xbridge®Shield RP18 3.5um, 3.0x100mm Column, combined with Xbridge®BEH Shield RP18 3.5μM, VanGuard® Cartridge (Waters Chromatography Ireland Limited, Dublin, Ireland)
MPP+	Cell lysate	0.39 – 25 ng/mL	5	0.3	90 (0.0) → 90 (0.1) → 15(1.0) → 15(3.5) → 90 (4.5) → 90 (6.0)	SeQuant® ZIC®-HILIC column (2.1 x 100 mm, 5 μm, 200Å, Merck KGaA, Darmstadt, Germany)

IS, internal standard; PAH, para-amino hippuric acid; E3S, Estrone-3-Sulfate; MPP+, 1-Methyl-4-phenylpyridinium.

<sup>a</sup> The gradient solvent systems for the compounds are as follows: Iohexol (Iohexol-d5) and MPP+ were analyzed with 0.1% formic acid in water (A) and acetonitrile with 0.1% formic acid (B); Metformin was assessed with 10 mM ammonium formate (pH 3.75) (A) and acetonitrile (B); PAH was determined using 10 mM ammonium acetate (pH 4) (A) and methanol with 0.1% formic acid (B); and E3S was evaluated using 10 mM ammonium acetate (pH 8.9) (A) and methanol (B)



**Table S2 Optimized tandem mass spectrometry parameters for analytes.**

Analyte	Mode	Ion transition (Da)	DP (volts)	CE (volts)	CXP (volts)
iohexol	positive	821.937 → 374.700	196.000	65.000	16.000
iohexol-d <sub>5</sub> (IS)	positive	826.911 → 607.900	146.000	39.000	28.000
PAH	positive	195.134 → 120.100	36.000	15.000	2.000
E3S	negative	349.142 → 269.000	-170.000	-48.000	-27.000
MPP+	positive	170.123 → 128.200	131.000	45.000	26.000
metformin	positive	130.176 → 60.000	81.000	19.000	14.000

DP, declustering potential; CE, collision energy; CXP, collision cell exit potential; IS, internal standard; PAH, para-amino hippuric acid; E3S, Estrone-3-Sulfate; MPP+, 1-Methyl-4-phenylpyridinium.

**Table S3 Evaluation of in vitro system quality and inhibitory effects of iohexol on these systems.**

Transporter	In vitro systems	Inhibitory effect (% reduction of specific activity) <sup>b</sup>		
	Expression on vs. off <sup>a</sup>	Prototypical inhibitors	1 mM or 2 mM iohexol	20 mM iohexol
hOAT1	250 (240 to 260)	70 (70 to 71)	-0.45 (-0.53 to 1.3)	3.1 (2.8 to 4.3)
hOAT3	13 (11 to 16)	94 (94 to 94)	-4 (-5.6 to -2.4)	-3.5 (-7.5 to -0.29)
hOCT1	17 (16 to 20)	90 (89 to 90)	-9.8 (-12 to -8)	-22 (-33 to -5.4)
hOCT2	19 (15 to 27)	49 (48 to 50)	-13 (-14 to -10)	-23 (-26 to -22)
hMATE1	18 (17 to 20)	95 (95 to 95)	5.4 (4.5 to 6.4)	12 (11 to 14)
hMATE2K	8 (7.3 to 8.8)	75 (75 to 76)	14 (13 to 16)	26 (25 to 28)
hOATP1B1	17 (16 to 20)	83 (82 to 83)	-6.9 (-9.2 to -4.5)	5.5 (4.6 to 7.6)
hOATP1B3	3.3 (3.3 to 3.8)	94 (90 to 96)	-2.5 (-3.8 to -1.6)	-21 (-24 to -18)
hMDR1	5.4 (4.8 to 5.9)	99 (97 to 100)	-4.9 (-10 to -1.2)	21 (17 to 24)

Stably transfected 293 cells, either with (expression on; n = 4 for hOAT3, n = 3 for other transporters) or without (expression off; n = 4 for hOAT3, n = 3 for other transporters) expression of hOAT1, hOAT3, hOCT1, hOCT2, hMATE1, or hMATE2K, were incubated with transporter-specific probe substrates alone, with prototypical inhibitors, or with 1 mM or 20 mM iohexol. Similarly, 293 cells stably expressing hOATP1B1, hOATP1B3, or hMDR1 vesicles (transporter-expressing; n = 3), and corresponding controls (empty-vector transfected cells or control vesicles; n = 3), were incubated with probe substrates alone, with prototypical inhibitors, or with 2 mM or 20 mM iohexol. Data are presented as the median values with 95% CIs across all experiments.

<sup>a</sup> Uptake rate ratios of probe substrates in transporter-expressing cells or vesicles were normalized to uptake rates in control cells or vesicles through element-wise division.

<sup>b</sup> Inhibitory effects of prototypical inhibitors and iohexol were calculated as the percentage reduction in transporter activity relative to activity with the probe substrate alone, using element-wise division within each experiment.

**Table S4 Iohexol accumulation and uptake ratios in transporter-expressing and non-expressing 293 cells.**

Transporter	Incubation time (minutes)	Differences in intracellular accumulation <sup>a</sup> (pmol/mg protein)	Uptake ratio <sup>b</sup>
hOAT1	10	-0.39 (-3.4 to 1.1)	0.91 (0.75 to 1.2)
	30	0.98 (-0.62 to 2.1)	1.1 (0.95 to 1.3)
hOAT3	10	0.6 (0.1 to 2)	1.1 (1 to 1.4)
	30	0.89 (0.19 to 1.5)	1.2 (1.1 to 1.3)
hOCT1	10	0.16 (-1.8 to 0.79)	1 (0.84 to 1.1)
	30	-0.51 (-1.1 to -0.15)	0.89 (0.79 to 0.97)
hOCT2	10	1.3 (0.007 to 2.6)	1.1 (1 to 1.2)
	30	1.5 (-1.4 to 2.9)	1.1 (0.9 to 1.3)
hMATE1	10	0.36 (-1.2 to 1.7)	1.1 (0.84 to 1.2)
	30	-0.67 (-1.6 to 0.61)	0.92 (0.78 to 1.1)
hMATE2K	10	-0.36 (-1.1 to 0.24)	0.95 (0.81 to 1.1)
	30	0.62 (-0.38 to 1.5)	1.1 (0.93 to 1.4)

Stably transfected 293 cells, either expressing (n = 4 for hOAT3; n = 3 for other transporters) or not expressing (n = 4 for hOAT3; n = 3 for other transporters) hOAT1, hOAT3, hOCT1, hOCT2, hMATE1, or hMATE2K, were incubated with 10  $\mu$ M iohexol for 10 and 30 minutes, respectively. Each experiment was performed in triplicate, with each assay conducted on a separate day. Data are presented as the median values with 95% CIs across all experiments.

<sup>a</sup> The difference in iohexol accumulation between transporter-expressing and control cells was determined by element-wise subtraction of intracellular iohexol accumulations under "expression off" from that under "expression on" conditions for each transporter and experimental group.

<sup>b</sup> The ratio of iohexol uptake rates in transporter-expressing cells compared to non-expressing cells was calculated through element-wise division within each transporter and experimental group.

**Table S5 Sensitivity analysis of parameter estimates from models using different datasets.**

	Final model <sup>a</sup>		Model 1 <sup>b</sup>		Model 2 <sup>c</sup>	
Parameters	Estimate	RSE (%)	Estimate	RSE (%)	Estimate	RSE (%)
CL <sub>R</sub> (L/h)	5.50	4.22	5.45	4.33	5.49	4.22
V <sub>1</sub> (L)	9.06	4.88	8.91	4.49	8.90	4.64
Q <sub>1</sub> (L/h)	0.221	14.7	0.219	15.3	0.227	16.2
V <sub>2</sub> (L)	1.56	7.74	1.54	8.31	1.57	8.24
Q <sub>2</sub> (L/h)	5.84	18.5	5.53	17.6	5.38	17.7
V <sub>3</sub> (L)	4.34	7.37	4.30	6.88	4.30	6.65
<b>Inter-individual variability (CV%)</b>						
CL <sub>R</sub>	14.0	29.5	14.4	28.9	14.2	28.5
V <sub>1</sub>	16.6	24.0	16.8	25.4	17.2	21.5
V <sub>2</sub>	14.0	21.3	15.1	20.1	13.8	22.9
V <sub>3</sub>	15.5	18.8	15.0	17.9	13.5	19.5
<b>Inter-occasion variability (CV%)</b>						
CL <sub>R</sub>	2.51	29.1	3.69	33.2	2.33	26.3
V <sub>1</sub>	6.23	39.2	4.82	48.4	3.87	36.2
Q <sub>2</sub>	29.2	50.0	23.7	40.6	17.1	47.9
<b>Residual variability (CV%)</b>						
plasma	11.3	17.9	8.94	4.40	8.84	4.85
urine	25.0	20.7	25.5	20.4	25.4	21.0

RSE%, relative standard error expressed as a percentage; CL<sub>R</sub>, renal clearance; Q<sub>1</sub> and Q<sub>2</sub>, intercompartmental clearances; V<sub>1</sub>, central volume of distribution; V<sub>2</sub> and V<sub>3</sub> peripheral volumes of distribution; CV%, coefficient of variation expressed as a percentage, CV% for Inter-individual and Inter-occasion variability computed as  $\sqrt{\exp(\omega^2) - 1}$ , CV% for residual unexplained variability computed as  $\sqrt{\exp(\sigma^2) - 1}$ .

<sup>a</sup> The final model was developed using the entire dataset.

<sup>b</sup> Model 1 was developed excluding samples taken within 45 minutes after the test dose for the subject with delayed absorption

<sup>c</sup> Model 2 was developed excluding all data from the subject with delayed absorption when receiving the iohexol test dose.

## SUPPLEMENTARY FIGURES

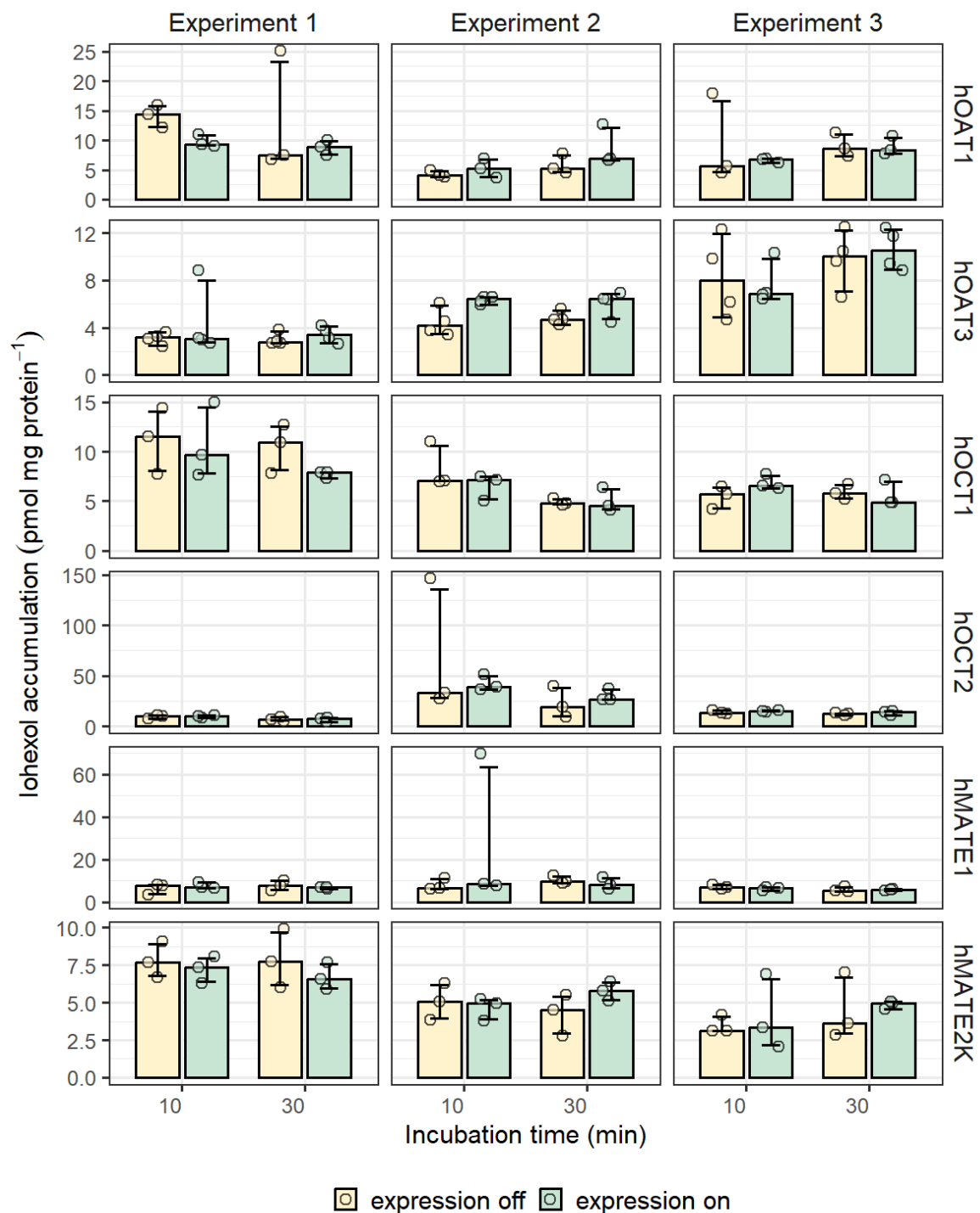


**Figure S1 The accumulation of iohexol in 293 cells with or without the expression of hOAT1, hOAT3, hOCT1, hOCT2, hMATE1, or hMATE2K.**

Stably transfected 293 cells, either expressing (expression on; n=3 or 4) or not expressing (expression off; n=3 or 4) hOAT1, hOAT3, hOCT1, hOCT2, hMATE1, or hMATE2K, were incubated with 10  $\mu$ M iohexol for 10 and 30 minutes, respectively. Each dot represents an individual dish. The columns and their error bars indicate the 5<sup>th</sup>, 50<sup>th</sup>, and 95<sup>th</sup> percentiles of the data.

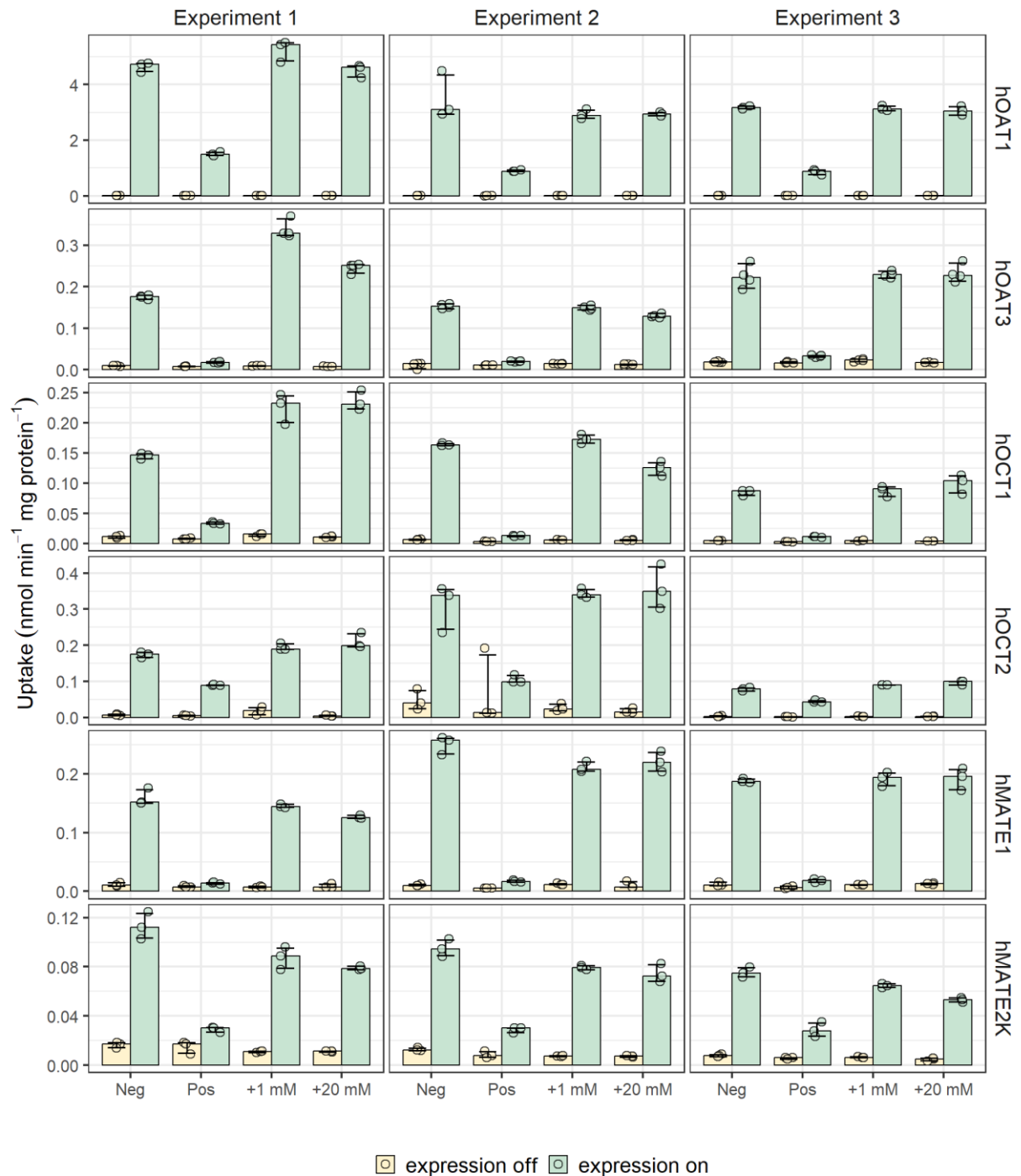


**Figure S2 Impact of iohexol on the transport of standard substrates mediated by hOAT1, hOAT3, hOCT1, hOCT2, hMATE1, or hMATE2K.**

Stably transfected 293 cells, either with (expression on; n=3 or 4) or without (expression off; n=3 or 4) the expression of hOAT1, hOAT3, hOCT1, hOCT2, hMATE1, or hMATE2K were incubated with the probe substrate for each transporter. The conditions included incubation with the standard substrate alone (Neg), with the respective positive inhibitor (Pos), or with 1 mM iohexol (+1 mM) or 20 mM iohexol (+20 mM). Each experiment was conducted three times. Each dot represents an individual dish. The columns and their error bars indicate the 5<sup>th</sup>, 50<sup>th</sup>, and 95<sup>th</sup> percentiles of the data.

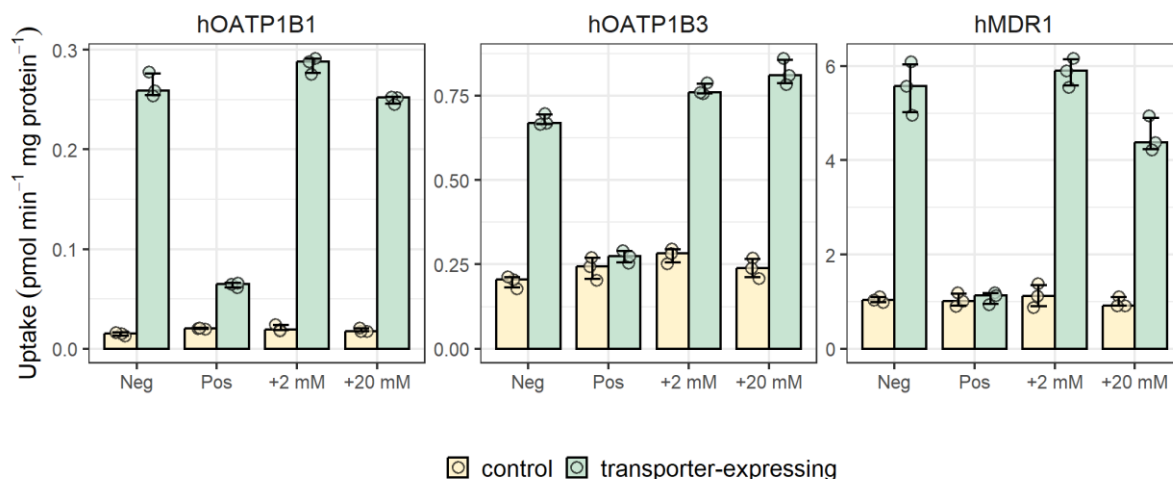
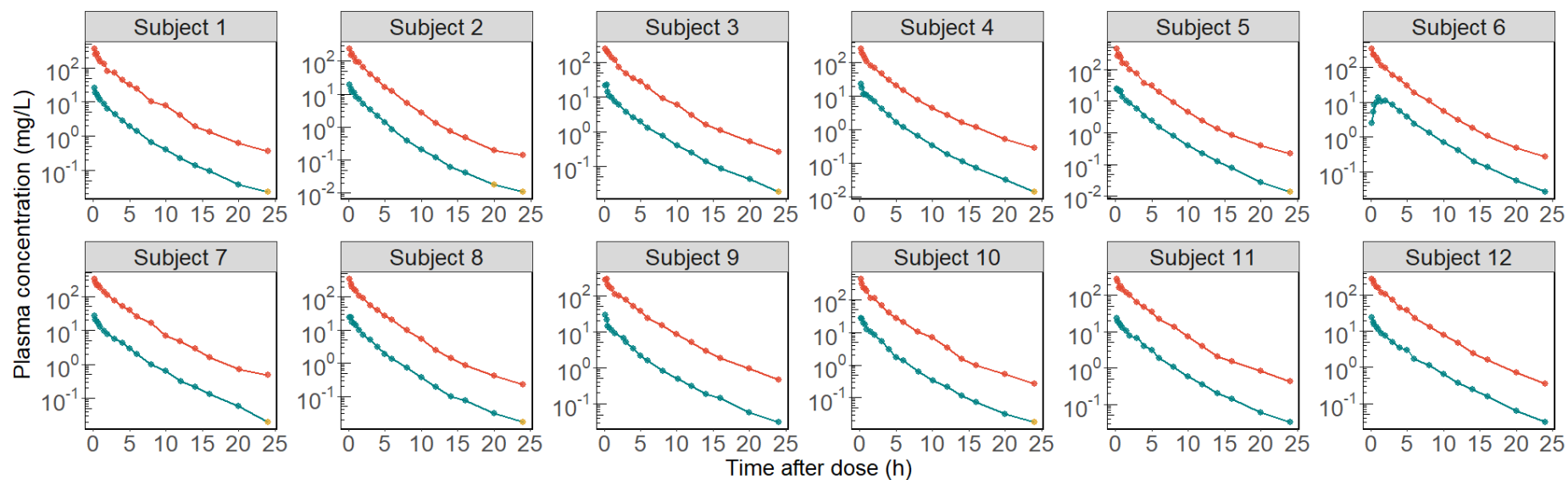


**Figure S3 Impact of iohexol on the transport of standard substrates mediated by hOATP1B1, hOATP1B3, or hMDR1.**

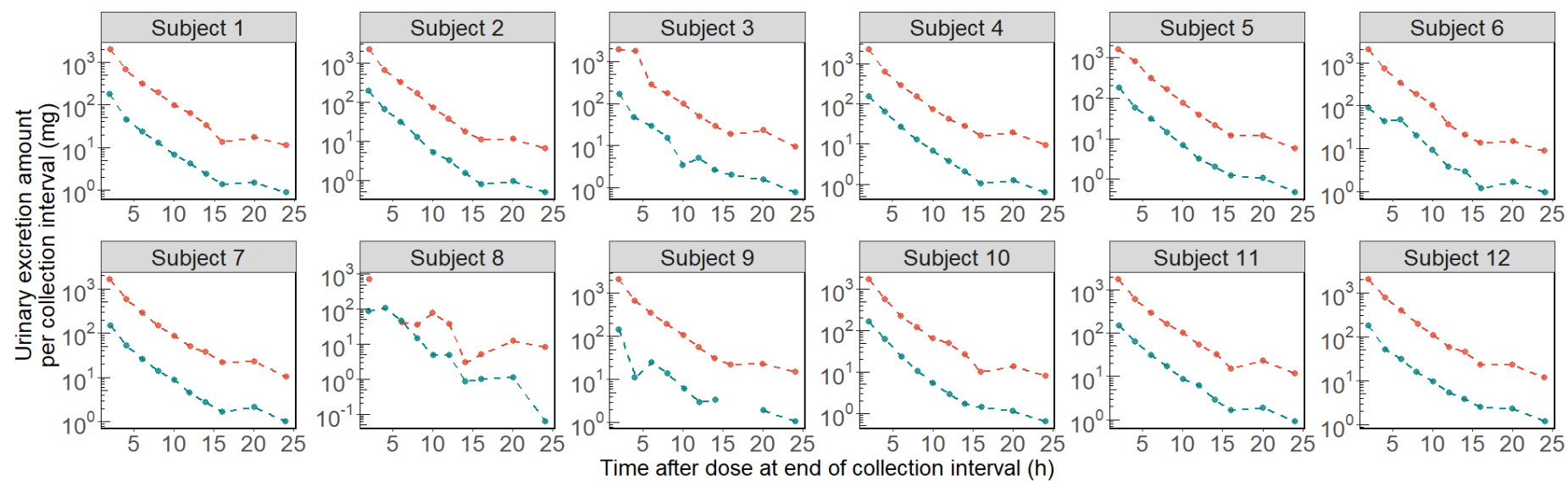
Stably transfected 293 cells expressing hOATP1B1, hOATP1B3, or hMDR1-expressing vesicles (transporter-expressing; n=3), along with control cells transfected with empty vectors or control vesicles (control; n=3), were incubated with transporter-specific probe substrates. Incubation conditions included: probe substrate alone (Neg), with a positive control inhibitor (Pos), or with iohexol at 2 mM (+2 mM) or 20 mM (+20 mM). Each dot represents a single well. Columns and error bars represent the 5<sup>th</sup>, 50<sup>th</sup>, and 95<sup>th</sup> percentiles.



(a)



(b)



—●— BQL —●— reference —●— test

**Figure S4 Time-course of log-scaled iohexol plasma concentrations and urinary excretion.**

(a) Log-scaled iohexol plasma concentrations over time following the reference and test doses, respectively. (b) Log-scaled urinary excretion amounts per collection interval following the reference and test doses, respectively. Data points are represented by dots: non-BQL (above the quantification limit) values are color-coded to match their respective lines, while BQL (below the quantification limit) values are highlighted in yellow. Note: urinary excretion data were unavailable for the 2–4 hour collection interval for Subject 8 after the reference dose, and for the 14–16 hour interval for Subject 9 after the test dose.

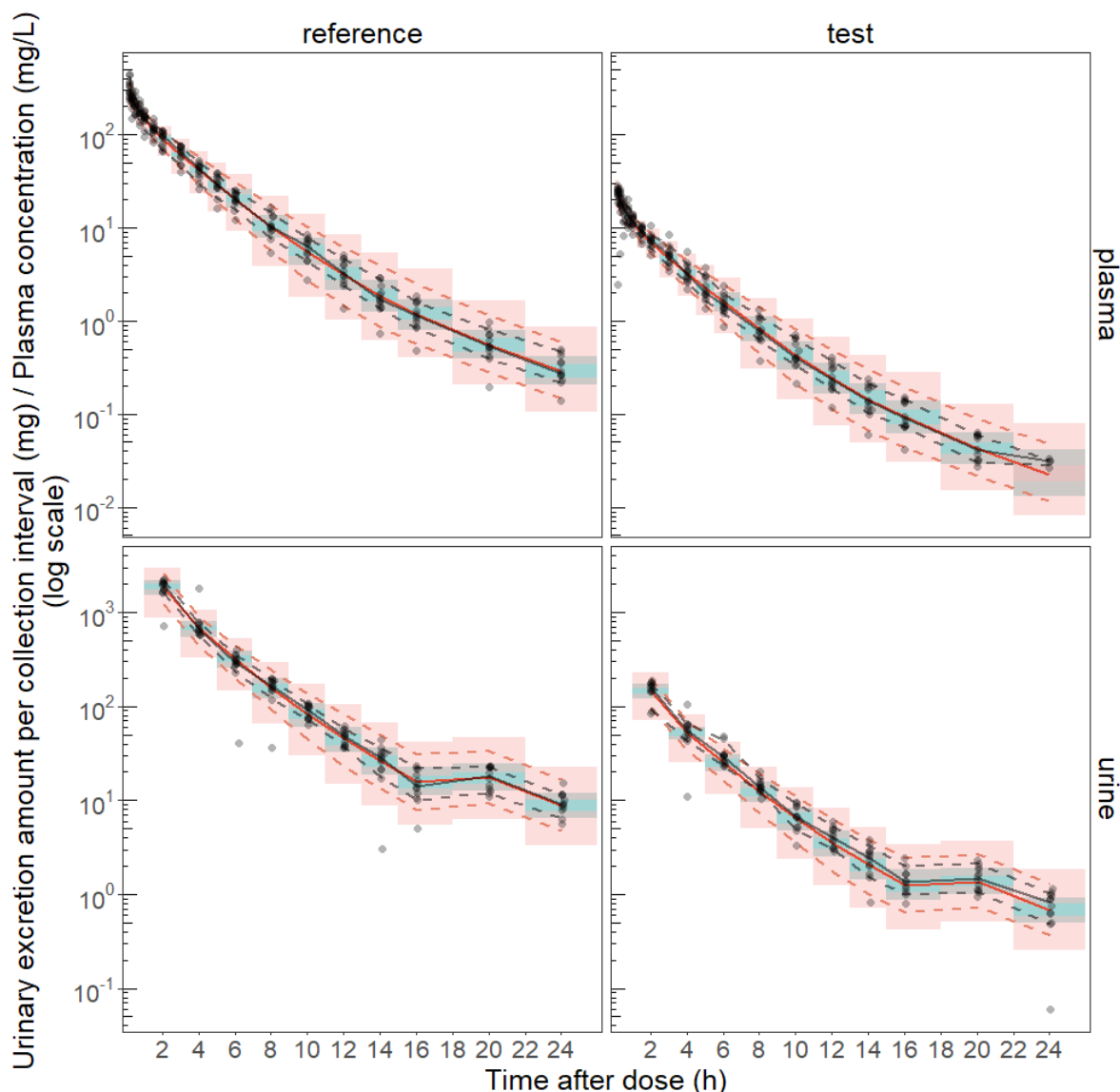


**Figure S5 Visual predictive check (n = 1000) for the final model stratified by plasma and urine data, and categorized by reference and test dose levels.**

Dots illustrate observed data points. Solid (dashed) black and red lines represent medians (10<sup>th</sup>, and 90<sup>th</sup> percentiles) of observations and simulated data, respectively; red, green, and red areas represent 95% confidence intervals of the 10<sup>th</sup>, 50<sup>th</sup>, and 90<sup>th</sup> percentiles of simulated data. The X-axis represents the sampling time (hours) for plasma data and the time at the end of the collection interval (hours) for urine data.

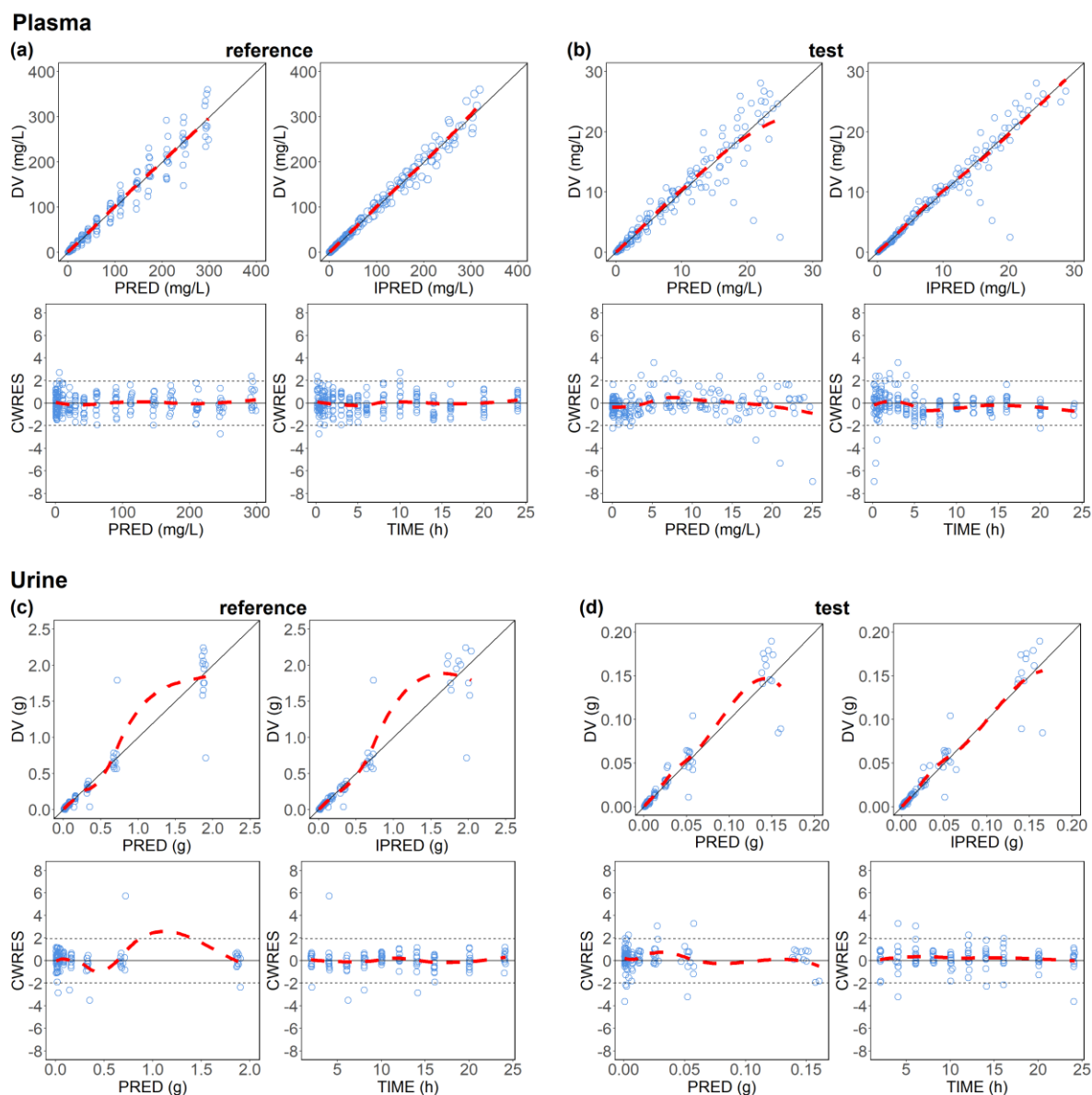


**Figure S6 Goodness-of-Fit plots for the final model.**

Panels (a) and (b) show plasma concentrations following the reference and test doses, respectively. Panels (c) and (d) display urinary excretion amounts following the reference and test doses, respectively. DV (dependent variable) represents observed plasma concentrations or urinary excretion amounts per collection interval. PRED (population prediction) indicates the predicted plasma concentration or urinary excretion amount per collection interval for the population; IPRED (individual prediction) denotes the predicted plasma concentration or urinary excretion amount per collection interval for each individual. CWRES represents conditional weighted residuals; TIME represents plasma sampling times or the end of each urine collection interval. Data points are depicted as open circles. Solid black lines represent the line of identity or a residual of 0, while dashed black lines show reference lines at  $y = \pm 1.96$ . Red dashed lines indicate locally weighted smoothing lines.



## Understanding adefovir pharmacokinetics as a component of a transporter phenotyping cocktail

Qian Dong<sup>1</sup> · Chunli Chen<sup>1,2</sup> · Max Taubert<sup>1</sup> · Muhammad Bilal<sup>1,3</sup> · Martina Kinzig<sup>4</sup> · Fritz Sörgel<sup>4</sup> · Oliver Scherf-Clavel<sup>5</sup> · Uwe Fuhr<sup>1</sup> · Charalambos Dokos<sup>1</sup>

Received: 10 December 2023 / Accepted: 11 March 2024 / Published online: 28 March 2024  
© The Author(s) 2024

### Abstract

**Purpose** Adefovir (as dipivoxil) was selected as a probe drug in a previous transporter cocktail phenotyping study to assess renal organic anion transporter 1 (OAT1), with renal clearance ( $CL_R$ ) as the primary parameter describing renal elimination. An approximately 20% higher systemic exposure of adefovir was observed when combined with other cocktail components (metformin, sitagliptin, pitavastatin, and digoxin) compared to sole administration. The present evaluation applied a population pharmacokinetic (popPK) modeling approach to describe adefovir pharmacokinetics as a cocktail component in more detail.

**Methods** Data from 24 healthy subjects were reanalyzed. After establishing a base model, covariate effects, including the impact of co-administered drugs, were assessed using forward inclusion then backward elimination.

**Results** A one-compartment model with first-order absorption (including lag time) and a combination of nonlinear renal and linear nonrenal elimination best described the data. A significantly higher apparent bioavailability (73.6% vs. 59.0%) and a lower apparent absorption rate constant ( $2.29\text{ h}^{-1}$  vs.  $5.18\text{ h}^{-1}$ ) were identified in the combined period compared to the sole administration period, while no difference was seen in renal elimination. The population estimate for the Michaelis-Menten constant ( $K_m$ ) of the nonlinear renal elimination was  $170\text{ nmol/L}$ , exceeding the observed range of adefovir plasma maximum concentration, while the maximum rate ( $V_{max}$ ) of nonlinear renal elimination was  $2.40\text{ }\mu\text{mol/h}$  at the median absolute estimated glomerular filtration rate of  $105\text{ mL/min}$ .

**Conclusion** The popPK modeling approach indicated that the co-administration primarily affected the apparent absorption and/or prodrug conversion of adefovir dipivoxil, resulting in the minor drug-drug interaction observed for adefovir as a victim. However, renal elimination remained unaffected. The high  $K_m$  value suggests that assessing renal OAT1 activity by  $CL_R$  has no relevant misspecification error with the cocktail doses used.

**Keywords** Adefovir · Population pharmacokinetics · Nonlinear renal elimination · OAT1-mediated drug-drug interactions

### Introduction

Membrane transporter proteins play a key role in the pharmacokinetics of drugs and are a potential target for transporter-based drug-drug interactions (DDIs) [1]. The

“cocktail approach,” which uses a combined administration of selective probe drugs for various transporters, is a valuable approach for the simultaneous investigation of several DDIs in a single clinical trial [2]. Although several cocktails have been established [3–5], the specificity of

✉ Qian Dong  
qdong2@smail.uni-koeln.de

<sup>1</sup> Department I of Pharmacology, Center for Pharmacology, Faculty of Medicine and University Hospital Cologne, University of Cologne, Gleueler Straße 24, Cologne 50931, Germany

<sup>2</sup> Heilongjiang Key Laboratory for Animal Disease Control and Pharmaceutical Development, College of Veterinary Medicine, Northeast Agricultural University, 600 Changjiang Road, Xiangfang District, Harbin 150030, People's Republic of China

<sup>3</sup> Department of Clinical Pharmacy, Institute of Pharmacy, University of Bonn, Bonn, Germany

<sup>4</sup> Institute for Biomedical and Pharmaceutical Research, Nürnberg-Heroldsberg, Germany

<sup>5</sup> Department Pharmazie, Ludwig-Maximilians-Universität München, Butenandtstr. 5, 81377 München, Germany

probe substances and the suitability of their pharmacokinetic (PK) parameters for characterizing transporter activities need to be investigated in more detail.

The organic anion transporter 1 (OAT1; gene name SLC22A6), predominantly located in the basolateral membrane of renal proximal tubular cells and mainly responsible for renal disposition of numerous prescribed drugs (e.g., diuretics and antivirals) [6], has been highlighted by regulatory agencies as a key transporter involved in potential DDIs [7, 8]. In order to establish a “more selective” cocktail, according to the suggestions by the FDA guideline [7], adefovir dipivoxil was selected as a specific probe drug for renal OAT1 activity in a previous clinical DDI cocktail study [3], as it is highly selective for OAT1 in vitro [9]. In addition, renal clearance ( $CL_R$ ), which only depends on renal excretion driven by plasma concentrations and is independent of other PK processes (e.g., drug absorption or conversion rate from its prodrug), was selected as the appropriate and practical primary metric to reflect renal OAT1 activity [3]. While the use of renal secretion of adefovir to assess OAT1 activity is considered the gold standard, this metric depends on a precise measurement of glomerular filtration rate (GFR) and fraction unbound ( $f_u$ ), which were unavailable in the study [3]. In the case of adefovir with  $f_u$  close to 1 [10], the unavailability of this parameter however is of little relevance.

Although the primary metric supported the absence of relevant interactions of adefovir with the other components of the cocktail (including 100 mg sitagliptin, 500 mg metformin, 2 mg pitavastatin, and 0.5 mg digoxin), an approximately 20% increase in systemic exposure for adefovir was observed during concomitant administration [3]. This indicated that there might still be some minor inhibition of OAT1, and/or an effect on other PK processes of adefovir might be present [3]. Extended in vitro analyses, however, did not support an effect of the other cocktail components on OAT1 activity [11]. Unfortunately, the non-compartmental analysis (NCA) applied in this trial could not explain the changes of PK processes in more detail.

Understanding the minor DDI observed for the victim drug adefovir in more detail also needs to take into account that OAT1-mediated secretion of adefovir (almost 60% of renal elimination [2]) might be saturable at studied concentrations. While this hypothesis might not be fully supported by in vitro findings, since adefovir peak plasma concentrations ( $C_{max}$ ) obtained in the clinical trial (5.56–91.0 nmol/L following a single dose of 10 mg adefovir dipivoxil [3]) were well below the Michaelis-Menten constant ( $K_m$ , mean  $\pm$  standard deviation [SD]  $23.8 \pm 4.2$   $\mu$ mol/L) observed in the studies [12, 13], there is evidence that such saturation may exist in vivo. Non-linearities in adefovir  $C_{max}$  and/or area under the curve (AUC) have been reported in infants, children infected

with HIV, and in adult volunteers [14, 15]. However, a detailed description of the PK processes contributing to the renal elimination of adefovir is currently lacking. If such non-linearities are not properly considered, the reliability of adefovir metrics for detection and quantification of potential DDIs might be affected in the cocktail.

Given these challenges, population pharmacokinetic (popPK) modeling might allow to gain a more mechanistic insight into the potential PK processes involved in the minor DDI observed for adefovir and to identify a possible nonlinear elimination process more precisely.

## Materials and methods

### Clinical study

Data from 24 healthy subjects in the previous clinical trial were reanalyzed [3]. The trial (ClinicalTrials.gov identifier: NCT02743260) was approved by the Ethics Committee of the Medical Faculty of the University of Cologne, Germany (application number 15-421; approval date: February 19, 2016). Conductance adhered to the pertinent version of the Declaration of Helsinki and to International Conference on Harmonization guidelines for Good Clinical Practice. All subjects gave informed consent. In this trial, a single 10 mg dose of adefovir dipivoxil was given alone and in combination with four aforementioned probe drugs in the reference and test periods, respectively. Plasma and urine concentrations of adefovir were measured up to 24 h using a validated HPLC–MS/MS method [16]. Lower limits of quantification (LLOQs) for adefovir were 0.998 nmol/L in plasma and 0.382  $\mu$ mol/L in urine, respectively [16]. The PK parameters of adefovir in reference and test periods were initially estimated via NCA using Phoenix WinNonlin™ (Version 7.0, Certara, NJ, USA), based on the concentration profiles in plasma and urine [3].

### Basic population pharmacokinetic analysis

A popPK model of adefovir was developed using the non-linear mixed-effects modeling program NONMEM 7.5.0 (ICON plc, Dublin, Ireland), Perl speaks NONMEM (PsN 5.2.6), and Pirana 3.0.0 (Certara, Princeton, NJ). R version 4.2.1 (R Foundation for Statistical Computing, Vienna, Austria) was used to build figures for model evaluations and for statistical summaries. The base model was developed starting from a one-compartment model, and model complexity was increased step by step. Inter-individual (IIV) and inter-occasion variability (IOV) of PK parameters were estimated assuming log-normally distributed individual PK parameters, and additive, proportional, and combined residual error models were evaluated. To identify a suitable base

model, we focus on Bayesian information criterion (BIC)-based comparisons, which penalize model complexity and mitigate the risk of overfitting [17].

The elimination of adefovir was modeled with two components: renal clearance ( $CL_R$ ) and nonrenal clearance ( $CL_{NR}$ ). Since adefovir exhibits negligible plasma protein binding (<3.0%) [10] and was not quantified in the study, we assumed that  $f_u=1$  for modeling purposes. Employing a one-compartment model with first-order absorption, two elimination models were considered. “Model 1” assumed linear kinetics for both renal and nonrenal elimination. In “Model 2”, renal elimination followed Michaelis-Menten-type nonlinear kinetics, while nonrenal elimination retained linear kinetics. The details of these models are presented in Table 1.

### Covariate evaluation

For covariate evaluations, we utilized objective function value (OFV)-based statistical tests, employing a forward inclusion and backward elimination approach to investigate the influence of co-administered drugs, demographic, and physiological variables. We evaluated the impact of concurrent administration of cocktail components on adefovir PK by separately determining all parameters for both reference and test periods after establishing a reasonable base model. To identify the impact of demographic and physiological factors on PK parameters, we individually added variables like age, sex, body weight, body mass index (BMI), body surface area (BSA), serum creatinine concentration, serum cystatin C concentration, and absolute estimated GFR (AGFR) to the base model. GFR was estimated via the Chronic Kidney Disease Epidemiology Collaboration (CKD-EPI) 2012 equation [18] and adjusted to AGFR based on individual BSA, determined using the Mosteller formula [19].

Covariates that resulted in a significant decrease ( $p < 0.05$ , chi-squared distribution with one degree of freedom) of at least 3.84 in the OFV from the basic model and a reduction in the variability of the PK parameter were included. All significant covariates were simultaneously integrated into

a comprehensive “full” model. Subsequently, each covariate was individually removed from the “full” model. If the increase in OFV exceeded 6.64 ( $p < 0.01$ , chi-squared distribution with one degree of freedom), indicating significant association with the PK parameter, it was retained in the final model.

### Model evaluation

Model validation was based on graphical and statistical criteria. Goodness-of-fit (GOF) plots, which included observed versus population prediction; observed versus individual prediction; conditional weighted residuals (CWRES) versus time and CWRES versus population prediction were initially used for diagnostic purposes [20]. The stability and predictive performance of the final model were further validated by non-parametric bootstrap analysis and visual predictive check (VPC) techniques [21, 22]. For the bootstrap analysis, resampling was repeated 1000 times, and medians and 95% confidence intervals (CIs) for the estimated parameters obtained from the bootstrap procedure were compared with the final model estimates [23]. Regarding the VPC, 1000 datasets were simulated using the final population model parameters, and 95% CIs for 2.5<sup>th</sup>, median (50<sup>th</sup>), and 97.5<sup>th</sup> percentiles of simulated data were calculated and then compared with the observations [21, 22].

### Calculation of individual average $CL_R$ and individual half-life ( $t_{1/2}$ )

The reliability of model parameter estimates were further evaluated by comparing them to previous NCA results [3]. While most parameters could be directly compared, the comparison of  $CL_R$  between NCA and popPK analysis required special consideration due to its dependence on concentration and changes over time in cases of saturable/nonlinear elimination. In the popPK analysis, individual average  $CL_R$  values were derived from the empirical Bayes estimates (EBEs) generated by our final model. The EBEs were obtained by

**Table 1** Summary of population pharmacokinetic models

Model	Model 1	Model 2
Absorption model	First-order absorption with lag time	
Elimination model	$CL_R$ Linear	Michaelis-Menten-type nonlinear
	$CL_{NR}$ Linear	Linear
Differential equation	$\frac{dA_1}{dt} = -K_a A_1$ $\frac{dA_2}{dt} = K_a A_1 - K_{NR} A_2 - K_R A_2$ $\frac{dA_3}{dt} = K_R A_2$	$\frac{dA_1}{dt} = -K_a A_1$ $\frac{dA_2}{dt} = K_a A_1 - K_{NR} A_2 - \frac{V_{max} A_2 / V}{K_m + A_2 / V}$ $\frac{dA_3}{dt} = \frac{V_{max} A_2 / V}{K_m + A_2 / V}$

$CL_R$  renal clearance,  $CL_{NR}$  nonrenal clearance,  $t$  time,  $A$  adefovir amount in a compartment, adefovir amounts in the absorption, central, and urine compartments are represented by  $A_1$ ,  $A_2$ , and  $A_3$ , respectively,  $K_a$  first-order absorption rate constant,  $V$  volume of distribution in the central compartment,  $K_{NR}$  linear nonrenal elimination rate constant,  $K_R$  linear renal elimination rate constant,  $K_m$  Michaelis-Menten constant for nonlinear renal elimination,  $V_{max}$  maximum rate of nonlinear renal elimination



integrating the Michaelis-Menten-type nonlinear renal clearance over the observation time period and dividing by the duration of the observation period. Therefore, this provides the average  $CL_R$  values during the observation period for each subject, accounting for the plasma concentrations of adefovir as described by the model.

Furthermore, individual  $t_{1/2}$  of adefovir was computed using the formula:  $t_{1/2} = \frac{0.693 \times V}{CL}$ , where  $CL$  represents individual total body clearance derived from  $CL_R + CL_{NR}$ . Here,  $CL_R$  represents the aforementioned individual values, while  $CL_{NR}$  and the volume of distribution ( $V$ ) represent the individual EBEs obtained from the final model.

## Results

Twenty-four healthy subjects (14 female) with the mean  $\pm$  SD BMI of  $24.5 \pm 3.10$  kg/m<sup>2</sup> and age of  $40.4 \pm 16.0$  years completed the clinical trial [3], resulting in 1101 adefovir plasma and urine concentrations for the popPK analysis. Detailed information on the demographic characteristics of subjects is provided in Supplemental Table 1s. A total of 9 (0.817%) samples with concentrations lower than the LLOQs were removed from the analysis. Supplemental Fig. 1s shows the plasma concentration and urine excretion profiles of adefovir over time.

### Population pharmacokinetic analysis

#### Adefovir base model

Plasma and urine samples were jointly analyzed using a one-compartment model, incorporating first-order absorption (including lag time) and combined renal and nonrenal elimination. This model adequately described adefovir concentrations in both plasma and urine and was selected as the base model. Implementation of nonlinear renal elimination decreased the OFV by 25.2 compared to linear renal elimination. IIV was found to be significant on the maximum rate ( $V_{max}$ ) of nonlinear renal elimination and  $V$ . Introduction of IOV for apparent bioavailability, apparent absorption rate constant ( $K_a$ ), lag time, and  $V$  improved the model significantly (OFV reduced by 400, 212, 61.6, 235 points, respectively). The residual unexplained variability of both plasma and urine data was best described by proportional error models.

#### Covariate model for effects of co-treatment

All potential PK parameters were separately assessed for reference and test periods. As a result, a significantly higher

apparent bioavailability was identified in the test period (point estimate 73.6%) compared to the published value of 59.0% [24] which was inputted for the reference period (drop in OFV by 7.39). Additionally, a significant decrease in apparent  $K_a$  was observed during the test period ( $2.29$  h<sup>-1</sup>) compared to the reference period ( $5.18$  h<sup>-1</sup>), resulting in a decrease of OFV by 9.11. Introducing additional PK parameters for reference and test periods separately did not result in significant model improvement.

#### Final model with demographic and physiological covariates

Several demographic and clinical parameters (age, body weight, body height, sex, BMI, BSA, serum creatinine and cystatin C concentrations, and AGFR) were tested as potential covariates on PK parameters. After stepwise covariate model building, AGFR on  $V_{max}$  was the only statistically significant covariate retained in the model (drop in OFV of 12.2 points). The final covariate model on  $V_{max}$  is therefore represented by  $TVV_{max} = \theta_{Vmax} \times (AGFR/105)$ , where  $TVV_{max}$  is the typical value of  $V_{max}$  and 105 mL/min is the median AGFR. Using a power relationship instead of a proportional relationship to describe the effect of AGFR did not improve the model. The key model development steps are summarized in Table 2.

#### Model evaluation

The VPC results (Fig. 1) showed that medians and 2.5<sup>th</sup> and 97.5<sup>th</sup> percentiles of the simulated data from the final model incorporating Michaelis-Menten-type nonlinear renal elimination (“Nonlinear model”) were in acceptable agreement with the observations. To facilitate a comparison between models with and without nonlinear renal elimination, an additional VPC is presented. This VPC is based on a linear renal elimination model (“Linear model”), which also incorporates AGFR as a covariate using a proportional equation, this time on  $CL_R$ , to adjust for individual differences in renal function. Apart from a higher population variability in simulated compared to observed urine excretion amounts with both models, the VPC of the “Nonlinear model” shows no obvious misspecification, while it performs slightly better than the “Linear model,” particularly concerning the initial high adefovir amounts excreted in urine. The GOF plots (Supplemental Fig. 2s) demonstrated that the final model adequately described the observed adefovir plasma concentrations and urinary excretion, exhibiting a satisfactory fit without notable trends. This suggests the absence of systematic deviations in the model. The final point estimates and bootstrap statistics of PK parameters are summarized in Table 3. There are no indications of overparameterization in any of the model diagnostics or the bootstrap results.

**Table 2** Summary of key model development steps

Model	Description	OFV
<b>Base model</b>		
1	One-compartment model with first-order absorption (including lag time) and combined Michaelis-Menten type nonlinear renal and linear nonrenal elimination	6401.44
<b>Covariate model for effects of co-treatment</b>		
2	Base model with separate estimates of apparent bioavailability for reference and test periods	6394.05
3	Model 2 with additional separate estimates for apparent $K_a$ for reference and test periods	6384.89
<b>Final model with demographic and physiological covariates</b>		
4	Final model with AGFR as a covariate on $V_{\max}$	6372.69

OFV objective function value,  $K_a$  first-order absorption rate constant, AGFR absolute estimated glomerular filtration rate

### Calculation of individual average $CL_R$ and individual $t_{1/2}$

The median (range) individual average  $CL_R$  and individual  $t_{1/2}$  values for adefovir during the reference and test periods were 12.4 (7.97–34.0) L/h and 6.59 (5.61–8.45) h, and 12.2 (7.82–31.0) L/h and 6.35 (5.07–9.01) h, respectively.

### Discussion

The present popPK analysis identified that changes in apparent absorption rate and apparent bioavailability, rather than changes in renal elimination, are the primary causes of the slight DDI that was found for adefovir as a victim when co-administered with other transporter probe substrates. Although the identified nonlinear renal clearance of adefovir is not saturated at the standard dose, further dose reduction in the existing transporter phenotyping cocktail might avoid even minor DDIs.

In this evaluation, plasma and urine data could be reasonably explained by a one-compartment model with first-order absorption (including lag time) and a combination of Michaelis-Menten-type nonlinear renal and linear nonrenal elimination. Despite previous studies reported that adefovir plasma levels declined biexponentially [10, 25, 26], our investigation did not reveal an observable biphasic decline in the semi-log plots (Supplemental Fig. 1s). Introducing a second compartment to the one-compartment base model did not significantly improve the BIC score (drop in BIC by 1.44), residual unexplained variability, or VPCs. Therefore, the one-compartment model was chosen as the final model.

The estimates for PK parameters of adefovir we present here are in line with the previous NCA conducted on the same dataset [3]. According to the final model, the individual apparent volume of distribution (V/F) for adefovir was calculated based on the individual EBEs of V divided by individual EBEs of F. The median of these individual values was 369 L and 308 L in the reference

and test periods, respectively. These values are comparable to the geometric mean values obtained from the previous NCA study, which reported 368 L and 307 L for the corresponding periods [3]. Additionally, the median (range)  $CL_R$  and  $t_{1/2}$  values for adefovir during the reference and test periods in this evaluation are in accordance with those reported in the NCA study [3]. According to the NCA, during the reference period, the geometric mean (95% CI)  $CL_R$  and the geometric mean (95% CI)  $t_{1/2}$  of adefovir were 12.3 (6.06–24.9) L/h and 6.38 (4.68–8.72) h, respectively. In the test period, these values were 11.3 (7.26–17.8) L/h and 6.58 (5.05–8.57) h, respectively [3].

In our analysis, after normalizing for body weight, median individual values for V/F,  $CL_R$ , and CL/F are 4.89 L/kg, 0.175 L/h/kg, and 0.493 L/h/kg, respectively. Moreover, the median urinary recovery over 24 h is 46.4%. These findings align with the characteristics reported in the summary of product characteristics for HEPSERA® (adefovir dipivoxil) tablets [23] and are consistent with observations by Sokal et al. [26]. Sokal et al. studied adolescents aged 12–17 years, finding mean  $\pm$  SD values of  $0.739 \pm 0.192$  L/h/kg for CL/F,  $7.16 \pm 1.6$  L/kg for V/F, and  $6.84 \pm 0.97$  h for  $t_{1/2}$  after a single oral dose of 10 mg adefovir dipivoxil [26]. However, our results were slightly lower than those reported by Hughes et al. [15] in infants and children (3 months–18 years) after a 1.5 mg/kg adefovir dipivoxil dose, showing a median CL/F of 1.0 L/h/kg and a median V/F of 8.1 L/kg. Conversely, our estimates of CL/F and V/F were slightly higher than those reported by Shiffman et al. [27] in patients with mild renal impairment (creatinine clearance  $\geq 50$  to  $< 80$  mL/min), reflecting a mean CL/F of 0.270 L/h/kg and a mean V/F of 2.6 L/kg [27]. These discrepancies may stem from physiological variations due to factors such as growth, development, and disease.

In the study by Cundy et al. [10], a comparable mean  $\pm$  SD value for  $CL_R$  was observed at  $0.205 \pm 0.078$  L/h/kg. Nevertheless, they reported a lower V at  $0.418 \pm 0.076$  L/kg, a shorter  $t_{1/2}$  of  $1.6 \pm 0.5$  h, and a reduced CL of  $0.223 \pm 0.053$



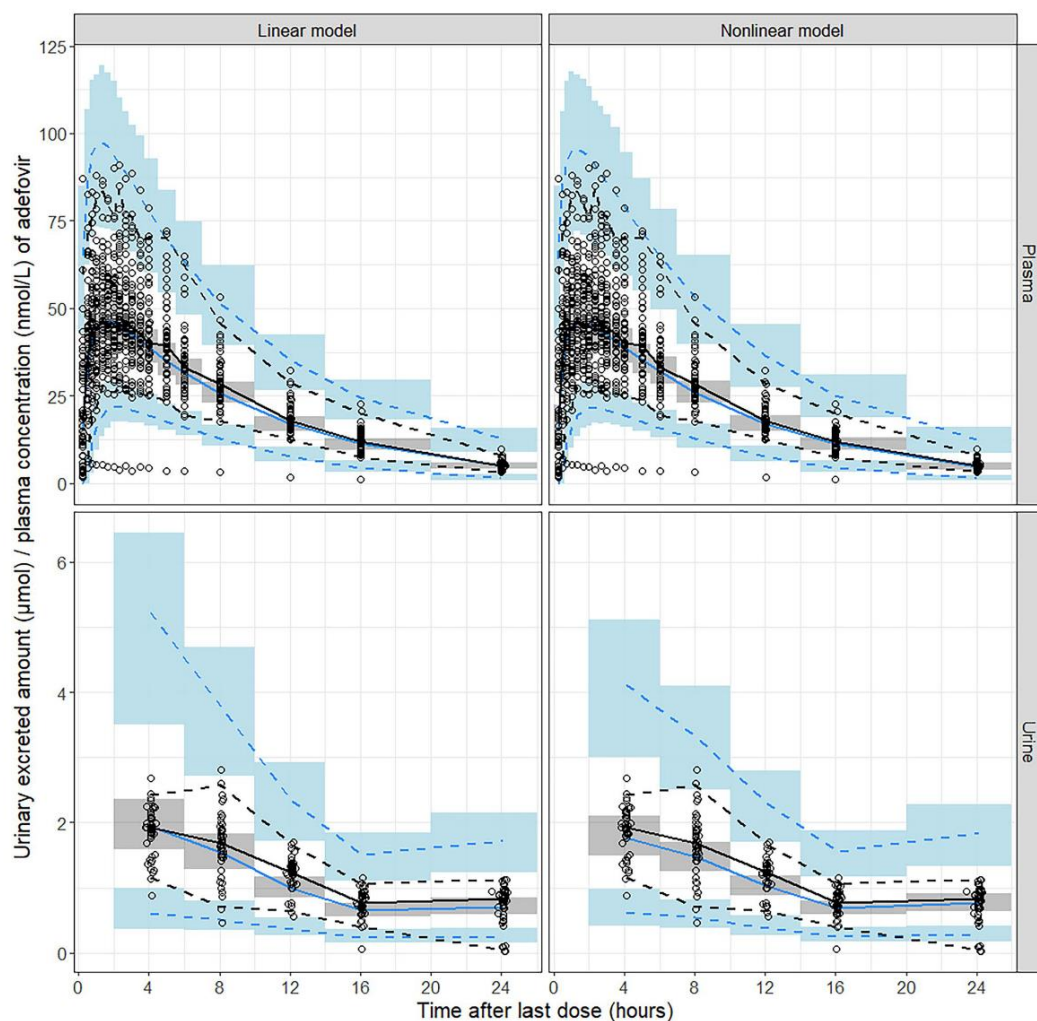


**Fig. 1** Visual predictive check ( $n=1000$ ) for the final model stratified by plasma and urine data, and categorized by renal elimination models: linear ("Linear model") and nonlinear ("Nonlinear model"). Open circles illustrate observed data points. Solid (dashed) black and blue

lines represent medians (2.5<sup>th</sup> and 97.5<sup>th</sup> percentiles) of observations and simulated data, respectively; blue, gray, and blue areas represent 95% confidence intervals of the 2.5<sup>th</sup>, median, and 97.5<sup>th</sup> percentiles of simulated data

L/h/kg compared to our study. This discrepancy was noted following the intravenous administration of adefovir at 1 or 3 mg/kg/day in HIV-infected patients [10]. Considering adefovir dipivoxil, an ester prodrug of adefovir, may rapidly convert to adefovir after administration [28], it is not probable that adefovir dipivoxil pharmacokinetics play an important role in estimating the PK parameters of adefovir. Therefore, the underlying mechanisms of this difference remain unclear.

While Sun et al. [14] and Huang et al. [25] reported  $t_{1/2}$  values similar to those in our study, Sun et al. presented notably low mean values for  $t$  (7.0 mL/kg) and CL (0.63 mL/h/kg) following a 10 mg oral dose of adefovir dipivoxil [14]. These values diverge from the mean serum concentration–time curves presented in their manuscript, prompting us to consider a potential unit mislabeling in the published results—suggesting "L" may be more appropriate than "mL." Should this correction prove accurate, it

**Table 3** Population pharmacokinetic parameters of adefovir and bootstrap results

Parameter (unit)	Point estimate	RSE %	Bootstrap median (95% CI)
<b>Fixed effects</b>			
ALAG (h)	0.122	17.2	0.123 (0.0819–0.162)
V (L)	235	14.1	233 (196–321)
CL <sub>NR</sub> (L/h)	11.8	25.7	11.6 (8.52–20.2)
K <sub>m</sub> (nmol/L)	170	26.3	170 (122–295)
V <sub>max</sub> (μmol/h)	2.40	23.5	2.42 (1.80–3.88)
<b>Impact of co-treatment</b>			
F <sub>R</sub>	0.590 fixed	–	–
F <sub>T</sub>	0.736	13.5	0.731 (0.629–0.999)
K <sub>aR</sub> (h <sup>-1</sup> )	5.18	20.5	5.14 (3.54–7.74)
K <sub>aT</sub> (h <sup>-1</sup> )	2.29	17.6	2.30 (1.66–3.30)
<b>Inter-individual variability (CV%)</b>			
V	17.1	22.1	16.3 (10.5–21.8)
V <sub>max</sub>	19.1	42.2	18.4 (6.32–29.6)
<b>Inter-occasion variability (CV%)</b>			
F	28.5	33.8	28.0 (11.6–48.1)
K <sub>a</sub>	104	14.9	101 (69.1–150)
ALAG	76.9	32.9	75.4 (43.0–129)
V	8.30	32.3	8.29 (4.90–11.2)
<b>Residual unexplained variability (CV%)</b>			
Proportional error, plasma	9.50	7.57	9.45 (8.23–10.9)
Proportional error, urine	28.1	18.7	27.7 (17.9–39.5)

RSE% relative standard error in percent, CI confidence interval, ALAG lag time for first-order absorption, V volume of distribution, CL<sub>NR</sub> linear nonrenal clearance, K<sub>m</sub> Michaelis-Menten constant for nonlinear renal elimination, V<sub>max</sub> maximum rate of nonlinear renal elimination, F bioavailability, the bioavailability of the reference and test periods are represented by F<sub>R</sub> and F<sub>T</sub> respectively, K<sub>a</sub> first-order absorption rate constant, the first-order absorption rate constant of the reference and test periods are represented by K<sub>aR</sub> and K<sub>aT</sub>, CV% coefficient of variation in percent, CV% for inter-individual and inter-occasion variability computed as  $\sqrt{\exp(\omega^2) - 1}$ , CV% for residual unexplained variability computed as  $\sqrt{\exp(\sigma^2) - 1}$

would better align with the results of our current study. In contrast, Huang et al. reported a higher CL (1.00 L/h/kg) and a higher V (10.7 L/kg) after a 10 mg dose of adefovir dipivoxil [25]. We attribute this discrepancy to an error in their article, where they indicate, “open circles represent observed adefovir dipivoxil concentrations” [25]. It appears they inadvertently used adefovir dipivoxil as the moiety for concentrations instead of adefovir, inflating both and CL in their analysis. Overall, published data on adefovir pharmacokinetics show a remarkable variability in clearance and volume of distribution.

To evaluate the influence of co-treatment on PK parameters, we employed two approaches. Firstly, we independently evaluated PK parameters for reference and test periods. Additionally, we integrated co-treatment effect as a covariate on the PK parameters. The relative differences in PK parameters between these periods, as estimated by both methods, are consistent and resulted in an equivalent reduction of the OFV. To allow for greater flexibility in identifying potentially more fundamental distinctions in the description of PK processes between periods, we finally conducted a separate

assessment of PK parameters for each of the reference and test periods, respectively. After a detailed assessment of the parameters in various PK processes using the popPK model, a higher apparent bioavailability, but a slower apparent absorption rate of adefovir when co-administered with the cocktail, has been identified. These findings indicate potential changes in the apparent absorption of adefovir dipivoxil or prodrug conversion, contributing to increased systemic exposure during co-administration with the cocktail, as observed in the previous DDI study [3]. Based on sporadic studies, a potential mechanism to explain this result may stem from the co-administered drugs exerting inhibitory effects on the intestinal multidrug resistance-associated protein 2 (MRP2, ABCC2). This protein mediates unidirectional transport of adefovir to the intestinal lumen within enterocytes [29–31]; thus, inhibition may enhance the bioavailability of adefovir. Furthermore, the model-based approach did not support the inclusion of V<sub>max</sub> for reference and test periods separately. Additionally, no significant difference was observed in the median CL<sub>R</sub> between reference and test periods. This suggests that CL<sub>R</sub> remains unaffected

by the other concomitantly administered probe drugs and may reliably reflect changes in the renal OAT1 activity, which is rate limiting for adefovir renal excretion [2, 9, 10].

The final model, incorporating a nonlinear renal elimination, provides an appropriate description of the data, as supported by the supplemental figures. The adefovir renal clearance plot (Supplemental Fig. 3s) indicates a deviation from linearity in urinary excretion at high concentrations, which is well described by the nonlinear renal clearance model. The residual plot (Supplemental Fig. 4s) illustrates clearly biased descriptions of urinary excretion with a linear model at high concentrations, supporting that the linear clearance model is inadequate. Furthermore a model with nonlinear renal elimination offers a physiologically plausible representation for adefovir renal elimination. Adefovir primarily undergoes OAT1-mediated tubular secretion, a process that could potentially saturate and complement kidney filtration. Calculated as  $CL_R - fu \cdot GFR$  (with a median GFR of 6.28 L/h in this study) [2], adefovir secretion accounts for over 50% of  $CL_R$  in this study, aligning with findings in previous reports [10, 24]. The population estimate (95% CI) for  $K_m$  in nonlinear renal elimination is 170 (122–295) nmol/L, which is lower than in vitro studies (mean  $\pm$  SD  $23.8 \pm 4.2$   $\mu$ mol/L) [11, 12]. This disparity may stem from challenges in replicating the dynamic in vivo environment in controlled in vitro settings and differences in techniques. Despite this, it exceeds the observed adefovir  $C_{max}$  range (5.56–91.0 nmol/L). Thus, this mechanism is expected to have little influence on systemic exposure and is considered clinically insignificant at therapeutic doses. However, this result suggests that a reduction of adefovir dose as part of the transporter probe cocktail may be considered in future studies to prevent relevant transporters to be saturated, and to minimize any impact on other cocktail components.

As discussed in the “Introduction” section, indeed there is some prior evidence for nonlinearity on adefovir pharmacokinetics [14, 15], albeit nonlinear renal clearance has not been shown yet [10, 25–27, 32–34]. The possible reason might be that such finding requires a popPK evaluation to gain a more detailed understanding of the role of individual PK processes for the pharmacokinetics of adefovir, while most of previous studies assessed the PK of adefovir by noncompartmental methods, which may provide insufficient information of individual PK processes [10, 14, 27]. Another possible reason could be that the extent of saturability in adefovir’s elimination, based on the recommended single dose of 10 mg, was relatively small. Therefore, both plasma measurements and urine collection might be necessary for a sound estimation of the nonlinearity. This could explain why Jihan Huang reported first-order elimination for adefovir in their popPK study [25].

The model could not be improved further by incorporating the AGFR as a component of  $CL_R$  in addition to nonlinear renal clearance. Although it might better reflect the physiological conditions of the renal excretion of adefovir, which involves both active tubular secretion and glomerular filtration, this approach resulted in unstable parameter estimates of  $K_m$  and  $V_{max}$  (RSEs > 1000%). As a result, we were unable to estimate the  $K_m$  value of true renal secretion, which might become more saturated at therapeutic adefovir concentrations.

Another limitation of this study is that it only included healthy adults who received a standard dose. To gain a comprehensive understanding of the nonlinear renal elimination of adefovir, future studies would need to include more dose levels, particularly higher doses, in diverse populations with varying degrees of renal function.

## Conclusion

In conclusion, the popPK modeling approach showed that the minor DDI observed for adefovir as a victim when co-administered with other transporter probe substrates is caused by an effect on apparent absorption and/or formation of adefovir from the prodrug, but not by an effect on renal elimination. Renal elimination of adefovir was found to be saturable, which should reflect its active renal secretion. The high  $K_m$  value suggests that the use of renal elimination of adefovir to assess renal OAT1 activity is not compromised by saturability, while using a lower adefovir dose (e.g., to 50%) may provide an additional safety margin.

**Supplementary Information** The online version contains supplementary material available at <https://doi.org/10.1007/s00228-024-03673-x>.

**Author contributions** All authors contributed to the conception and design of the research. U.F. provided the data. Q.D., C.C., M.T., and M.B. organized the database and performed the analyses. U.F. supervised the project. Q.D. wrote the first draft of the manuscript. All authors reviewed and approved the submitted version of the manuscript.

**Funding** Open Access funding enabled and organized by Projekt DEAL. Qian Dong received a scholarship from the China Scholarship Council (CSC) for support of her Ph.D. studies. Dr. Chunli Chen is supported by the 2022 ESI International High Impact Research Article Cooperation Program (No. 212-54900112), the National Natural Science Foundation of Heilongjiang Province (No. YQ2022C017) and the International Postdoctoral Exchange Fellowship Program from the Office of China Postdoctoral Council (No. 2020106 and PC2020013). The Higher Education Commission of Pakistan provided financial support in the form of a Ph.D. scholarship for Muhammad Bilal through the German Academic Exchange Service (DAAD). The study’s design, data collection and analysis, and the choice to submit the work for publication were all independent of the sponsor.

**Data availability** The data that support the findings of this study are available from the corresponding author upon reasonable request.

## Declarations

**Competing interests** The authors declare no competing interests.

**Open Access** This article is licensed under a Creative Commons Attribution 4.0 International License, which permits use, sharing, adaptation, distribution and reproduction in any medium or format, as long as you give appropriate credit to the original author(s) and the source, provide a link to the Creative Commons licence, and indicate if changes were made. The images or other third party material in this article are included in the article's Creative Commons licence, unless indicated otherwise in a credit line to the material. If material is not included in the article's Creative Commons licence and your intended use is not permitted by statutory regulation or exceeds the permitted use, you will need to obtain permission directly from the copyright holder. To view a copy of this licence, visit <http://creativecommons.org/licenses/by/4.0/>.

## References

1. Mooij MG, Nies AT, Knibbe CA, Schaeffeler E, Tibboel D, Schwab M, de Wildt SN (2016) Development of human membrane transporters: drug disposition and pharmacogenetics. *Clin Pharmacokinet* 55(5):507–524. <https://doi.org/10.1007/s40262-015-0328-5>
2. Fuhr U, Hsin C-H, Li X, Jabrane W, Sörgel F (2019) Assessment of pharmacokinetic drug–drug interactions in humans: in vivo probe substrates for drug metabolism and drug transport revisited. *Annu Rev Pharmacol Toxicol* 59:507–536. <https://doi.org/10.1146/annurev-pharmtox-010818-021909>
3. Truock C, Hsin Ch, Scherf-Clavel O, Schaeffeler E, Lenssen R, Gazzaz M, Gersie M, Taubert M, Quasdorff M, Schwab M (2019) A clinical drug–drug interaction study assessing a novel drug transporter phenotyping cocktail with adefovir, sitagliptin, metformin, pitavastatin, and digoxin. *Clin Pharmacol Ther* 106(6):1398–1407. <https://doi.org/10.1002/cpt.1564>
4. Wiebe ST, Giessmann T, Hohl K, Schmidt-Gerets S, Huel E, Jambrecina A, Bader K, Ishiguro N, Taub ME, Sharma A (2020) Validation of a drug transporter probe cocktail using the prototypical inhibitors rifampin, probenecid, verapamil, and cimetidine. *Clin Pharmacokinet* 59(12):1627–1639. <https://doi.org/10.1007/s40262-020-00907-w>
5. Prueksaritanont T, Tatossian D, Chu X, Railkar R, Evers R, Chavez-Eng C, Lutz R, Zeng W, Yabut J, Chan G (2017) Validation of a microdose probe drug cocktail for clinical drug interaction assessments for drug transporters and CYP3A. *Clin Pharmacol Ther* 101(4):519–530. <https://doi.org/10.1002/cpt.525>
6. Burckhardt G, Burckhardt BC (2011) In vitro and in vivo evidence of the importance of organic anion transporters (OATs) in drug therapy. *Handb Exp Pharmacol* (201):29–104. [https://doi.org/10.1007/978-3-642-14541-4\\_2](https://doi.org/10.1007/978-3-642-14541-4_2)
7. U.S. Food and Drug Administration. Clinical drug interaction studies — cytochrome P450 enzyme- and transporter-mediated drug interactions guidance for industry. Guidance as of January 2020. <https://www.fda.gov/regulatory-information/search-fda-guidance-documents/clinical-drug-interaction-studies-cytochrome-p450-enzyme-and-transporter-mediated-drug-interactions>
8. European Medicines Agency. Guideline on the investigation of drug interactions CPMP/EWP/560/95/Rev. 1 Corr. 2\*\*, 21 June 2012. [https://www.ema.europa.eu/en/documents/scientific-guideline/guideline-investigation-drug-interactions-revision-1\\_en.pdf](https://www.ema.europa.eu/en/documents/scientific-guideline/guideline-investigation-drug-interactions-revision-1_en.pdf)
9. Maeda K, Tian Y, Fujita T, Ikeda Y, Kumagai Y, Kondo T, Tanabe K, Nakayama H, Horita S, Kusuhara H (2014) Inhibitory effects of p-aminohippurate and probenecid on the renal clearance of adefovir and benzylpenicillin as probe drugs for organic anion transporter (OAT) 1 and OAT3 in humans. *Eur J Pharm Sci* 59:94–103. <https://doi.org/10.1016/j.ejps.2014.04.004>
10. Cundy KC, Barditch-Crovo P, Walker RE, Collier AC, Ebeling D, Toole J, Jaffe HS (1995) Clinical pharmacokinetics of adefovir in human immunodeficiency virus type 1-infected patients. *Antimicrob Agents Chemother* 39(11):2401–2405. <https://doi.org/10.1128/AAC.39.11.2401>
11. Hsin C-H, Kuehne A, Gu Y, Jedlitschky G, Hagos Y, Gründemann D, Fuhr U (2023) In vitro validation of an in vivo phenotyping drug cocktail for major drug transporters in humans. *Eur J Pharm Sci* 186:106459. <https://doi.org/10.1016/j.ejps.2023.106459>
12. Cihlar T, LaFlamme G, Fisher R, Carey AC, Vela JE, Mackman R, Ray AS (2009) Novel nucleotide human immunodeficiency virus reverse transcriptase inhibitor GS-9148 with a low nephrotoxic potential: characterization of renal transport and accumulation. *Antimicrob Agents Chemother* 53(1):150–156. <https://doi.org/10.1128/AAC.01183-08>
13. Ho ES, Lin DC, Mendel DB, Cihlar T (2000) Cytotoxicity of antiviral nucleotides adefovir and cidofovir is induced by the expression of human renal organic anion transporter 1. *J Am Soc Nephrol* 11(3):383–393. <https://doi.org/10.1681/ASN.V113383>
14. Sun DQ, Wang HS, Ni MY, Wang BJ, Guo RC (2007) Pharmacokinetics, safety and tolerance of single- and multiple-dose adefovir dipivoxil in healthy Chinese subjects. *Br J Clin Pharmacol* 63(1):15–23. <https://doi.org/10.1111/j.1365-2125.2006.02728.x>
15. Hughes WT, Shenep JL, Rodman JH, Fridland A, Willoughby R, Blanchard S, Purdue L, Coakley DF, Cundy KC, Culnane M (2000) Single-dose pharmacokinetics and safety of the oral antiviral compound adefovir dipivoxil in children infected with human immunodeficiency virus type 1. *Antimicrob Agents Chemother* 44(4):1041–1046. <https://doi.org/10.1128/AAC.44.4.1041-1046.2000>
16. Scherf-Clavel O, Kinzig M, Stoffel MS, Fuhr U, Sörgel F (2019) Quantification of adefovir and pitavastatin in human plasma and urine by LC-MS/MS: a useful tool for drug–drug interaction studies. *J Chromatogr B* 1125:121718. <https://doi.org/10.1016/j.jchromb.2019.121718>
17. Mould DR, Upton RN (2013) Basic concepts in population modeling, simulation, and model-based drug development-part 2: introduction to pharmacokinetic modeling methods. *CPT Pharmacometrics Syst Pharmacol* 2(4):e38. <https://doi.org/10.1038/psp.2013.14>
18. Inker LA, Schmid CH, Tighiouart H, Eckfeldt JH, Feldman HI, Greene T, Kusek JW, Manzi J, Van Lente F, Zhang YL (2012) Estimating glomerular filtration rate from serum creatinine and cystatin C. *N Engl J Med* 367(1):20–29. <https://doi.org/10.1056/NEJMoa1114248>
19. Mosteller R (1987) Simplified calculation of body surface area. *New Engl J Med* 317:1098. <https://doi.org/10.1056/NEJM198710223171717>
20. Hooker AC, Staats CE, Karlsson MO (2007) Conditional weighted residuals (CWRES): a model diagnostic for the FOCE method. *Pharm Res* 24(12):2187–2197. <https://doi.org/10.1007/s11095-007-9361-x>
21. Post TM, Freijer JJ, Ploeger BA, Danhof M (2008) Extensions to the visual predictive check to facilitate model performance evaluation. *J Pharmacokinet Pharmacodyn* 35(2):185–202. <https://doi.org/10.1007/s10928-007-9081-1>
22. Nguyen T, Ms Mouksassi, Holford N, Al-Huniti N, Freedman V, Hooker AC, John J, Karlsson MO, Mould D, Pérez Ruixo J (2017) Model evaluation of continuous data pharmacometric models: metrics and graphics. *CPT Pharmacometrics Syst Pharmacol* 6(2):87–109. <https://doi.org/10.1002/psp4.12161>

23. Ette EI (1997) Stability and performance of a population pharmacokinetic model. *J Clin Pharmacol* 37(6):486–495. <https://doi.org/10.1002/j.1552-4604.1997.tb04326.x>
24. Gilead Sciences International Limited. Fachinformation für Hepsera® 10 mg Tabletten as of April 2021. In: ed. <https://www.fachinfo.de/suche/fi/003016>
25. Huang J, Zhang Y, Huang X, Li L, Li Y, Wang K, Yang J, He Y, Lv Y, Zheng Q (2014) Population pharmacokinetics of adefovir dipivoxil tablets in healthy Chinese volunteers. *Int J Clin Pharmacol Ther* 52(1):8–14. <https://doi.org/10.5414/CP201928>
26. Sokal EM, Kelly D, Wirth S, Mizerski J, Dhawan A, Frederick D (2008) The pharmacokinetics and safety of adefovir dipivoxil in children and adolescents with chronic hepatitis B virus infection. *J Clin Pharmacol* 48(4):512–517. <https://doi.org/10.1177/0091270007313325>
27. Shiffman ML, Pol S, Rostaing L, Schiff E, Thabut D, Zeuzem S, Zong J, Frederick D, Rousseau F (2011) Efficacy and pharmacokinetics of adefovir dipivoxil liquid suspension in patients with chronic hepatitis B and renal impairment. *J Clin Pharmacol* 51(9):1293–1301. <https://doi.org/10.1177/0091270010381385>
28. Noble S, Goa KL (1999) Adefovir dipivoxil. *Drugs* 58(3):479–487. <https://doi.org/10.2165/00003495-199958030-00010>
29. Chen Z, Shi T, Zhang L, Zhu P, Deng M, Huang C, Hu T, Jiang L, Li J (2016) Mammalian drug efflux transporters of the ATP binding cassette (ABC) family in multidrug resistance: a review of the past decade. *Cancer Lett* 370(1):153–164. <https://doi.org/10.1016/j.canlet.2015.10.010>
30. Motoki K, Taniguchi T, Ashizawa N, Sakai M, Chikamatsu N, Yamano K, Iwanaga T (2023) Uricosuric agents affect plasma and kidney concentration of adefovir via inhibition of oat1 and Mrp2 in rats. *Biol Pharm Bull* 46(2):170–176. <https://doi.org/10.1248/bpb.b22-00384>
31. Shin E, Shin N, Oh JH, Lee YJ (2017) High-dose metformin may increase the concentration of atorvastatin in the liver by inhibition of multidrug resistance-associated protein 2. *J Pharm Sci* 106(4):961–967. <https://doi.org/10.1016/j.xphs.2016.11.020>
32. Fok BS, Gardner S, Piscitelli S, Chen S, Chu TT, Chan JC, Tomlinson B (2013) Pharmacokinetic properties of single-dose lamivudine/adevovir dipivoxil fixed-dose combination in healthy Chinese male volunteers. *Clin Ther* 35(1):68–76. <https://doi.org/10.1016/j.clinthera.2012.12.001>
33. Barditch-Crovo P, Toole J, Hendrix C, Cundy K, Ebeling D, Jaffe H, Lietman P (1997) Anti-human immunodeficiency virus (HIV) activity, safety, and pharmacokinetics of adefovir dipivoxil (9-[2-(bis-pivaloyloxymethyl)-phosphonylmethoxyethyl] adenine) in HIV-infected patients. *J Infect Dis* 176(2):406–413. <https://doi.org/10.1086/514057>
34. Deeks SG, Collier A, Lalezari J, Pavia A, Rodrigue D, Drew WL, Toole J, Jaffe HS, Mulato AS, Lamy PD (1997) The safety and efficacy of adefovir dipivoxil, a novel anti-human immunodeficiency virus (HIV) therapy, in HIV-infected adults: a randomized, double-blind, placebo-controlled trial. *J Infect Dis* 176(6):1517–1523. <https://doi.org/10.1086/514150>

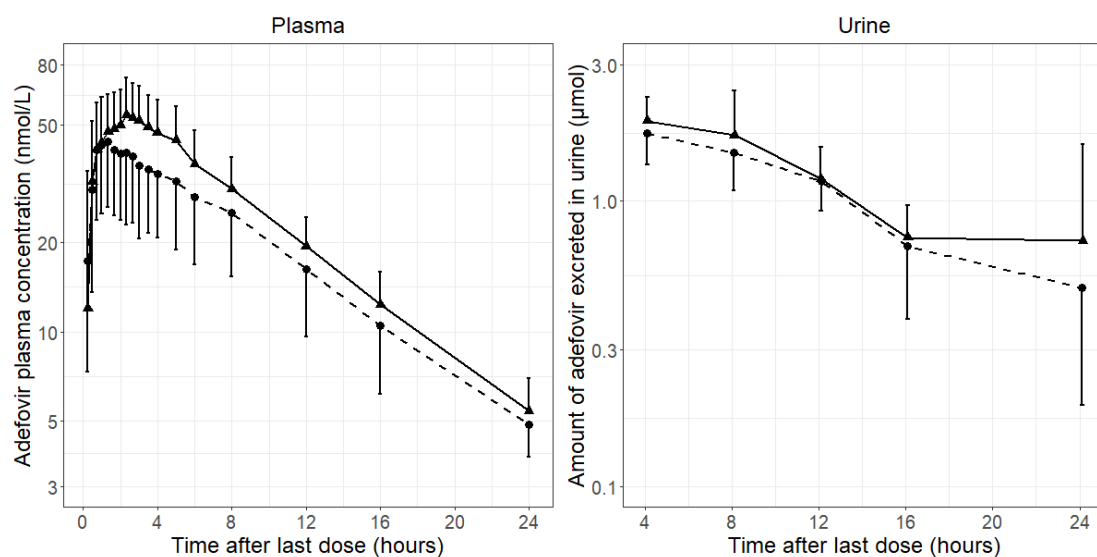
**Publisher's Note** Springer Nature remains neutral with regard to jurisdictional claims in published maps and institutional affiliations.

### Supplementary Material for Publication III

**Supplemental Table 1s** Demographic characteristics of subjects

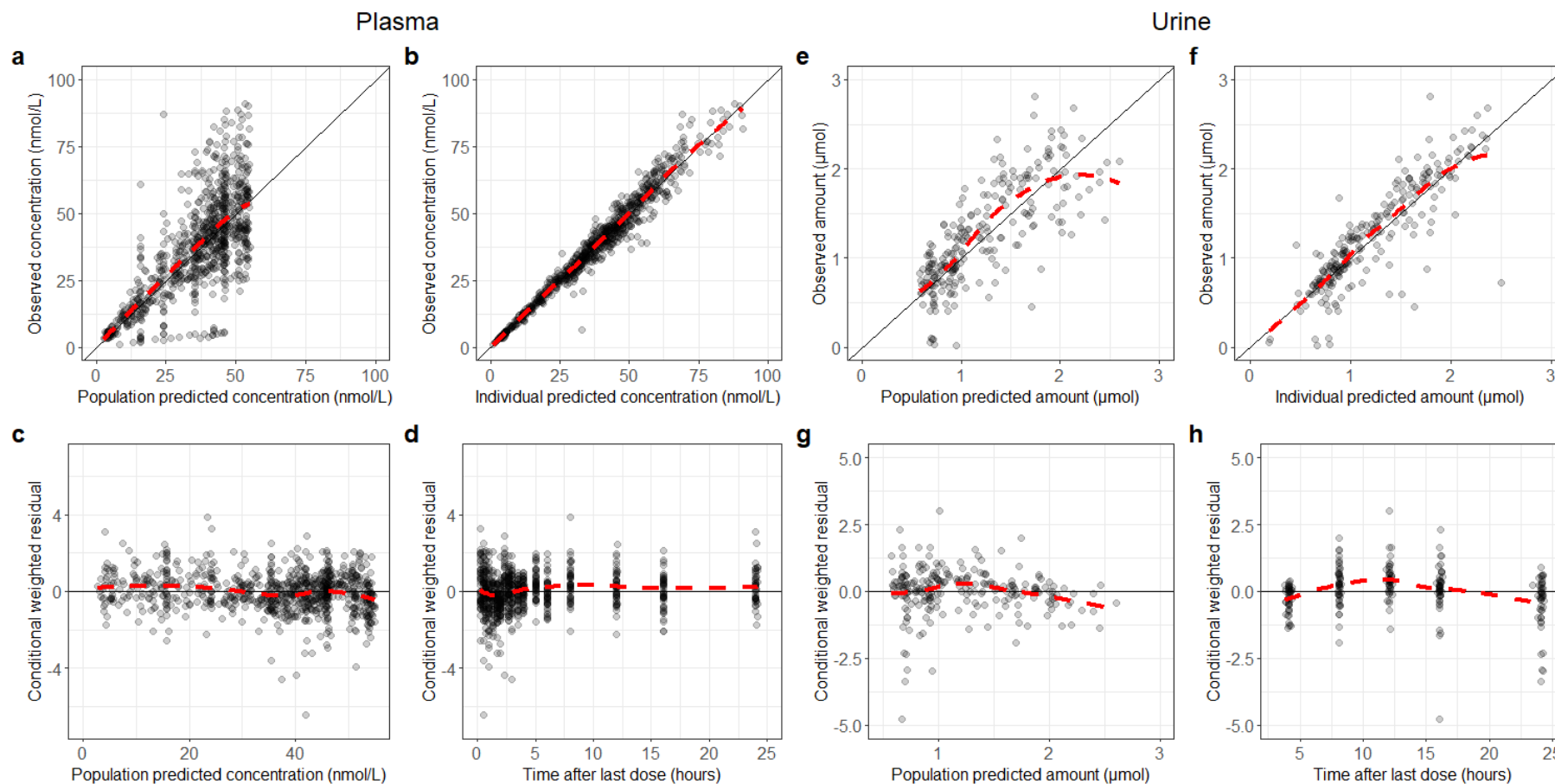
Demographic characteristics	No. or median (range)
No. of subjects (male/female)	24 (10/14)
Age (y)	35 (20 - 68)
Body weight (kg)	71.3 (55.5 - 94.9)
Body height (cm)	172 (160 - 188)
BMI (kg/m <sup>2</sup> )	24.5 (19.5 - 29.7)
BSA (m <sup>2</sup> )	1.83 (1.59 - 2.18)
AGFR (mL/min)	105 (77.5 - 136)
Serum creatinine concentration (mg/dL)	0.855 (0.660 - 1.14)
Serum cystatin C concentration (mg/L)	0.835 (0.660 - 1.10)

*BMI* body mass index, *BSA* body surface area, determined using the Mosteller formula<sup>259</sup>, *AGFR* absolute estimated glomerular rate. Glomerular filtration rate (GFR) was estimated using the Chronic Kidney Disease Epidemiology Collaboration (CKD-EPI) 2012 equation<sup>126</sup> and adjusted to AGFR based on individual BSA<sup>259</sup>.



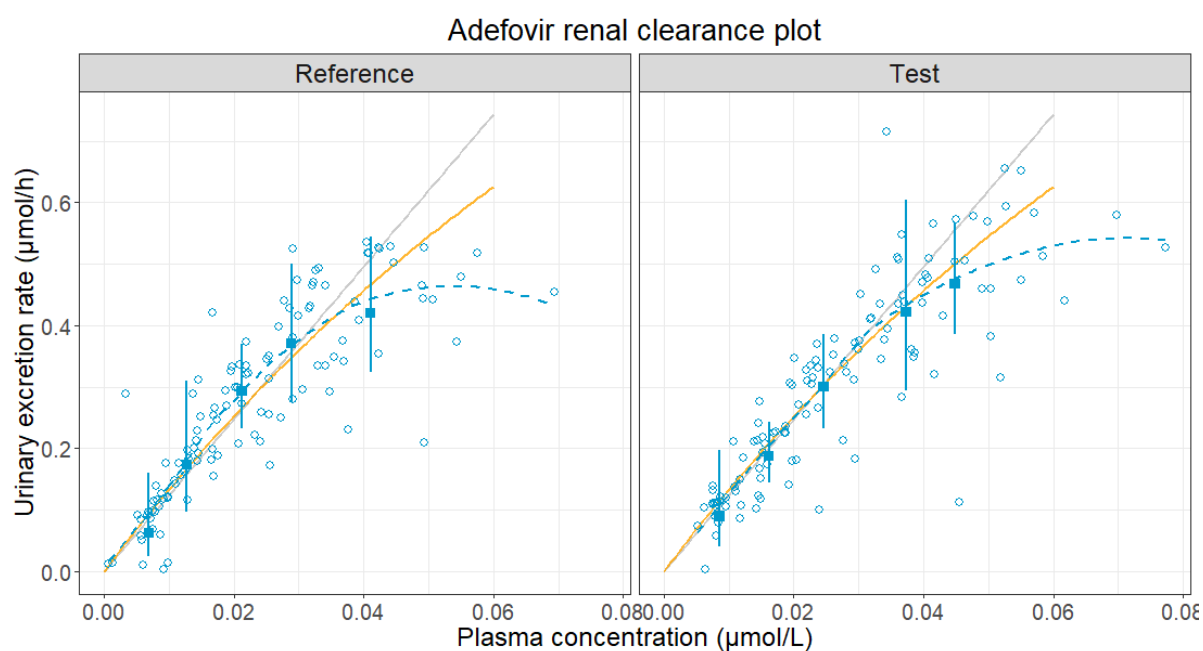
**Supplemental Fig. 1s** Semi-logarithmic plots illustrate the adefovir plasma concentration and the amount of adefovir excreted during the urine collection period over time in both the reference (circle points and dashed lines) and test (triangle points and solid lines) periods. The associated symbols and error bars represent geometric means and geometric standard deviations (SD), respectively.



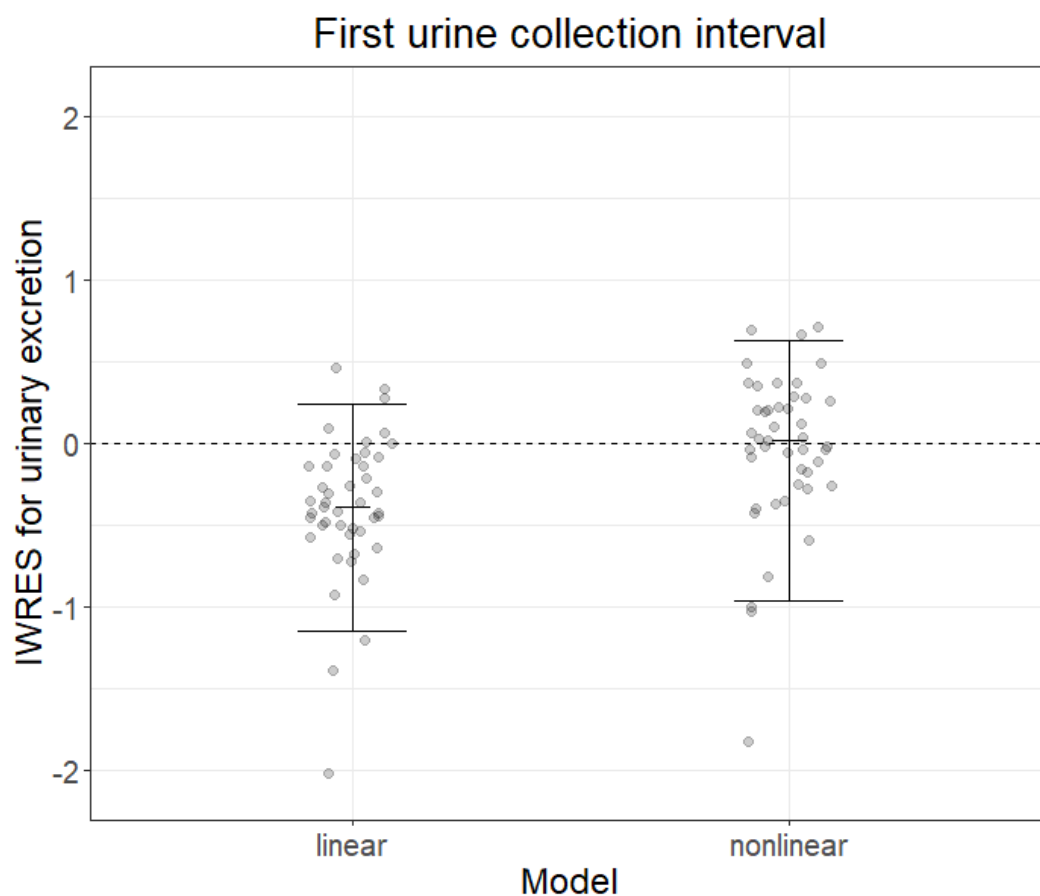


**Supplemental Fig. 2s** Goodness-of-fit plots of the final model for plasma concentrations (a-d) and amounts excreted in urine (e-h). a, e: Population predicted *versus* observed for plasma concentrations and amounts excreted in urine; b, f: Individual predicted *versus* observed for plasma concentrations and amounts excreted in urine; c, g: Conditional weighted residual *versus* population predicted for plasma concentrations and amounts excreted in urine; d, h: Conditional weighted residual *versus* time after last dose for plasma concentrations and amounts excreted in urine. Red dashed lines represent locally weighted smoothing lines.





**Supplemental Fig. 3s** Adefovir renal clearance plots illustrate a comparison between observed and estimated urinary excretion rates using both nonlinear and linear renal elimination models against the geometric mean of individual average adefovir plasma concentrations across the five urine collection intervals in both reference and test periods. The blue open circles represent individual observations of urinary excretion rate *versus* average plasma concentrations in each urine collection interval. The individual average plasma concentrations result from dividing the area under the curve of observed plasma concentrations by the duration of each urine collection interval. Dashed blue lines represent locally weighted smoothing lines of these individual observation pairs. Blue solid square points and error bars depict geometric means and  $\pm$  one geometric SD of observed individual urinary excretion rates in comparison to the geometric means of individual average plasma concentrations during each of the five urine collection intervals. Orange and grey lines represent population predictions of renal excretion rate from the nonlinear and linear models, respectively.



**Supplemental Fig. 4s** Residual plots compare the urinary adefovir excretion for both the linear and nonlinear models during the first urine collection interval. Scatter points represent individual weighted residuals (IWRES) calculated from the final nonlinear and linear models. Error bars show the 5<sup>th</sup>, 50<sup>th</sup>, and 95<sup>th</sup> percentiles of the data.

## Erklärung

Hiermit versichere ich an Eides statt, dass ich die vorliegende Dissertationsschrift selbstständig und ohne die Benutzung anderer als der angegebenen Hilfsmittel angefertigt habe. Alle Stellen - einschließlich Tabellen, Karten und Abbildungen -, die wörtlich oder sinngemäß aus veröffentlichten und nicht veröffentlichten anderen Werken im Wortlaut oder dem Sinn nach entnommen sind, sind in jedem Einzelfall als Entlehnung kenntlich gemacht. Ich versichere an Eides statt, dass diese Dissertationsschrift noch keiner anderen Fakultät oder Universität zur Prüfung vorgelegen hat; dass sie - abgesehen von unten angegebenen Teilpublikationen - noch nicht veröffentlicht worden ist sowie, dass ich eine solche Veröffentlichung vor Abschluss der Promotion nicht ohne Genehmigung der / des Vorsitzenden des IPHS-Promotionsausschusses vornehmen werde. Die Bestimmungen dieser Ordnung sind mir bekannt. Die von mir vorgelegte Dissertation ist von Univ.-Prof. Dr. Uwe Fuhr betreut worden.

Darüber hinaus erkläre ich hiermit, dass ich die Ordnung zur Sicherung guter wissenschaftlicher Praxis und zum Umgang mit wissenschaftlichem Fehlverhalten der Universität zu Köln gelesen und sie bei der Durchführung der Dissertation beachtet habe und verpflichte mich hiermit, die dort genannten Vorgaben bei allen wissenschaftlichen Tätigkeiten zu beachten und umzusetzen.

Übersicht der Publikationen:

- (1) **Dong, Q.**, Fuhr, U., Schaeffner, E., van der Giet, M., Ebert, N., & Taubert, M. (2023). Improved correction formulas to estimate iohexol clearance from simple models. *European journal of clinical pharmacology*, 79(9), 1215–1217. <https://doi.org/10.1007/s00228-023-03535-y>
- (2) **Dong, Q.**, Chen, Z., Boland, J., Dokos, C., Hagos, Y., Kühne, A., Taubert, M., Gründemann, D., & Fuhr, U. (2025). Validating Low-Dose Iohexol as a Marker for Glomerular Filtration Rate by In vitro and In Vivo Studies. *Clinical and translational science*, 18(2), e70141. <https://doi.org/10.1111/cts.70141>
- (3) **Dong, Q.**, Chen, C., Taubert, M., Bilal, M., Kinzig, M., Sörgel, F., Scherf-Clavel, O., Fuhr, U., & Dokos, C. (2024). Understanding adefovir pharmacokinetics as a component of a transporter phenotyping cocktail. *European journal of clinical pharmacology*, 80(7), 1069–1078. <https://doi.org/10.1007/s00228-024-03673-x>

Ich versichere, dass ich alle Angaben wahrheitsgemäß nach bestem Wissen und Gewissen gemacht habe und verpflichte mich, jedmögliche, die obigen Angaben betreffenden Veränderungen, dem IPHS-Promotionsausschuss unverzüglich mitzuteilen.

04.07.2025

Datum

Qian Dong

Unterschrift